

SYNTHESIS AND CHARACTERIZATION OF ORGANIC AND  
ORGANOMETALLIC CONDUCTING POLYMERS AND OLIGOMERS

by

Michael Oliver Wolf

B.Sc., Dalhousie University  
(1989)

Submitted to the Department of Chemistry  
in Partial Fulfillment of the Requirements  
for the Degree of

DOCTOR OF PHILOSOPHY

at the

MASSACHUSETTS INSTITUTE OF TECHNOLOGY

February 1994

© Massachusetts Institute of Technology, 1994

Signature of Author \_\_\_\_\_  
Department of Chemistry  
January 14, 1994

Certified by \_\_\_\_\_  
Mark S. Wrighton  
Thesis Supervisor

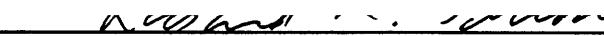
Accepted by \_\_\_\_\_  
Glenn A. Berchtold  
Chairman, Departmental Committee on Graduate Students

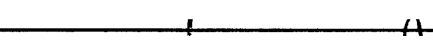
MASSACHUSETTS INSTITUTE  
OF TECHNOLOGY

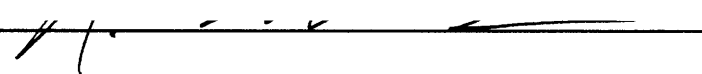
MAR 21 1994

LIBRARIES Science

This doctoral thesis has been examined by a Committee of the Department of Chemistry  
as Follows:

Professor Richard R. Schrock  \_\_\_\_\_  
Chairman

Professor Mark S. Wrighton  \_\_\_\_\_  
Thesis Supervisor

Professor Hans-Conrad zur Loye  \_\_\_\_\_

SYNTHESIS AND CHARACTERIZATION OF ORGANIC AND  
ORGANOMETALLIC CONDUCTING POLYMERS AND OLIGOMERS

by

Michael Oliver Wolf

Submitted to the Department of Chemistry, January 14, 1994,

in partial fulfillment of the requirements

for the Degree of Doctor of Philosophy in Chemistry

ABSTRACT

**Chapter 1: General Introduction**

A brief review of the field of conducting polymers and their applications is given. An overview of the research described in the thesis is included.

**Chapter 2: Tunable Electron Density at a Rhenium Carbonyl Complex  
Coordinated to the Conducting Polymer Poly[5,5'-(2-thienyl)-2,2'-bithiazole]**

The synthesis of a conducting polymer by electropolymerization of 5,5'-(2-thienyl)-2,2'-bithiazole is reported. Films of this polymer exhibit electrochemical behavior typical of conducting polymers and have a conductivity of  $0.2 \Omega^{-1}\text{cm}^{-1}$  in 0.1 M  $[n\text{-Bu}_4\text{N}]\text{PF}_6/\text{CH}_2\text{Cl}_2$  25 °C at the potential of maximum conductivity (approx. +1.5 V vs. Ag). The activation energy for conductivity for partially oxidized (approx. +1.3 V vs. Ag) films is 0.25 eV. Reaction of these polymer films with refluxing solutions of  $\text{Re}(\text{CO})_5\text{Cl}$  in  $\text{CHCl}_3$  yields polymers in which the  $[\text{Re}(\text{CO})_3\text{Cl}]$  moiety is bound to the bithiazolyl sites in the polymer. Subsequent reaction with  $\text{AgPF}_6$  converts the Re centers to cationic  $[\text{Re}(\text{CO})_3(\text{CH}_3\text{CN})]^+$  groups. These polymers were characterized by XPS and surface reflectance FTIR. The polymer containing the cationic Re groups is conducting (approx.  $2 \times 10^{-3} \Omega^{-1}\text{cm}^{-1}$  at +1.5 V vs. Ag). The potential region in which the polymer is conducting does not overlap with any Re-centered oxidations, but oxidation of films of the polymer to the conducting state causes electron density to be removed from the Re center resulting in a reversible shift of the carbonyl stretching frequencies to higher energy. At the potential of maximum conductivity this shift is 4-6  $\text{cm}^{-1}$ .

### Chapter 3: Synthesis and Reactivity of Novel Conducting Polymers Containing Platinum(II) in the Backbone: Polymers Derived from Oxidation of *cis*(5'-(2,5-Bithienyl))<sub>2</sub>(4-isocyanophenylferrocene)<sub>2</sub>platinum(II) and *cis*(2-Thienyl)<sub>2</sub>(4-isocyanophenyl-ferrocene)<sub>2</sub>platinum(II)

The preparation and characterization of *cis*(5'-(2,5-bithienyl))<sub>2</sub>(4-isocyanophenylferrocene)<sub>2</sub>platinum(II), **1a** and a novel conducting polymer prepared by oxidative polymerization of this complex, poly[*cis*(5'-(2,5-bithienyl))(4-isocyanophenylferrocene)<sub>2</sub>platinum(II)], is described. The polymer is characterized by X-ray photoelectron spectroscopy, specular reflectance infrared spectroscopy and electrochemical techniques. The polymer has a conductivity of approximately 0.1  $\Omega^{-1}\text{cm}^{-1}$  at the potential of maximum conductivity (+1.1 V vs. Ag). Reversible substitution of the isonitrile ligands by 4-isocyanophenylferrocenoate at the Pt(II) center of the polymer is demonstrated. Preparation and characterization of *cis*(2-thienyl)<sub>2</sub>(4-isocyanophenylferrocene)<sub>2</sub>platinum(II), **1c** is also described. Oxidative polymerization of this complex occurs at +1.75 V vs. Ag, but it was not possible to grow films thick enough to measure the potential dependence of the conductivity. The polymers from both **1a** and **1c** show Pt/S ratios which are lower than in the respective monomers, suggesting that oxidative polymerization is accompanied by some degradation. The "purity" of the polymer depends on deposition conditions. For comparison to the oxidatively prepared polymers the related oligomer, [Pt(1,5-cyclooctadiene)(2,2':5',2'':5'',2''':5''''-tetrathiophene)]<sub>n</sub> (n = 2-3) was prepared by reaction of (1,5-cyclooctadiene)dichloroplatinum with 5,5'''-di(tributylstannyl)-2,2':5',2'':5'',2'''-tetrathiophene. Substitution of the 1,5-cyclooctadiene in this oligomer by *t*-butylisonitrile yields a derivative which is soluble and of which thin films can be cast. Electrochemical techniques show that the *t*-butylisonitrile derivative has a conductivity of approximately 0.03  $\Omega^{-1}\text{cm}^{-1}$  at the positive limit of the cyclic voltammogram (+1.0 V vs. Ag). The *t*-butylisonitrile can be displaced by 4-isocyanophenylferrocene to introduce discrete redox-active centers into the polymer.

### Chapter 4: Electrochemical Properties of Cyclopolymers of 1,6-Heptadiyne Derivatives Prepared Using Well-Defined Alkylidene Complexes.

The electrochemical behaviour of polymers prepared by the living cyclopolymerization of diethyl dipropargylmalonate (**2**), and optically active di-(1R,2S,5R)-(-)-menthyl dipropargylmalonate (**3(-)**), di-(1S,2R,5S)-(+)-menthyl dipropargylmalonate (**3(+)**), using Mo(NAr)(CHCMe<sub>2</sub>Ph)(OR<sub>F6</sub>)<sub>2</sub> (**1**; Ar = 2,6-*i*-Pr<sub>2</sub>-C<sub>6</sub>H<sub>3</sub>, OR<sub>F6</sub> = OMe(CF<sub>3</sub>)<sub>2</sub>) as the initiator in 1,2-dimethoxyethane (DME) is described. Solution cyclic voltammetry of poly-(**2**) and poly-(**3(-)**), and well as cyclic voltammograms of thin-films of these homopolymers are obtained. None of the homopolymers are conducting when oxidized. Random and block copolymers of **3(+)** and TCDT (**4a - 4c**) as well as **2** and 7,8-bistrifluoromethyl-tricyclo[4.2.2.0<sup>2,5</sup>]deca-3,7,9-triene (TCDT) (**4d - 4e**) were characterized electrochemically. These copolymers have conductivities ranging from 3 x 10<sup>-4</sup> to 2 x 10<sup>-2</sup>  $\Omega^{-1}\text{cm}^{-1}$ . The average conductivity of the triblock copolymer [poly(TCDT)<sub>10</sub>]<sub>2</sub>poly(**3(+)**)<sub>20</sub> (**4f**), is 3 x 10<sup>-4</sup>  $\Omega^{-1}\text{cm}^{-1}$ .

### Chapter 5: Preparation and Characterization of Photovoltaic and Photoelectrochemical Devices Based on $\alpha$ -Sexithiophene.

Vacuum deposited thin films of  $\alpha$ -sexithiophene are shown to behave as active materials in both photovoltaic and photoelectrochemical cells. Solid state cells in which the  $\alpha$ -sexithiophene thin film is sandwiched between Al and ITO as well as Al and Pt were studied. The Al/ $\alpha$ -sexithiophene/Pt devices have open circuit potentials (V<sub>oc</sub>) of as high as 0.99 V and operated at an overall power efficiency ( $\eta$ ) of 1.2% under polychromatic illumination of 25  $\mu\text{W}/\text{cm}^2$ . These devices had low fill factors (0.11). Thin films of sexithiophene on Pt may be used as photocathodes when the films are

contacted on the other side with an electrolyte solution containing a redox couple. The  $\alpha$ -sexithiophene photocathodes have a photovoltage of  $\sim 1.4$  V when  $[\text{Cp}_2\text{Co}][\text{PF}_6]$  is used as the solution redox couple. Steady-state experiments demonstrated these cells to have high fill-factors (0.42) under polychromatic illumination, however the cells have low overall efficiencies (0.01%).

Thesis Supervisor: Dr. Mark S. Wrighton

Title: Provost and Ciba-Geigy Professor of Chemistry

## TABLE OF CONTENTS

	<u>page</u>
Title Page .....	1
Signature Page.....	2
Abstract .....	3
Table of Contents .....	6
List of Figures .....	9
List of Tables .....	12
Lists of Charts and Schemes .....	13
Dedication .....	14
Acknowledgments.....	15
<b>Chapter 1: General Introduction.....</b>	<b>16</b>
References.....	25
<b>Chapter 2: Tunable Electron Density at a Rhenium Carbonyl Complex Coordinated to the Conducting Polymer Poly[5,5'-(2-thienyl)-2,2'- bithiazole].....</b>	<b>28</b>
Introduction.....	29
Results and Discussion.....	32
Preparation and Characterization of Poly-1 .....	32
UV-vis Spectroelectrochemistry .....	39
Derivatization of Poly-1.....	39
Electrochemistry of Complexes 4 and 5 .....	51
Electrochemistry of Poly-2 and Poly-3 .....	56
IR of Reduced and Oxidized Poly-3 .....	57
Conclusions .....	58
Experimental Section .....	60

References .....	64
<b>Chapter 3: Synthesis and Reactivity of Novel Conducting Polymers Containing Platinum(II) in the Backbone: Polymers Derived from Oxidation of <i>cis</i>(5'-(2,5-Bithienyl)<sub>2</sub>(4-isocyanophenylferrocene)<sub>2</sub>platinum(II) and <i>cis</i>(2-Thienyl)<sub>2</sub>(4-isocyanophenyl-ferrocene)<sub>2</sub>platinum(II) .....</b>	<b>66</b>
Introduction .....	67
Results and Discussion.....	71
Preparation and Characterization of Monomers <b>1a-1c</b> .....	71
Preparation and Characterization of Oxidatively Formed Polymers from <b>1a</b> and <b>1c</b> .....	71
Isonitrile Exchange Reactions.....	85
Preparation and Characterization of <b>3a</b> and <b>3b</b> .....	90
Conclusions .....	100
Experimental Section .....	102
References .....	108
<b>Chapter 4: Properties of Cyclopolymers of 1,6-Heptadiyne Derivatives Prepared Using Well-Defined Alkylidene Complexes.....</b>	<b>111</b>
Introduction .....	112
Results and Discussion.....	115
Solution Electrochemistry of Poly ( <b>2</b> ) and Poly ( <b>3(-)</b> ).....	115
Thin Film Electrochemistry of Poly ( <b>3(-)</b> ) .....	115
Thin Film Electrochemistry of Copolymers .....	123
Experimental Section .....	132
References .....	133
<b>Chapter 5: Preparation and Characterization of Photovoltaic and Photoelectrochemical Devices Based on <math>\alpha</math>-Sexithiophene.....</b>	<b>136</b>
Introduction .....	137

Results and Discussion.....	140
Preparation and Characterization of Photovoltaic Devices.....	140
Photoelectrochemical Devices .....	151
Experimental Section .....	159
References .....	161



## List of Figures

	page
<b>Chapter 2</b>	
Figure 1. Absorption and emission spectra of <b>1</b> .....	34
Figure 2. (a) Cyclic voltammogram of a film of poly- <b>1</b> on Au microelectrodes, in 0.1 M [ <i>n</i> -Bu <sub>4</sub> N]PF <sub>6</sub> /CH <sub>2</sub> Cl <sub>2</sub> at 100 mV/s. (b) I <sub>D</sub> -V <sub>G</sub> of poly- <b>1</b> on Au microelectrodes with V <sub>D</sub> = 50 mV at 100 mV/s. (c) Cyclic voltammogram of a film of poly- <b>3</b> on Au microelectrodes, in 0.1 M [ <i>n</i> -Bu <sub>4</sub> N]PF <sub>6</sub> /CH <sub>2</sub> Cl <sub>2</sub> at 100 mV/s. (d) I <sub>D</sub> -V <sub>G</sub> of poly- <b>3</b> on Au microelectrodes with V <sub>D</sub> = 100 mV at 100 mV/s. Note the different current scales in (b) and (d).....	36
Figure 3. Temperature dependence of the conductivity of a partially oxidized film of poly- <b>1</b> . Inset: Log conductivity vs. 1/T for the same data .....	40
Figure 4. (a) UV-vis spectrum of poly- <b>1</b> on ITO/glass. (b) UV-vis spectrum of poly- <b>1</b> held at + 1.5 V vs. Ag. (c) UV-vis spectrum of poly- <b>1</b> returned to 0 V vs. Ag.....	42
Figure 5. (a) Surface reflectance FTIR spectrum of CO stretching region of a film of poly- <b>2</b> on Pt. (b) IR of the same region of a CH <sub>2</sub> Cl <sub>2</sub> solution of <b>4</b> . (c) Surface reflectance FTIR spectrum of CO stretching region of a film of poly- <b>3</b> on Pt. (d) IR of the same region of a CH <sub>2</sub> Cl <sub>2</sub> solution of <b>5</b> .....	47
Figure 6. XPS survey scan of (a) poly- <b>1</b> on Pt; (b) poly- <b>2</b> on Pt; (c) poly- <b>3</b> on Pt .....	49
Figure 7. (a) UV-vis spectrum of a film of poly- <b>1</b> on ITO/glass. (b) UV-vis spectrum of a film of poly- <b>2</b> on ITO/glass. (c) UV-vis spectrum of a film of poly- <b>3</b> on ITO/glass.....	52
Figure 8. (a) Cyclic voltammogram of (2,2'-bithiazole)Re(CO) <sub>3</sub> Cl, <b>4</b> in 0.1 M [ <i>n</i> -Bu <sub>4</sub> N]PF <sub>6</sub> /CH <sub>3</sub> CN at 100 mV/s. (b) Same solution scanning to +2.0 V vs. SCE. (c) Cyclic voltammogram of [(2,2'-bithiazole)Re(CO) <sub>3</sub> (CH <sub>3</sub> CN)] <sup>+</sup> , <b>5</b> in 0.1 M [ <i>n</i> -Bu <sub>4</sub> N]PF <sub>6</sub> /CH <sub>3</sub> CN at 100 mV/s .....	54
<b>Chapter 3</b>	
Figure 1. (a) Cyclic voltammetry of electrodeposited film of poly- <b>1a</b> on Au microelectrodes in 0.1 M [( <i>n</i> -Bu) <sub>4</sub> N]PF <sub>6</sub> /CH <sub>2</sub> Cl <sub>2</sub> . (b) I <sub>D</sub> -V <sub>G</sub> characteristic in the same medium for the same pair of derivatized microelectrodes. (c) Cyclic voltammogram of the same film of poly- <b>1a</b> after 15 minutes immersed in <b>2b</b> /CH <sub>2</sub> Cl <sub>2</sub> . (d) I <sub>D</sub> -V <sub>G</sub> characteristic of the film shown in (c). (e) Cyclic voltammogram of the same film of poly- <b>1a</b> after 15 minutes further immersion in <b>2a</b> /CH <sub>2</sub> Cl <sub>2</sub> . (f) I <sub>D</sub> -V <sub>G</sub> characteristic of the film shown in (e)..	74
Figure 2. (a) Solution infrared spectra of the isonitrile stretching region of <b>1a</b> and <b>2a</b> in CH <sub>2</sub> Cl <sub>2</sub> . (b) Specular reflectance infrared spectrum of poly- <b>1a</b> on a Au macroelectrode in the same region.....	76

Figure 3.	XPS spectrum of (a) thin film of <b>1a</b> on Au and (b) poly- <b>1a</b> on Au .....	81
Figure 4.	(a) Cyclic voltammometry of electrodeposited film of poly- <b>1c</b> on a Pt macroelectrode in 0.1 M [( <i>n</i> -Bu) <sub>4</sub> N]PF <sub>6</sub> /CH <sub>2</sub> Cl <sub>2</sub> . (b) Cyclic voltammogram of the same film of poly- <b>1c</b> after 15 minutes immersed in <b>2b</b> /CH <sub>2</sub> Cl <sub>2</sub> . (c) Cyclic voltammogram of the same film of poly- <b>1c</b> after 15 minutes further immersion in <b>2a</b> /CH <sub>2</sub> Cl <sub>2</sub> .....	86
Figure 5.	XPS spectrum of (a) thin film of <b>1c</b> on Au and (b) poly- <b>1c</b> on Au .....	88
Figure 6.	UV-vis spectrum of (a) <b>3a</b> , (b) <b>3b</b> , (c) <b>3c</b> in CHCl .....	92
Figure 7.	(a) Cyclic voltammometry of film of <b>3c</b> on Pt microelectrodes in 0.1 M [( <i>n</i> -Bu) <sub>4</sub> N]PF <sub>6</sub> /CH <sub>3</sub> CN. (b) I <sub>D</sub> -V <sub>G</sub> characteristic in the same medium for the same pair of derivatized microelectrodes.....	95
Figure 8.	(a) Cyclic voltammometry of film of <b>3c</b> on Pt microelectrodes in 0.1 M [( <i>n</i> -Bu) <sub>4</sub> N]PF <sub>6</sub> /CH <sub>3</sub> CN after immersion for 15 min in <b>2a</b> /CH <sub>3</sub> CN. (b) I <sub>D</sub> -V <sub>G</sub> characteristic in the same medium for the same pair of derivatized microelectrodes .....	97

#### Chapter 4

Figure 1.	Cyclic voltammogram of a thin film of poly ( <b>2</b> ) <sub>20</sub> at a Pt electrode in 0.1 M [ <i>n</i> -Et <sub>4</sub> N]AsF <sub>6</sub> / CH <sub>3</sub> CN at 100 mV/s.....	118
Figure 2.	(a) Cyclic voltammogram of a thin film of poly ( <b>3(-)</b> ) <sub>40</sub> on a Pt electrode in 0.1 M [ <i>n</i> -Bu <sub>4</sub> N]PF <sub>6</sub> / CH <sub>3</sub> CN from -1.0 V to 1.0 V vs. Ag; (b) Cyclic voltammogram of poly ( <b>3(-)</b> ) <sub>40</sub> from 0 V to 1.25 V .....	120
Figure 3.	(a) UV/vis spectrum of a thin film of poly ( <b>3(-)</b> ) <sub>20</sub> on an indium-tin oxide electrode held at 0 V vs. Ag in 0.1 M [ <i>n</i> -Bu <sub>4</sub> N]PF <sub>6</sub> / CH <sub>3</sub> CN; (b) Same film held at 1.0 V; (c) Same film held at 0 V again .....	124
Figure 4.	Cyclic voltammogram of a thin film of polymer <b>4c</b> on a Pt electrode in 0.1 M [ <i>n</i> -Bu <sub>4</sub> N]PF <sub>6</sub> / CH <sub>3</sub> CN.....	126
Figure 5.	Cyclic voltammograms of copolymer films on Pt electrodes in 0.1 M [ <i>n</i> -Bu <sub>4</sub> N]PF <sub>6</sub> / CH <sub>3</sub> CN: (a) polymer <b>4a</b> ; (b) polymer <b>4d</b> . I <sub>D</sub> -V <sub>G</sub> characteristics for copolymer films on interdigitated Pt electrode arrays in 0.1 M [ <i>n</i> -Bu <sub>4</sub> N]PF <sub>6</sub> / CH <sub>3</sub> CN: (c) polymer <b>4a</b> ; (d) polymer <b>4d</b> .....	130

#### Chapter 5

Figure 1.	Photocurrent density as a function of potential for irradiation of an Pt/ $\alpha$ -sexithiophene/Al device for different incident light intensities. Illumination is through the Al side of the device with 488 nm laser light, and intensities are corrected for the aluminum absorption .....	141
-----------	--	-----

- Figure 2. Photocurrent density as a function of potential for irradiation of an ITO/ $\alpha$ -sexithiophene/Al device for different incident light intensities. Illumination is through the Al side of the device with 488 nm laser light, and intensities are corrected for the aluminum absorption ..... 142
- Figure 3. (a)  $V_{oc}$  vs.  $I_{inc}$  and (b)  $I_{sc}$  vs.  $I_{inc}$  for an ITO/ $\alpha$ -sexithiophene/Al device . Illumination is through the Al side of the device with 488 nm laser light, and intensities are corrected for Al absorption. Inset:  $\log I_{sc}$  vs.  $\log I_{inc}$  ..... 147
- Figure 4. (a) Absorbance spectrum of the  $\alpha$ -sexithiophene film on ITO/glass. (b) photoaction spectra for irradiation through aluminum side and (c) ITO side. Photocurrents are corrected for Al and ITO/glass absorption and lamp intensity variations ..... 149
- Figure 5. (a)  $I_{sc}$  vs.  $I_{inc}$  and (b)  $V_{oc}$  vs.  $I_{inc}$  for a Pt/-sexithiophene/Al device. Illumination is through the Al side of the device with 488 nm laser light, and intensities are corrected for Al absorption ..... 152
- Figure 6. (a) Photoaction spectra for irradiation through aluminum side of a Pt/-sexithiophene/Al device and (b) absorbance spectrum of the  $\alpha$ -sexithiophene film on ITO/glass. Photocurrents are corrected for Al absorption and lamp intensity variations ..... 154
- Figure 7. Photocurrent density as a function of potential vs. SCE for irradiation of a sexithiophene/Pt device in 0.05 M  $Cp_2CoPF_6$  / 0.1 M  $[n-Bu_4]NPF_6$  ..... 157

## List of Tables

	page
<b>Chapter 2</b>	
Table I. Electrochemical and Infrared Spectral Data in the CO Stretching Region for 2,2'-Bithiazole and 2,2'-Bipyridine complexes .....	44
<b>Chapter 3</b>	
Table I. IR and UV-vis spectroscopic data.....	73
Table II. XPS Compositions and Element Ratios of Polymers and Monomer <b>1a</b> .....	80
<b>Chapter 4</b>	
Table I. Data for Homopolymers, Random and Block Copolymers .....	117
<b>Chapter 5</b>	
Table I. Performance Characteristics of Photovoltaic and Photoelectrochemical Cells Based on $\alpha$ -Sexithiophene .....	146

## List of Charts

**Chapter 1**

Chart I.	Structure of some of the common organic conducting polymers .....	18
Chart II.	Examples of metal coordination polymers, linear dithiolene polymers and ladder polymers.....	20

## List of Schemes

**Chapter 1**

Scheme I.	Schematic of highly interdigitated microelectrode devices.....	22
Scheme II.	Schematic of a conducting polymer microelectrochemical transistor.....	23

**Chapter 2**

Scheme I	Synthesis of poly- <b>1-3</b> .....	30
Scheme II	Synthesis of 5,5'-(2-thienyl)-2,2'-bithiazole, <b>1</b> .....	33
Scheme III	Synthesis of (2,2'-bithiazole)Re(CO) <sub>3</sub> Cl, <b>4</b> and (2,2'-bithiazole)Re(CO) <sub>3</sub> (CH <sub>3</sub> CN)PF <sub>6</sub> , <b>5</b> .....	45

**Chapter 3**

Scheme I	Synthesis of <b>1a-1c</b> .....	68
Scheme II	Synthesis of <b>3b</b> .....	70

**Chapter 4**

Scheme I	Synthesis of polymers.....	116
----------	----------------------------	-----

**Chapter 5**

Scheme I	Schematic of $\alpha$ -sexithiophene photovoltaic and photoelectrochemical devices .....	139
----------	--	-----

To Jennifer

## Acknowledgments

I would like to thank Mark Wrighton for teaching me to be a careful scientist and to do *all* the experiments, for encouraging me to pursue chemistry that I found interesting, and most importantly for helping me learn to develop ideas independently. It has been a pleasure to be a colleague.

Thanks to the Wrighton group, most particularly my friends Ivan, Larry, Eric Lee, Dave Ofer, Dave Albagli, Chris Hable, and Dan Frisbie. Ron, you made a fantastic labmate and friend, you taught me a lot about how to do things the right way. I can't think of anyone I'd rather change pump oil with.

Thanks to my friends who have travelled the same road with me the last few years. Tu - for putting me up while I finished this thesis. Dan - coffee and beer and breaking in the Blue Thing. Mathai - I couldn't ask for a better roommate and friend for the last 14 years (yes, it's been that long).

Thanks to Dick Schrock and Howie Fox for the collaboration from which some of the results are in Chapter 4 of this thesis.

Thanks to the people at MIT who worked hard and were always willing to do more than the job required, in particular Bob D., Rich P., Lee and Joan at Graphic Arts, Dena, and Christine.

Thanks to both my families, Pa, Ma, Tom, Peter, Joel, Judy, and Missy. Your support helped make this easy.

Thanks to NSERC and NSF for financial support.

Finally, thanks to Jen, for staying here an extra year, for pushing me when I needed it, but most of all for having an unreliable car battery, for without that we might never have met. I dedicate this work to you.

## **Chapter 1**

### **General Introduction**

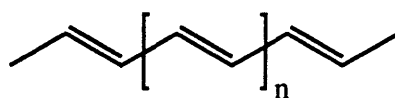


The discovery that oxidation or reduction of polymeric materials with conjugated backbones could dramatically increase their electrical conductivities opened a large field of research which spans material science, physics and chemistry. The seminal discovery that polyacetylene could be "doped" to extraordinarily high conductivity ( $1000 \Omega^{-1}\text{cm}^{-1}$ )<sup>1</sup> stimulated intense interest in these conjugated materials. Although this finding is often cited as the first example of a polymer with "metallic" conductivity, other workers had previously discovered similar properties in other materials. In 1968, a material which was called "pyrrole black", prepared by electrochemical oxidation of pyrrole, was found to have a conductivity of  $8 \Omega^{-1}\text{cm}^{-1}$ .<sup>2</sup> Concurrently,  $(\text{SN})_n$ , first prepared by Burt in 1910 by topochemical solid-state polymerization,<sup>3</sup> was also shown to be conducting.

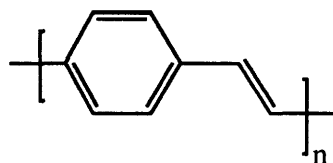
Over the last 25 years, many other conjugated, conducting polymers have been prepared and studied.<sup>4-11</sup> Some of the well-studied systems are shown in Chart I. Many routes to these polymers are known including both chemical and electrochemical syntheses. In addition to the simple polymers shown in Chart I, countless derivatives of these have been prepared, much of this chemistry with the design of specific properties in mind. Highly soluble polymers have been prepared to avoid many of the processing problems associated with insoluble materials, such as those shown in Chart I. The use of well-controlled polymerization techniques has led to the preparation of materials in which the polydispersity can be controlled, as well as chain length. Methods of introducing bulk order to polymer samples have been developed, and resulting increases in conductivity have been studied. These new polymers, along with theoretical studies have led to a better understanding of the electronic structure of conducting polymers.<sup>4</sup>

Despite the obvious utility of conducting organic materials with conductivities on the order of metals, practical applications of conducting polymers have been slower to arrive than originally predicted. New applications of conducting polymers in the areas of nonlinear optics,<sup>12</sup> device fabrication,<sup>13,14</sup> and light-emitting diodes<sup>15-21</sup> are

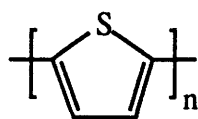
**Chart I.** Structure of some of the common organic conducting polymers.



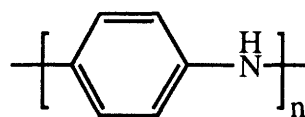
polyacetylene



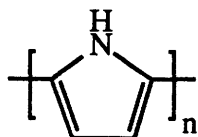
poly-*p*-phenylenevinylene



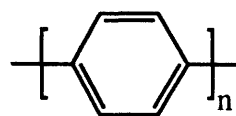
polythiophene



polyaniline



polypyrrole



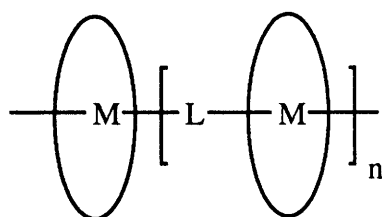
poly-*p*-phenylene

beginning to be explored, and it is hoped that these new developments will reinvigorate interest in such polymers. The ease in which properties such as the color of a light-emitting diode can be tuned by chemical modification of the backbone structure is important, as it illustrates how organic synthesis can be used to effect changes in property.

Although much of the research in this area has focused on the organic conducting polymers, there has also been interest in materials in which the conduction pathway involves elements other than carbon. Some examples include the polysilanes,<sup>22</sup> metal coordination polymers,<sup>23,24</sup> linear dithiolenes<sup>25-29</sup> and ladder polymers<sup>30-32</sup>, Chart II. The mechanism of charge transport in these polymers may differ from that in the organic conducting polymers, as the structures are dramatically different in some cases. Recently, the preparation of short, well-defined oligomers of some of the conducting polymers has been carried out. In some cases the oligomers have been found to have properties superior to those of the parent polymers,<sup>33-39</sup> stimulating interest in molecular materials which are structurally related to conducting polymers. The processibility of oligomers, as much a problem as in the polymers, has been improved by increasing the solubility via alkyl side groups.<sup>40,41</sup> Since oligomers may be prepared easily as pure materials, the defects and structural incongruities present in polymeric systems can be avoided, possibly giving rise to the improvements in properties which have been observed.

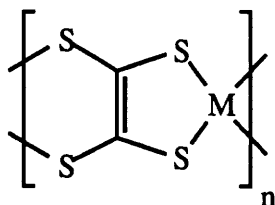
Previous work in the Wrighton group has shown that using microelectrochemical devices, the potential dependence of the conductivity of conducting polymers can be measured.<sup>42-49</sup> The significance of this technique is that it gives one a way to simultaneously control and monitor the oxidation or reduction of a conducting polymer. In the same way that a cyclic voltammogram reveals information about redox processes as a function of the applied potential, the measurement of conductivity of a material as a function of potential yields information about the process, which cannot be obtained

**Chart II.** Examples of metal coordination polymers, linear dithiolene polymers and ladder polymers.



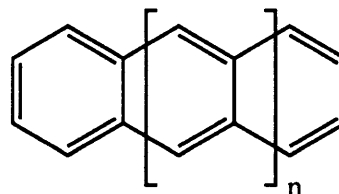
M = metal porphyrin or metal pthalocyanine  
L = O,S, -CN-, -CC-

**Metal pthalocyanine polymer**



M = metal

**linear dithiolene polymer**



**polyacene (ladder polymer)**

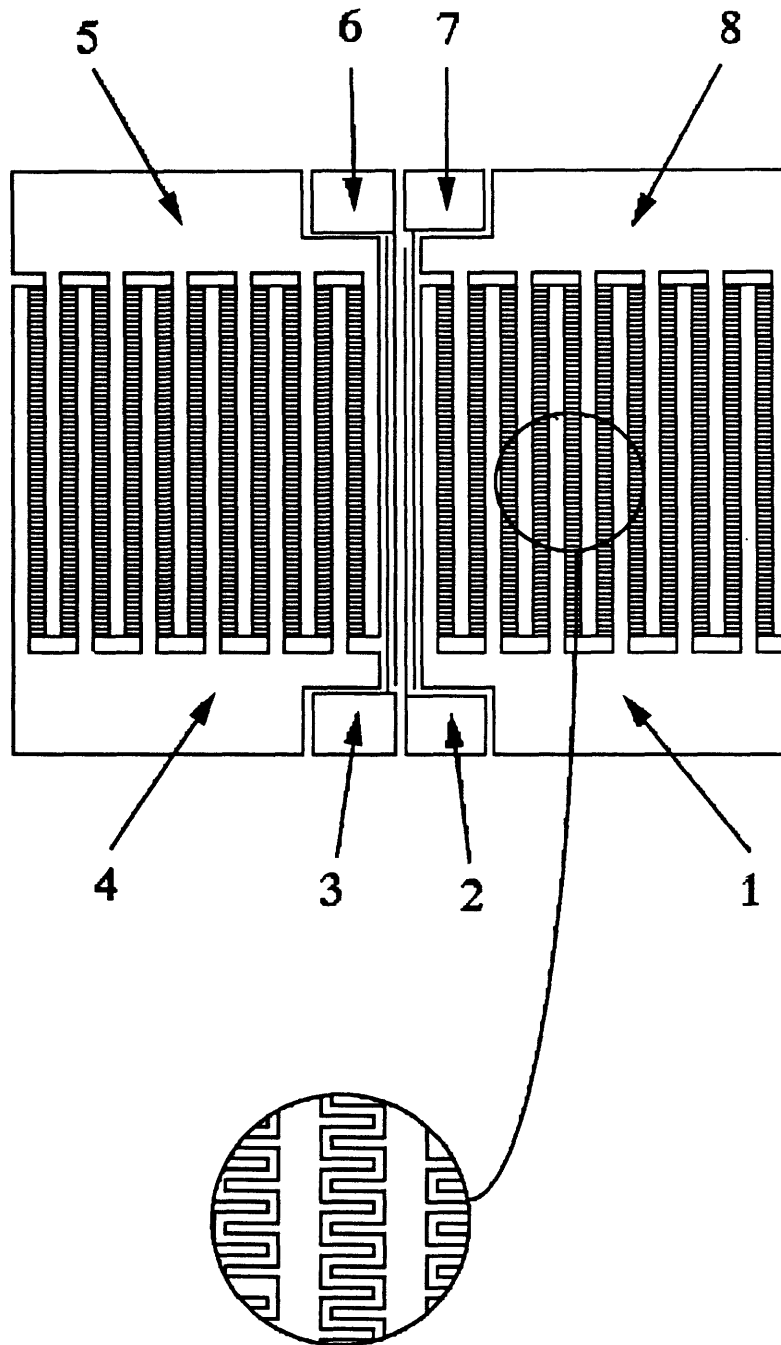
from a bulk conductivity measurement alone. The microelectrode arrays used in the work described in this thesis are of two types. The first consists of arrays of eight, closely spaced, individually addressable Pt or Au microelectrodes. The dimensions of each electrode are ( $\sim 2 \mu\text{m} \times 100 \mu\text{m} \times 0.1 \mu\text{m}$ ) and the spacing in between electrodes  $\sim 2 \mu\text{m}$ . The second type consists of eight electrodes. The outer four consist of six  $1.5 \text{ mm} \times 50 \mu\text{m}$  bars which have  $50 \mu\text{m} \times 4 \mu\text{m}$  teeth protruding on each side, Scheme I. In this configuration electrodes 1 and 8, and 4 and 5 are highly interdigitated. The inner electrodes, 2, 3, 6, and 7 are band electrodes  $1.5 \text{ mm} \times 4 \mu\text{m}$  in size. All the electrodes are separated from one another by  $4 \mu\text{m}$ . The size of the entire array is  $\sim 1.5 \text{ mm} \times \sim 2.5 \text{ mm}$ .

The first type of device is used for experiments in which electrodeposited polymers are to be studied. To measure the conductivity as a function of potential, polymer is first deposited over two of the microelectrodes called source and drain, Scheme II. The array is then configured such that a small, constant potential is applied between the source and drain,  $V_D$ . At the same time the potential of both electrodes versus a reference electrode,  $V_G$ , is varied, thus changing the state of charge and conductivity of the polymer. In the potential regime where the polymer is conducting, significant drain current,  $I_D$ , flows between the source and drain electrodes; when the polymer is insulating,  $I_D$  is negligible. The conductivity is directly proportional to  $I_D$ . Using eq. 1, actual conductivities can be calculated, where  $l$  and  $A$  are the distance between the microelectrodes and the cross-sectional area between, respectively. The larger devices

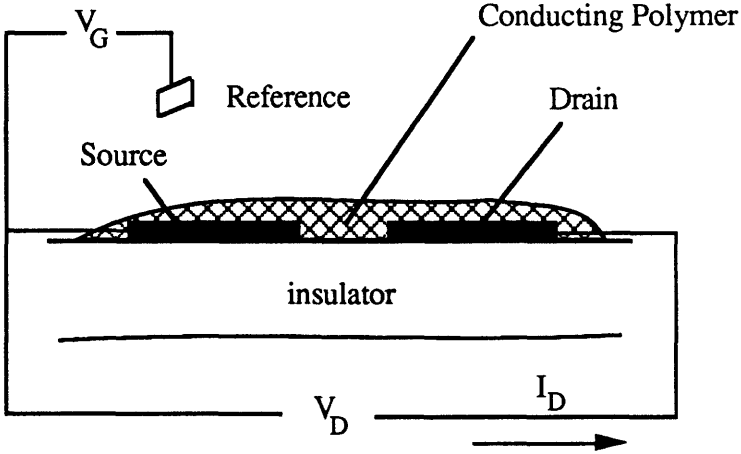
$$\sigma = I_D l / V_D A \quad (1)$$

are convenient to perform  $I_D$ - $V_G$  measurements on cast films of polymers. The experiment is identical, except electrodes 1 and 8 are configured as the source, and electrodes 4 and 5 as the drain.

**Scheme I.** Schematic of highly interdigitated microelectrode devices.



**Scheme II.** Schematic of a conducting polymer microelectrochemical transistor.



The work described in this thesis makes contributions in four areas of conducting polymer chemistry. Chapter 2 describes the synthesis of a new conducting polymer, containing 2,2'-bithiazolyl groups in the backbone. The 2,2'-bithiazolyl groups are analogous to other  $\alpha$ -diimine ligands such as 2,2'-bipyridyl and can be used to coordinate metal complexes to the polymer backbone. In this way the interaction between the conducting polymer in various states of oxidation and the pendant metal center can be probed. This is the first example of using a conducting polymer to "tune" electron density in a metal complex. Chapter 3 describes the synthesis of conducting polymers prepared from electropolymerizable platinum(II) containing monomers. Chemical synthesis of oligomers with analogous structures to the polymers is also demonstrated, and the potential dependence of the conductivity of all of these materials discussed. Although metal-containing polymers have been shown to be conducting, these systems are unique in that the reversible substitution of ligands at the metal centers is possible.

In Chapter 4, the electrochemistry of a series of well-defined polymers prepared by metal catalyzed cyclopolymerization of 1,6-heptadiynes is described. These polymers are soluble in many common solvents. Although the homopolymers are very poor conductors, soluble copolymers with polyacetylene can be prepared, and these are shown to be conducting. The magnitude of the conductivity varies depending on the constitution of the copolymers. In Chapter 5, the photovoltaic properties of an oligomer of thiophene,  $\alpha$ -sexithiophene, are investigated. The charge mobility in thin-films of  $\alpha$ -sexithiophene has been shown to be extraordinarily high. Photovoltaic devices using  $\alpha$ -sexithiophene as the active component are described.



**References.**

- (1) Shirikawa, H.; Louis, E. J.; MacDiarmid, A. G.; Chiang, C. K.; Heeger, A. J. *J. Chem. Soc. Chem. Commun.* **1977**, 578.
- (2) Dall'Olio, A.; Dascola, Y.; Varacca, V.; Bocchi, V. *Comptes Rendus* **1968**, C267, 433.
- (3) Burt, F. P. *J. Chem. Soc.* **1910**, 1171.
- (4) *Conjugated Polymers*; Brédas, J. L.; Silbey, R., Ed.; Kluwer: Dordrecht, 1991.
- (5) Kanatzidis, M. G. *Chem. and Eng. News* **1990**, 68, 36.
- (6) Kaner, R. B.; MacDiarmid, A. G. *Scient. Amer.* **1988**, 258, 106.
- (7) Aldissi, M. *Makromol. Chem. Macromol. Symp.* **1989**, 24, 1.
- (8) Frommer, J. E.; Chance, R. R. in "Encyclopedia of Polymer Science and Engineering"; M. Grayson and J. Kroschwitz, Ed.; John Wiley and Sons: New York, 1985; Vol. 5; pp 462.
- (9) Diaz, A. F.; Rubinson, J. F.; Mark, H. B. *J. Adv. Polym. Sci.* **1988**, 84, 113.
- (10) Chandler, G. K.; Pletcher, D. in "Specialist Periodical Reports: Electrochemistry" Royal Society of Chemistry: London, 1985.
- (11) *Handbook of Conducting Polymers*; Skotheim, T. A., Ed.; Marcel Dekker: New York, 1986.
- (12) Kajzar, F.; Messier, J. in "Conjugated Polymers"; J. L. Brédas and R. Silbey, Ed.; Kluwer: Dordrecht, 1991; pp 509.
- (13) Bradley, D. C. *Chemistry in Britain* **1991**, 719.
- (14) Burroughs, J. H.; Friend, R. H. in "Conjugated Polymers"; J. L. Brédas and R. Silbey, Ed.; Kluwer: Dordrecht, 1991; pp 555.
- (15) Braun, D.; Heeger, A. J. *Appl. Phys. Lett.* **1991**, 58, 1982.
- (16) Burroughs, J. H.; Bradley, D. D. C.; Brown, A. R.; Marks, R. N.; Mackay, K.; Friend, R. H.; Burns, P. L.; Holmes, A. B. *Nature* **1990**, 347, 539.

- (17) Greenham, N. C.; Moratti, S. C.; Bradley, D. D. C.; Friend, R. H.; Holmes, A. B. *Nature* **1993**, *365*, 628.
- (18) Ohmori, Y.; Uchida, M.; Muro, K.; Yoshino, K. *Jpn. J. Appl. Phys.* **1991**, *30*, L1938.
- (19) Ohmori, Y.; Uchida, M.; Muro, K.; Yoshino, K. *Jpn. J. Appl. Phys.* **1991**, *30*, L1941.
- (20) Grem, G.; Leditzky, G.; Ullrich, B.; Leising, G. *Adv. Mater.* **1992**, *4*, 36.
- (21) Burn, P. L. *Nature* **1992**, *356*, 47.
- (22) Miller, R. D.; Michl, J. *Chem. Rev.* **1989**, *89*, 1359.
- (23) Snow, A. W.; Griffith, J. R. in "Encyclopedia of Polymer Science and Engineering" John Wiley and Sons: New York, 1985; Vol. 11; pp 212.
- (24) Hanack, M.; Datz, A.; Fay, R.; Fischer, K.; Keppeler, U.; Koch, J.; Metz, J.; Mezger, M.; Schneider, O.; Schulze, H. in "Handbook of Conducting Polymers"; T. A. Skotheim, Ed.; Marcel Dekker, Inc.: New York, 1986; Vol. 1; pp 133.
- (25) Pittman, C. U.; Carraher, C. E.; Reynolds, J. R. in "Encyclopedia of Polymer Science and Engineering" John Wiley and Sons: New York, 1985; Vol. 10; pp 541.
- (26) Reynolds, J. R.; Lillya, C. P.; Chien, J. C. W. *Macromolecules* **1987**, *20*, 541.
- (27) Vicente, R.; Ribas, J.; Cassoux, P.; Valade, L. *Synth. Met.* **1986**, *13*, 265.
- (28) Dirk, C. W.; Bosseau, M.; Barrett, P. H.; Moraes, F.; Wudl, F.; Heeger, A. J. *Macromolecules* **1986**, *19*, 266.
- (29) Alcacer, L.; Novais, H. in "Extended Linear Chain Compounds" Plenum Press: New York, 1983; Vol. 3; pp 319.
- (30) Tanaka, K.; Ohzeki, K.; Yamabe, T.; Yata, S. *Synth. Met.* **1984**, *9*, 41.
- (31) Kiji, J.; Iwamoto, M. *J. Polym. Sci. Polym. Lett. Ed.* **1968**, *6*, 53.
- (32) Bohlmann, F.; Inhoffen, E. *Chem. Ber.* **1956**, *89*, 1276.
- (33) Martinez, F.; Voelkel, R.; Naegele, D.; Naarmann, H. *Mol. Cryst. Liq. Cryst.* **1989**, *167*, 227.

- (34) Kagan, J.; Arora, S. K. *J. Org. Chem.* **1983**, *48*, 4317.
- (35) Kagan, J.; Arora, S. K. *Heterocycles* **1983**, *20*, 1937.
- (36) Kagan, J.; Arora, S. K. *Tetrahedron Lett.* **1983**, *24*, 4043.
- (37) Fichou, D.; Horowitz, G.; Nishikitani, Y.; Roncali, J.; Garnier, F. *Synth. Met.* **1989**, *28*, C729.
- (38) Fichou, D.; Horowitz, G.; Nishikitani, Y.; Garnier, F. *Synth. Met.* **1989**, *28*, C723.
- (39) Garnier, F.; Horowitz, G.; Fichou, D. *Synth. Met.* **1989**, *28*, C705.
- (40) Bauerle, P.; Segelbacher, U.; Gaudl, K.-U.; Huttenlocher, D.; Mehring, M. *Angew. Chem. Int. Ed. Engl.* **1993**, *32*, 76.
- (41) Havinga, E. E.; Rotte, I.; Meijer, E. W.; Ten Hoeve, W.; Wynberg, H. *Synth. Met.* **1991**, *41-43*, 473.
- (42) Paul, E. W.; Ricco, A. J.; Wrighton, M. S. *J. Phys. Chem.* **1985**, *89*, 1441.
- (43) Natan, M. J.; Wrighton, M. S. in "Progress in Inorganic Chemistry"; S. J. Lippard, Ed.; John Wiley and Sons: New York, 1989; Vol. 37.
- (44) Kittlesen, G. P.; White, H. S.; Wrighton, M. S. *J. Am. Chem. Soc.* **1984**, *106*, 7389.
- (45) Thackerey, J. W.; White, H. S.; Wrighton, M. S. *J. Phys. Chem.* **1985**, *89*, 5133.
- (46) Ofer, D.; Wrighton, M. S. *J. Am. Chem. Soc.* **1988**, *110*, 4467.
- (47) Ofer, D.; Crooks, R. M.; Wrighton, M. S. *J. Am. Chem. Soc.* **1990**, *112*, 7869.
- (48) Ofer, D.; Park, L. Y.; Wrighton, M. S.; Schrock, R. R. *Chem. Mater.* **1991**, *3*, 573.
- (49) Park, L. Y.; Ofer, D.; Gardner, T. J.; Schrock, R. R.; Wrighton, M. S. *Chem. Mater.* **1992**, *4*, 1388.

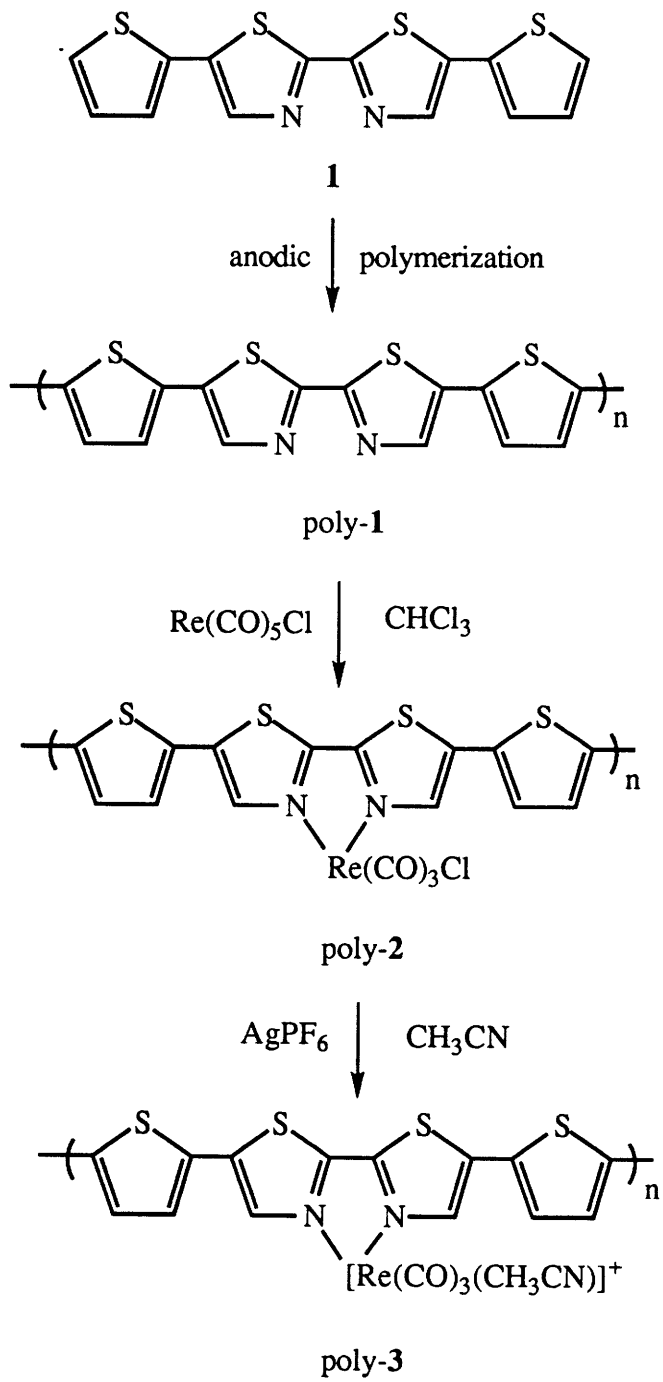
## Chapter 2

Tunable Electron Density at a Rhenium Carbonyl Complex Coordinated to the Conducting  
Polymer Poly[5,5'-(2-thienyl)-2,2'-bithiazole]

In this chapter the synthesis and properties of a novel conducting polymer, poly-**1**, prepared by anodic electropolymerization of 5,5'-(2-thienyl)-2,2'-bithiazole, **1** and subsequent reaction of the polymer to incorporate a cationic Re center, Scheme I are discussed. By incorporating a metal center into a conducting polymer so that the metal is coordinated to the conjugated backbone, we hoped to be able to demonstrate modulation of the electron density at the metal by varying the redox state of the polymer. We have been interested in organometallic complexes containing redox-active ligands because changing the oxidation state of such a ligand affects the properties and reactivity of the metal center.<sup>1-3</sup> By using a conducting polymer as the ligand, we have a continuous progression of "oxidation states" accessible to us, since changing the redox state by gradual oxidation of the polymer results in the charge being delocalized, at least partially, over the polymer backbone.<sup>4</sup>

Tuning the properties and reactivity of metal centers by changing the electronic properties of ligands is common.<sup>1-3</sup> However, such changes are inevitably a combination of both steric and electronic changes, and these factors are difficult to separate. Redox-active ligands may be used to tune properties with only small changes in sterics at the metal center. Moreover, these ligands permit *in situ* tuning by accessing the different redox states using electrochemical techniques. We have shown previously that changes in the oxidation state of a ferrocene pendant to a Re carbonyl complex affects the carbonyl stretching frequency in the infrared region.<sup>5</sup> The shifts obtained range from 2 to 33 cm<sup>-1</sup> depending on the proximity and number of bonds separating the ferrocene and the metal center. Other workers have also demonstrated carbonyl shifts upon oxidation or reduction of a redox-active ligand.<sup>6-14</sup> Recently, we have demonstrated that changing the oxidation state of a pendant cobaltocene containing ligand on a Re carbonyl complex causes changes in the rate of a nucleophilic reaction at the carbonyl groups in the complex.<sup>15</sup>

Scheme I.



In this chapter we establish that oxidation of poly-3 results in electron density changes at the Re center. Importantly, these changes are reversible upon returning the polymer to its neutral state. We chose the cationic Re species to demonstrate this effect for several reasons. The preparation of the complexes is straightforward, and they are inert to oxygen and substitution reactions. Moreover, the metal center in these complexes is not oxidized in the potential range where the polymer is expected to be conducting, allowing investigation of the consequences of changes in the state of charge of the conducting polymer ligand. Additionally, the carbonyl ligands provide an infrared handle by which the changes in electron density at the metal center can be monitored.<sup>5</sup>

In order to introduce the metal center as close to the conjugated backbone as possible, we chose a derivative of the previously characterized Re complexes containing 2,2'-bipyridine as a ligand.<sup>16,17</sup> In this respect a ligand based on 2,2'-bithiazole was attractive, because this compound has the same structural basis as 2,2'-bithiophene which can be used as a precursor to polythiophene, yet it also contains an  $\alpha$ -diimine ligating site analogous to 2,2'-bipyridine. Conducting polymers<sup>18-23</sup> and oligomers<sup>24</sup> containing bound transition metal complexes have been previously prepared; however, in most of these systems the metals are too easily oxidized and are not stable when oxidized, or the metals are too remote from the backbone of the polymer to be substantially affected by the redox changes in the polymer.

Electrochemical polymerization of thiazole and 4,4'-dimethyl-2,2'-bithiazole has been attempted,<sup>25,26</sup> but the resulting materials are poorly conducting. The electropolymerization of monomers such as 1,4-(2'-thienyl)benzene, 2,5-(2'-thienyl)pyridine or 2,5-(2'-thienyl)thiazole has been shown to yield polymers which are conducting.<sup>27</sup> These results provide evidence that aromatic groups that do not readily electropolymerize by themselves can be incorporated into conducting polymers by using a monomer in which the aromatic group is inserted between two thiophene groups.

## Results and Discussion

**Preparation and Characterization of Poly-1.** The simplest polymer incorporating 2,2'-bithiazolyl units is poly-5,5'-(2,2'-bithiazole). Unfortunately, previous attempts to electropolymerize both thiazole and 4,4'-dimethyl-2,2'-bithiazole were unsuccessful.<sup>25,26</sup> Polythiazole was prepared chemically from 2,5-dibromothiazole using a Grignard coupling, but the measured conductivity of the material after doping was very low ( $10^{-7}$  -  $10^{-8} \Omega^{-1}\text{cm}^{-1}$ ).<sup>25</sup> We attempted to electropolymerize 2,2'-bithiazole but were unsuccessful. Although anodic current was observed, no polymer deposited on the electrode. Hence, it became necessary to synthesize modified bithiazoles from which polymers could be prepared. To this end we prepared 5,5'-(2-thienyl)-2,2'-bithiazole, **1** prepared as shown in Scheme II. **1** has an intense absorption band with  $\lambda_{\text{max}} = 400 \text{ nm}$  ( $\epsilon = 35,000 \text{ M}^{-1}\text{cm}^{-1}$ ), and strong, short-lived ( $< 10 \text{ ns}$ ) fluorescence showing vibrational structure, Figure 1.

**1** can be electropolymerized from a  $\text{CH}_2\text{Cl}_2$  solution at +1.5 V vs. Ag wire. The deposited films are black when oxidized and become red upon stepping the electrode back to 0 V. The films are insoluble in  $\text{CH}_2\text{Cl}_2$  or  $\text{CH}_3\text{CN}$  and were characterized by cyclic voltammetry in 0.1 M [*n*-Bu<sub>4</sub>N]PF<sub>6</sub>/ $\text{CH}_2\text{Cl}_2$ , Figure 2a. The films are durable to oxidative cycling between 0 and +1.4 V, and the cyclic voltammogram has the broad reversible appearance typical of the polythiophene class of conducting polymers.<sup>4,28</sup> Although both  $\text{CH}_3\text{CN}$  and propylene carbonate were tried as electrochemical solvents, neither solvent was suitable for characterization of the films, as degradation of the oxidized film was very rapid in these media. For example, in  $\text{CH}_3\text{CN}$  the cyclic voltammogram disappeared completely after one scan to +1.5 V.

Microelectrode devices developed in these laboratories may be used for *in situ* potential dependent measurement of the conductivities of electropolymerized polymer films. This method has been described previously for the measurement of the conductivities of polythiophene, polypyrrole and polyacetylene films.<sup>28-30</sup> Using this technique we



## Scheme II

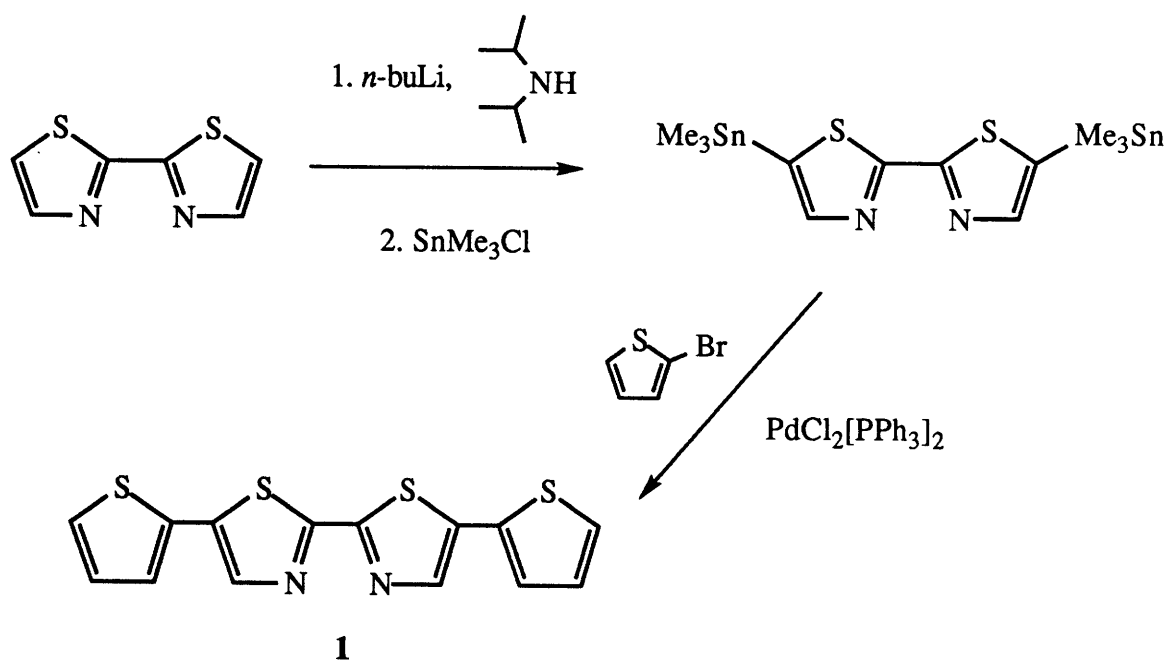


**Figure 1.** Absorption and emission spectra of **1**.

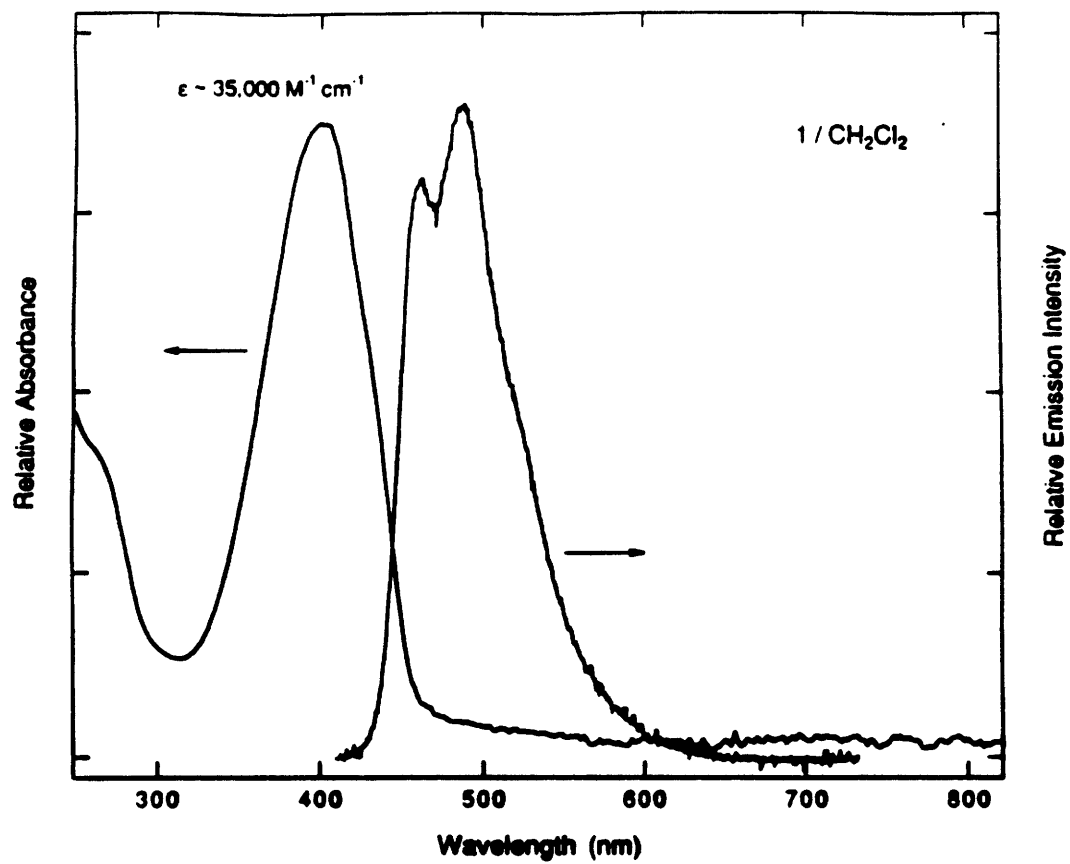
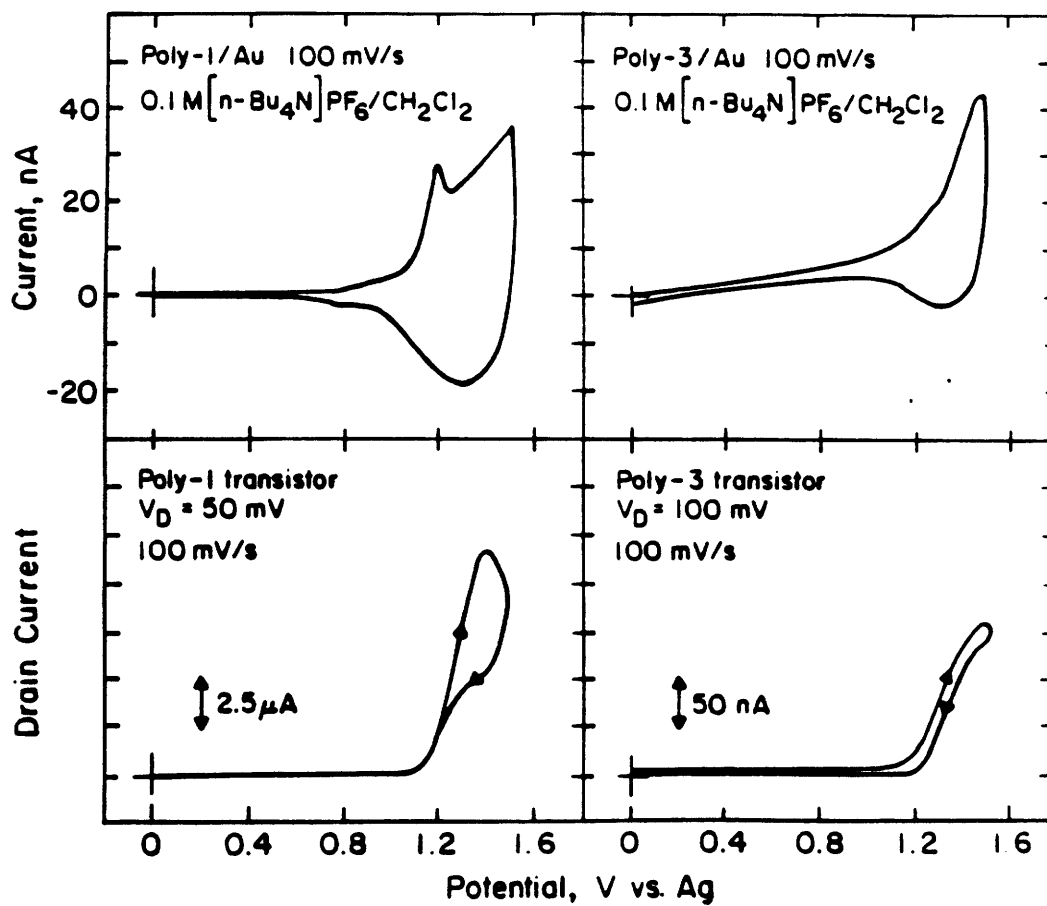


**Figure 2.** (a) Cyclic voltammogram of a film of poly-1 on Au microelectrodes, in 0.1 M  $[n\text{-Bu}_4\text{N}]\text{PF}_6/\text{CH}_2\text{Cl}_2$  at 100 mV/s. (b)  $I_D\text{-}V_G$  of poly-1 on Au microelectrodes with  $V_D = 50$  mV at 100 mV/s. (c) Cyclic voltammogram of a film of poly-3 on Au microelectrodes, in 0.1 M  $[n\text{-Bu}_4\text{N}]\text{PF}_6/\text{CH}_2\text{Cl}_2$  at 100 mV/s. (d)  $I_D\text{-}V_G$  of poly-3 on Au microelectrodes with  $V_D = 100$  mV at 100 mV/s. Note the different current scales in (b) and (d).



measured the drain current,  $I_D$ , as a function of gate potential,  $V_G$ , for electropolymerized films of poly-1. The drain current flows between the "source" and "drain" microelectrodes when the sample is conducting due to the small applied drain voltage,  $V_D$ . The drain current is proportional to the conductivity of the polymer at a given potential; hence we are able to examine the conductivity of poly-1 as a function of potential, Figure 2b. The polymer becomes conducting at a gate potential of +1.1 V, and the conductivity reaches a maximum at +1.5 V vs. Ag. At this maximum the conductivity is approximately  $0.2 \Omega^{-1}\text{cm}^{-1}$ . In comparison, polythiophene becomes conducting at approximately +0.75 V vs. Ag.<sup>28</sup> The shift to more positive potentials in both the  $I_D$ - $V_G$  and cyclic voltammogram of poly-1 vs. polythiophene is attributed to the electron withdrawing nature of the nitrogen in the thiazole rings.

The transport of charge carriers in conducting polymers containing more than one type of heterocycle (in poly-1 both bithiazole and thiophene moieties) may differ from that in conducting polymers in which the backbone contains only one type of heterocycle. In poly-1, the bithiazole unit may present an energy barrier which charge carriers must overcome. Poly-1 is only moderately conducting, compared to polythiophene, suggesting that the bithiazole/bithiophene alternation in the backbone gives rise to the lower conductivity of poly-1. We studied the temperature dependence of the conductivity of poly-1, in order to measure the activation energy for conductivity. Because of the reactivity of highly oxidized films of poly-1, it was only possible to study a partially oxidized film. We find that the conductivity of a film of poly-1 increased with increasing temperature. A plot of  $\log \sigma$  as a function of  $1/T$  plot is linear over the temperature range studied (213 -298 K), and the activation energy,  $E_A$ , obtained from the slope of this plot is 0.25 eV, Figure 3. Undoped, electrochemically synthesized polythiophene is reported to have an  $E_A$  of 0.36 eV, whereas the doped material has  $E_A = 0.023$  eV.<sup>4</sup> The sample we examined was oxidized to approximately 50% of the oxidation level at maximum conductivity, yet  $E_A$  is close to that measured for undoped polythiophene.

**UV/vis Spectroelectrochemistry of Poly-1.** Spectral changes in the visible part of the spectrum upon oxidation of conducting polymers are well documented.<sup>31</sup> Typically, a broad band in the infrared replaces the high-energy  $\pi-\pi^*$  absorption upon oxidation. The UV/vis spectrum of a film of poly-1 which was electrochemically oxidized in 0.1 M [*n*-Bu<sub>4</sub>N]PF<sub>6</sub>/CH<sub>2</sub>Cl<sub>2</sub> to +1.5 V vs. Ag, Figure 4b, shows that the  $\pi-\pi^*$  absorption of the neutral film, Figure 4a, is reduced in intensity, and a low-energy absorption appears. There is residual absorption in the 400-600 nm range suggesting incomplete oxidation. When the potential of the film is returned to 0 V vs. Ag, Figure 4c, the original absorption band reappears, although there is more absorption at the low-energy end of the spectrum than previously. We attribute this to decomposition of the film when oxidized, consistent with the electrochemical results.

**Derivatization of Poly-1.** Electropolymerized films of poly-1 react readily with Re(CO)<sub>5</sub>Cl to give poly-2 under mild conditions. Immersion in a refluxing CHCl<sub>3</sub> solution of the Re reagent for 5 minutes yields derivatized films. The Re complexes (2,2'-bithiazole)Re(CO)<sub>3</sub>Cl, **4** and (2,2'-bithiazole)Re(CO)<sub>3</sub>(CH<sub>3</sub>CN)PF<sub>6</sub>, **5** were prepared in order to compare their electrochemical and spectroscopic properties, Table I, to those of the analogous polymer confined complexes. Complexes **4** and **5** were prepared in a manner similar to that reported for the analogous (2,2'-bipyridine)Re(CO)<sub>3</sub>Cl and [(2,2'-bipyridine)Re(CO)<sub>3</sub>(CH<sub>3</sub>CN)]<sup>+</sup> complexes by reaction of 2,2'-bithiazole with Re(CO)<sub>5</sub>Cl followed by reaction with AgPF<sub>6</sub>, Scheme III.<sup>16,17</sup> Attempted reaction of 2,2'-bithiophene with Re(CO)<sub>5</sub>Cl under the same conditions yielded only starting materials, supporting the proposal that the 2,2'-bithiazole is not ligated in a *S,S*- fashion. The <sup>1</sup>H NMR spectrum of **4** shows only two resonances (8.35 and 8.25 ppm) suggesting that the 2,2'-bithiazole is bound symmetrically and ruling out the possibility of a *N,S*-bound complex. 2,2'-bithiazole has been previously used as a ligand and in iridium and

**Figure 3.** Temperature dependence of the conductivity of a partially oxidized film of poly-1. Inset: Log conductivity vs.  $1/T$  for the same data.



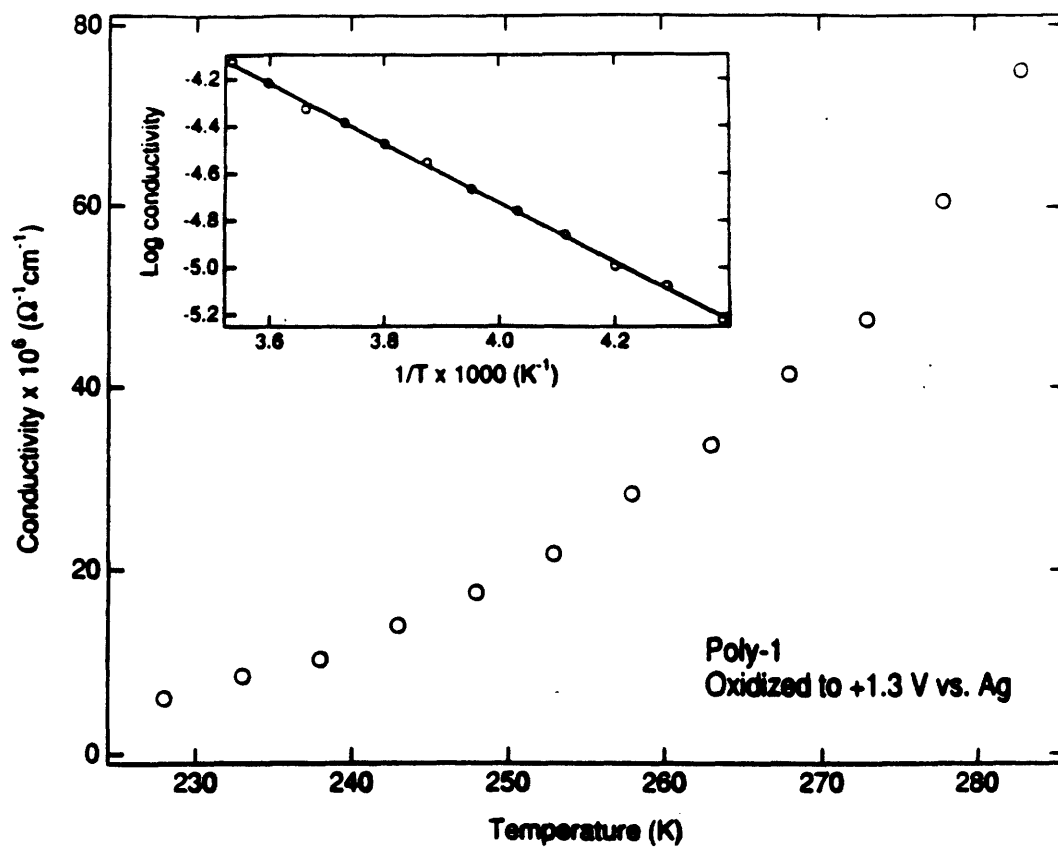


**Figure 4.** (a) UV-vis spectrum of poly-1 on ITO/glass. (b) UV-vis spectrum of poly-1 held at + 1.5 V vs. Ag. (c) UV-vis spectrum of poly-1 returned to 0 V vs. Ag.

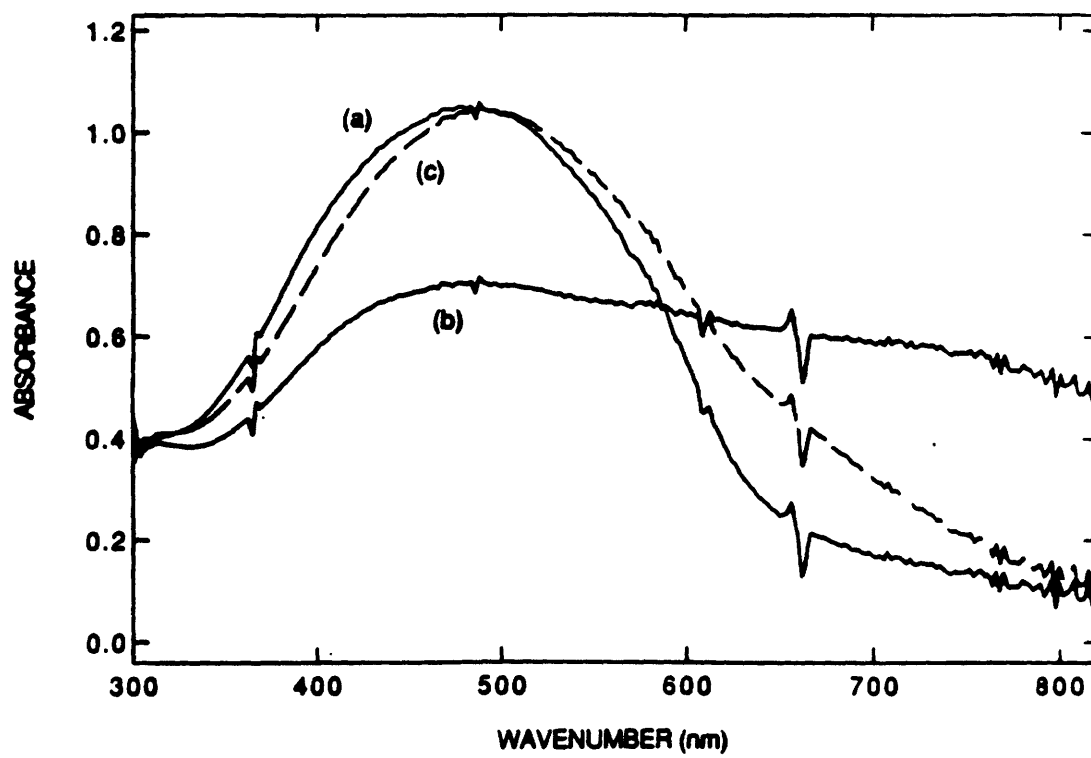
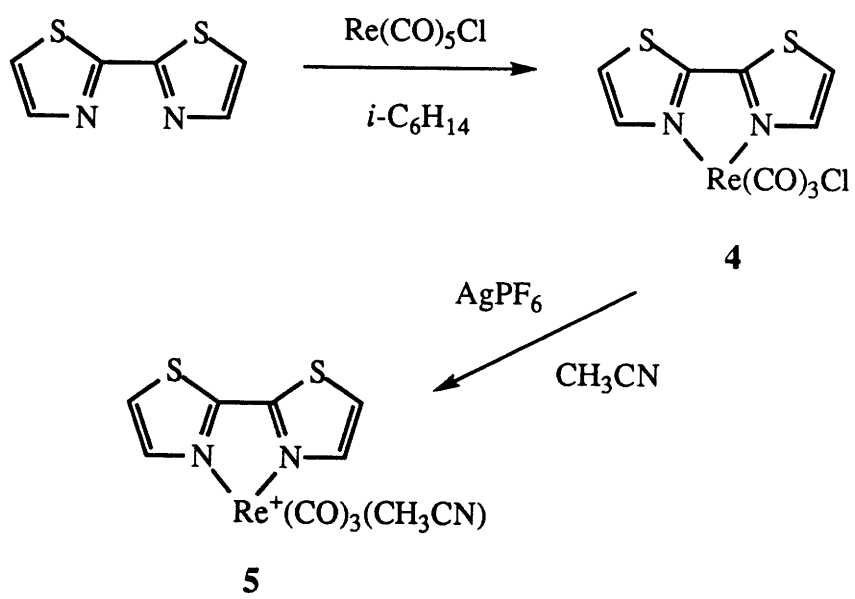


**Table I.** Electrochemical and Infrared Spectral Data in the CO Stretching Region for 2,2'-Bithiazole and 2,2'-Bipyridine complexes.

Complex	IR Bands (cm <sup>-1</sup> )	E <sub>PA</sub> (E <sub>1/2</sub> ) (V)	E <sub>PC</sub> (E <sub>1/2</sub> ) (V)
(2,2'-bithiazole)Re(CO) <sub>3</sub> Cl, <b>4</b>	2026; 1926; 1901 <sup>a</sup>	+1.38 <sup>b</sup>	(-1.11)
(2,2'-bipyridine)Re(CO) <sub>3</sub> Cl	2025; 1923; 1896 <sup>c,d</sup>	+1.35 <sup>e,f</sup>	(-1.41)
[(2,2'-bithiazole)-Re(CO) <sub>3</sub> (CH <sub>3</sub> CN)] <sup>+</sup> , <b>5</b>	2044; 1944 <sup>a</sup>	(+1.77) <sup>b</sup>	(-1.00); -1.35
[(2,2'-bipyridine)-Re(CO) <sub>3</sub> (CH <sub>3</sub> CN)] <sup>+</sup>	2032; 1942 <sup>a,g</sup>	(+1.77) <sup>g,h</sup>	(-1.25)

<sup>a</sup> CH<sub>2</sub>Cl<sub>2</sub>. <sup>b</sup> 0.1 M [*n*-Bu<sub>4</sub>N]PF<sub>6</sub>/CH<sub>3</sub>CN vs. SCE. <sup>c</sup> CHCl<sub>3</sub>. <sup>d</sup> Reference 32. <sup>e</sup> 0.1 M [*n*-Bu<sub>4</sub>N]PF<sub>6</sub>/CH<sub>3</sub>CN vs. SCE. <sup>f</sup> Reference 17. <sup>g</sup> Reference 33. <sup>h</sup> 0.1 M [*n*-Et<sub>4</sub>N]ClO<sub>4</sub>/CH<sub>3</sub>CN vs. SSCE.

## Scheme III



rhodium complexes has been demonstrated to ligate through the two nitrogen atoms.<sup>34</sup> Films of poly-2 were analyzed by surface reflectance IR and X-ray photoelectron spectroscopy (XPS) to confirm that the reaction took place. The surface reflectance IR spectrum of a film of poly-2 in the carbonyl stretching region clearly confirms that the Re is coordinated to the available bithiazole sites in the polymer in a manner analogous to that in 4, Figure 5a and 5b. The peak positions of the metal carbonyl bands are close to those observed in solution for 4. The IR spectrum shows no evidence of residual  $\text{Re}(\text{CO})_5\text{Cl}$  in the film.

The XPS spectrum of a poly-2 film contains peaks which are assigned to Re and Cl in addition to the C, N and S observed in XPS spectra of films of poly-1, Figure 6. By comparison of the integrated areas of the Re 4f peaks with the areas of the S and N peaks in the XPS spectrum of poly-2, it is possible to calculate the extent that 2,2'-bithiazole sites in the polymer have reacted with  $\text{Re}(\text{CO})_5\text{Cl}$ . This comparison shows that the amount of Re remains the same whether reaction was stopped after 5 min. or 30 min. However, the ratio of Re to N indicates that only 60-75% of the available reaction sites are occupied by Re. In addition, we were able to use the N 1s peaks to verify the extent of reaction with  $\text{Re}(\text{CO})_5\text{Cl}$ . The N 1s peak appears at 399 eV in the spectrum of poly-1. After the film is reacted with  $\text{Re}(\text{CO})_5\text{Cl}$  the N 1s splits into two distinct peaks, one at 399 eV, which we assign to N in unreacted 2,2'-bithiazolyl groups, and one at 400 eV assigned to N in groups which had reacted with the  $[\text{Re}(\text{CO})_3\text{Cl}]$  moiety. The N 1s peak in the XPS spectrum of a thin-film of 4 on Au appears at 400 eV. The integrated areas of the two N peaks for poly-2 indicates that approximately 60% of the N at the surface of the sample has reacted in good accord with the conclusion drawn from the Re/N ratio.

Poly-2 can be converted quantitatively to poly-3 by reaction of the polymer film with a solution of refluxing  $\text{AgPF}_6$  in  $\text{CH}_3\text{CN}$  for 1 h, Scheme I. Surface reflectance IR of a film of poly-3, shown in Figure 5c, demonstrates that complete conversion to the cationic Re occurs. The correspondence between the characteristic carbonyl bands of 5, shown in

**Figure 5.** (a) Surface reflectance FTIR spectrum of CO stretching region of a film of poly-2 on Pt. (b) IR of the same region of a CH<sub>2</sub>Cl<sub>2</sub> solution of 4. (c) Surface reflectance FTIR spectrum of CO stretching region of a film of poly-3 on Pt. (d) IR of the same region of a CH<sub>2</sub>Cl<sub>2</sub> solution of 5.

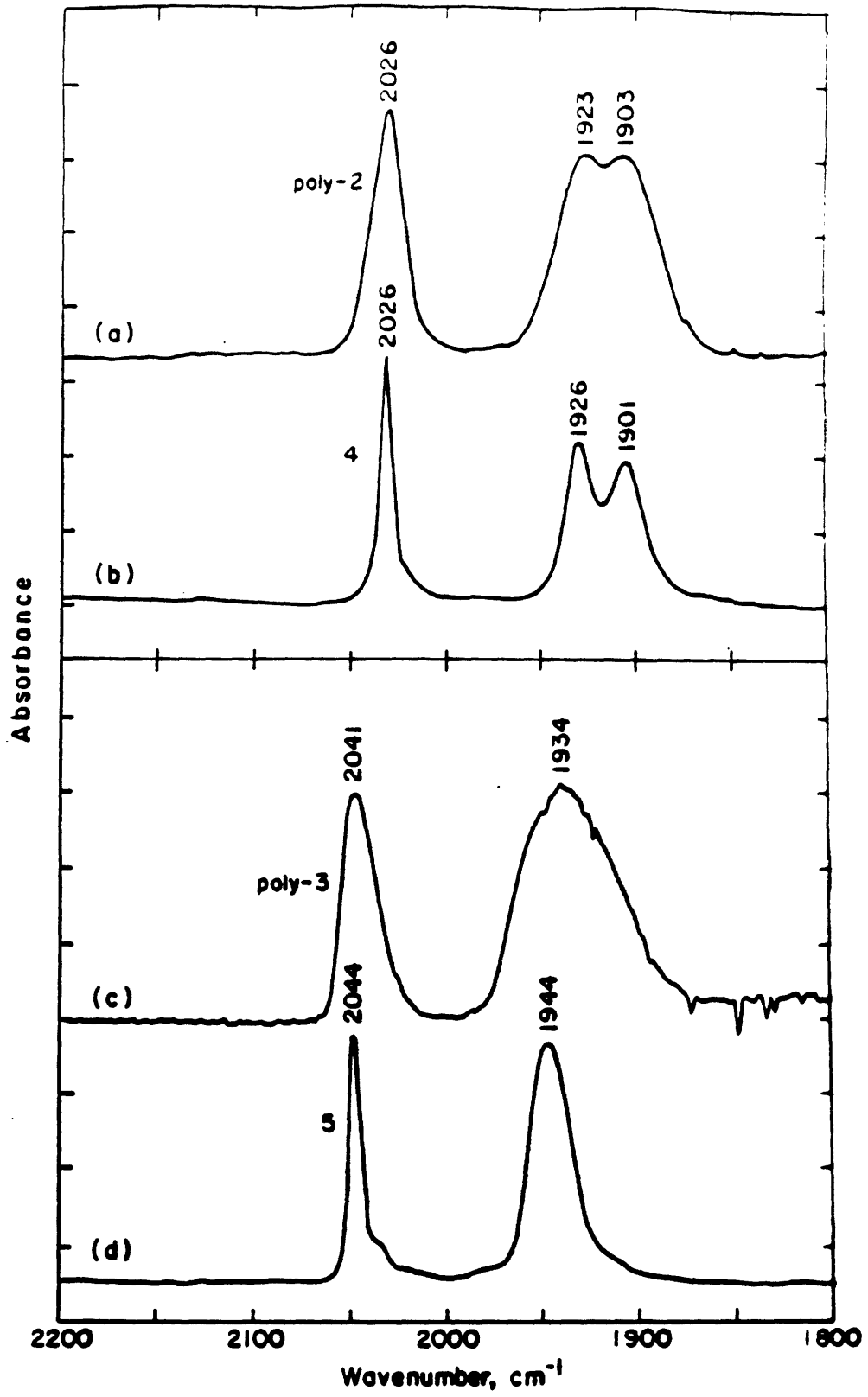




**Figure 6.** XPS survey scan of (a) poly-1 on Pt; (b) poly-2 on Pt; (c) poly-3 on Pt.

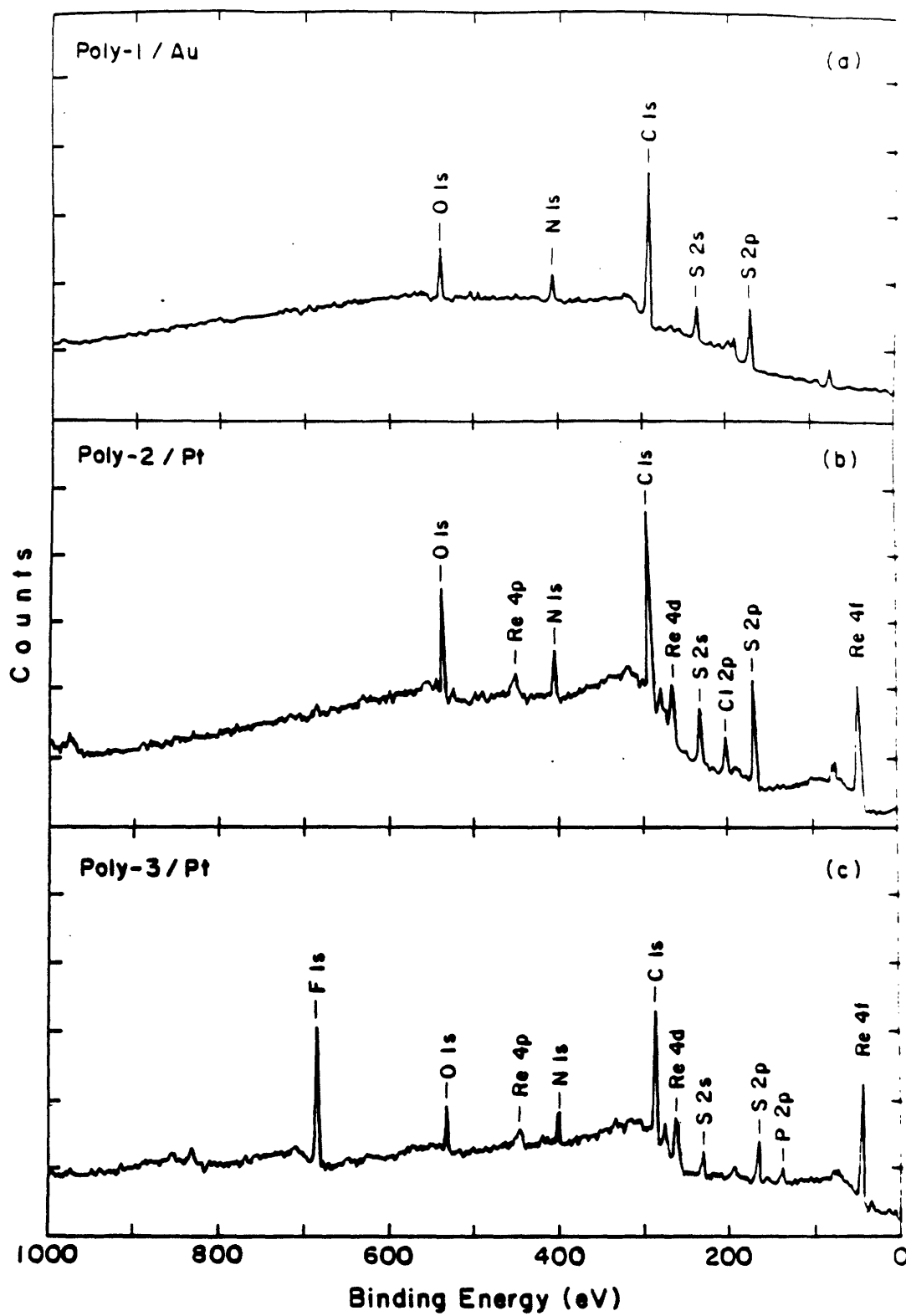


Figure 5d, and the IR spectrum of poly-3 in the CO stretching region confirms the binding mode of the Re. XPS analysis of a film of poly-3 confirms the presence of Re, S, N as well as the unique elements F and P, Figure 6c.

The sequence of reactions to make poly-3 may also be followed by UV-vis spectroscopy. The spectrum of poly-1 contains a broad peak with  $\lambda_{\text{max}} = 510$  nm, Figure 7a. Upon reaction with  $\text{Re}(\text{CO})_5\text{Cl}$  to give poly-2, the maximum in the absorbance spectrum shifts to 530 nm, Figure 7b. The shift in the maximum is the result of the overlap of the polymer absorption band and a low energy Re→LCT band. In **4** the Re→LCT is found at 412 nm, and the extended conjugation in poly-2 should shift this band to lower energy. Reaction of poly-2 with  $\text{AgPF}_6$  to give poly-3 results in a shift in  $\lambda_{\text{max}}$  back to 510 nm and the development of a shoulder at approximately 400 nm, Figure 7c. We assign the band at 510 nm to the  $\pi-\pi^*$  of the polymer backbone, and the band at 400 nm to the Re→LCT. The absorption spectrum of **5** has a peak at 336 nm with no lower energy peaks present, so in this complex the Re→LCT band must be shifted to higher energy compared to **4**. In the polymer confined complex, the extended conjugation is expected to shift this Re→LCT to lower energy than in **4**, therefore it is reasonable that the band would appear at 400 nm.

**Electrochemistry of Complexes 4 and 5.** The cyclic voltammetry of **4** in 0.1 M [*n*-Bu<sub>4</sub>N]PF<sub>6</sub> / CH<sub>3</sub>CN is shown in Figure 8a. There is no evidence for electropolymerization in the potential region examined (-1.4 V to 2.0 V vs. SCE). However, two waves are present, an irreversible oxidation wave and a reversible reduction wave at +1.38 V and -1.11 V vs. SCE respectively, Table I. This electrochemical behavior is very similar to that observed for other ( $\alpha$ -diimine)Re(CO)<sub>3</sub>X (X=halide) species such as (2,2'-bipyridine)Re(CO)<sub>3</sub>Cl, both in the reversibility and potentials of the waves.<sup>17</sup>

The cyclic voltammetry of **5** in 0.1 M [*n*-Bu<sub>4</sub>N]PF<sub>6</sub> / CH<sub>3</sub>CN is shown in Figure 8c. We observe a reversible oxidation (+1.77 V vs. SCE) and two reduction waves (-1.00

**Figure 7.** (a) UV-vis spectrum of a film of poly-1 on ITO/glass. (b) UV-vis spectrum of a film of poly-2 on ITO/glass. (c) UV-vis spectrum of a film of poly-3 on ITO/glass.

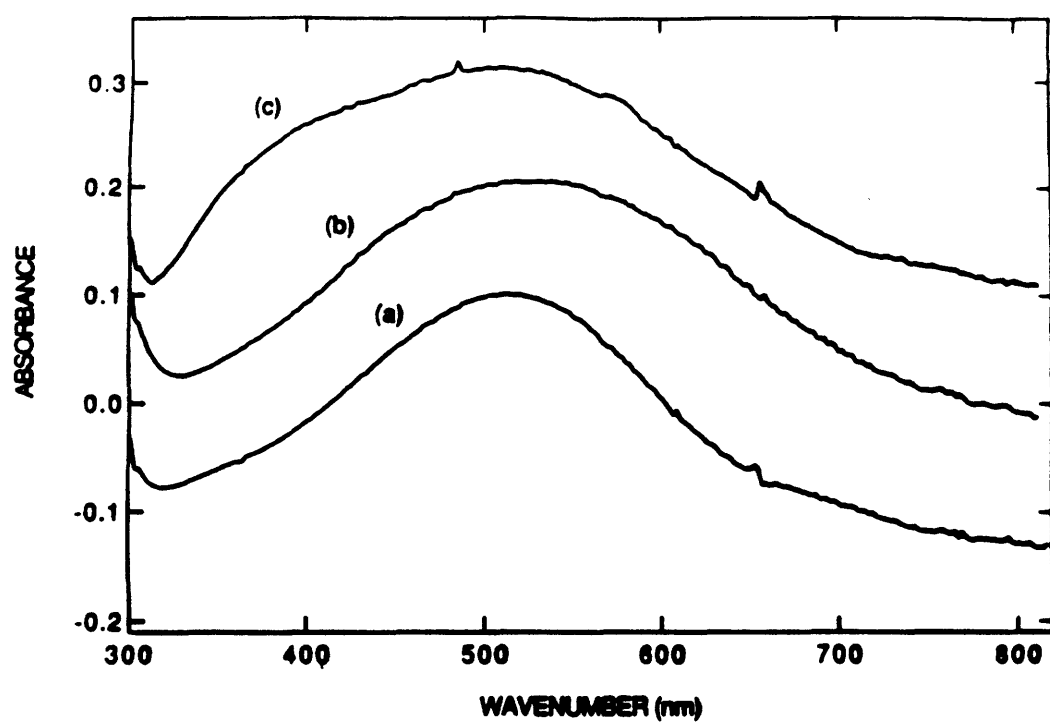
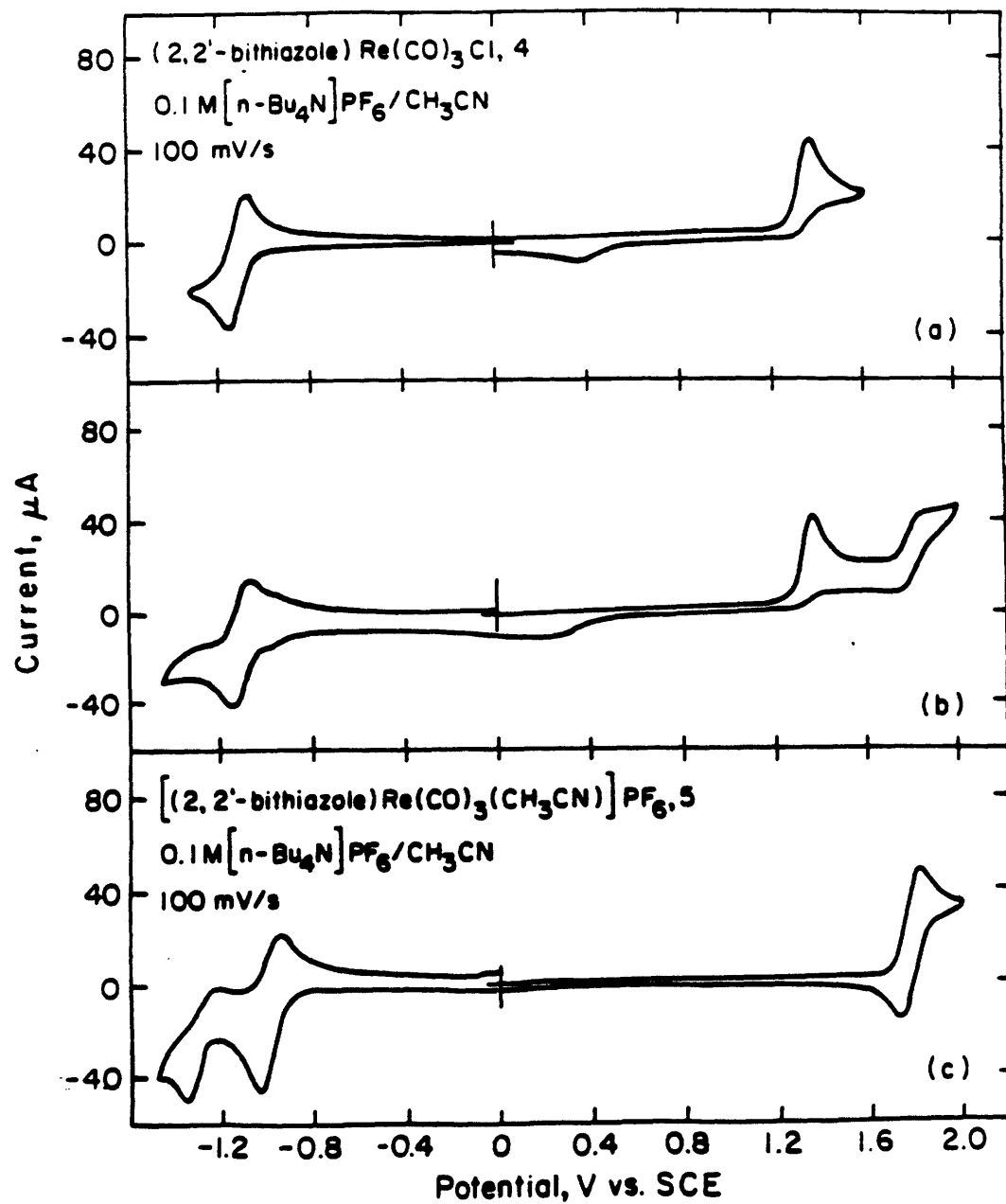


**Figure 8.** (a) Cyclic voltammogram of (2,2'-bithiazole)Re(CO)<sub>3</sub>Cl, **4** in 0.1 M [*n*-Bu<sub>4</sub>N]PF<sub>6</sub>/CH<sub>3</sub>CN at 100 mV/s. (b) Same solution scanning to +2.0 V vs. SCE. (c) Cyclic voltammogram of [(2,2'-bithiazole)Re(CO)<sub>3</sub>(CH<sub>3</sub>CN)]<sup>+</sup>, **5** in 0.1 M [*n*-Bu<sub>4</sub>N]PF<sub>6</sub>/CH<sub>3</sub>CN at 100 mV/s.



and -1.35 V vs. SCE). The first reduction wave is reversible when the scan was reversed at -1.2 V; the second reduction was irreversible even at a high scan rate. We also found that if we scan positive of the irreversible oxidation of **4** we find a smaller reversible oxidation with  $E_{1/2} = +1.81$  V vs. SCE, (Figure 8b). This wave corresponds closely to the cyclic voltammogram observed for **5**. We conclude that **4** is oxidized electrochemically to a species which loses Cl to give **5** in CH<sub>3</sub>CN solution, analogous to the behavior of (2,2'-bipyridine)Re(CO)<sub>3</sub>Cl upon electrochemical oxidation.<sup>17</sup>

The similarities between the electrochemical and spectroscopic characteristics of the 2,2'-bithiazolyl and 2,2'-bipyridyl complexes are great enough that they can be considered analogs for most purposes. Importantly, the cationic Re species **5** is difficult to oxidize, and hence should not interfere with the oxidative doping of a conducting polymer to which it is pendant, provided that the potential region in which the polymer is conducting is < +1.6 V vs. SCE.

**Electrochemistry of Poly-2 and Poly-3.** Characterization of the films of poly-2 by cyclic voltammetry is difficult, because the potential region in which the polymer is oxidized overlaps with the region where the Re is expected to be oxidized, based on the cyclic voltammetry studies on the model complex **4**. Holding the poly-2 film for several minutes at +1.8 V vs. Ag, a potential at which we expect the Re to be oxidized, causes the growth of carbonyl bands in the IR region the same as those observed for the cationic complex **5**. In addition, XPS analysis of a film which was subjected to the same procedure showed the presence of F and P in the resulting film, additional evidence of conversion of the Re to a cationic center, with PF<sub>6</sub><sup>-</sup> from the electrolyte solution as counterion. However, the XPS results may be ambiguous since holding the films at such oxidizing potentials causes degradation of the polymer, rendering it non-conducting. For this reason, electrochemical oxidation cannot be used to quantitatively convert poly-2 to poly-3, and the reaction of poly-2 with AgPF<sub>6</sub> is therefore the preferred synthetic route to poly-3.



The cyclic voltammogram and  $I_D$ - $V_G$  plot<sup>28-30</sup> of poly-3 are shown in Figure 2c and 2d respectively. The cyclic voltammogram looks fundamentally the same as that of poly-1 although the small peak at +1.2 V is gone and the area under the curve is slightly reduced. The plot of the conductivity as a function of  $V_G$  indicates that the onset of conductivity is shifted slightly more positive than for poly-1, and the maximum drain current is about three order of magnitude less than for poly-1, corresponding to a peak conductivity of  $2 \times 10^{-3} \Omega^{-1}\text{cm}^{-1}$ . Incorporation of the Re cation into the film reduces the conductivity significantly compared to underivatized poly-1. Interestingly, poly-3 can be cycled to +1.5 V several times without any significant decrease in conductivity. The mechanism by which oxidized poly-1 degrades during electrochemical cycling to positive potentials may therefore involve the unprotected nitrogen atom. In poly-3 the nitrogen is "protected" by ligation with the Re and degradation by this mechanism is minimized.

**IR of Reduced and Oxidized Poly-3.** Electrochemical oxidation of the films of poly-3 on an electrode surface demonstrates that the electron density at the cationic Re center can be tuned as a function of the state of charge of the polymer backbone. Surface reflectance IR measurements on films of poly-3 which were oxidized to +1.5 V vs. Ag wire in 0.1 M  $[n\text{-Bu}_4\text{N}]\text{PF}_6/\text{CH}_2\text{Cl}_2$  and removed from solution under potential control shows that in the oxidized film the carbonyl stretching bands shift from 2040 to 2044  $\text{cm}^{-1}$  and from 1934 to 1940  $\text{cm}^{-1}$ . When the same film was returned to 0 V vs. Ag and the surface IR acquired the bands did not shift back completely to the original values; we attribute this to partial degradation of the oxidized film when removed from solution for an extended time. However, scanning a different sample to +1.5 V vs. Ag, holding at that potential for 30 s and returning the potential to 0 V, results in a film in which the IR bands remained at the original positions.

The magnitude of the shifts in the CO stretching frequencies upon oxidation of poly-3 is related to the extent of oxidation and charge distribution in the polymer ligand. Unlike the systems we have studied previously where the redox-active pendant group has

two discrete and well-defined states, the conducting polymer ligand system described in this work has an ill-defined structure in which the exact nature of the oxidized and reduced states is unclear. The shift in the carbonyl stretching frequencies upon oxidation represents the average effect on the system.

## Conclusions

A conducting polymer system containing 2,2'-bithiazole groups derivatized with  $[\text{Re}(\text{CO})_3(\text{CH}_3\text{CN})]^+$  groups has been described. The modified polymer is the first example of a conducting polymer system in which a metal complex has been attached using the polymer as a ligand and the metal moiety remains intact when the polymer is oxidized and conducting. This stability allowed us to study the electron density at the Re as a function of the state of charge of the polymer backbone. The electron density changes which we observed were small, as measured by a shift in the carbonyl stretching frequency, but this result is not entirely unexpected since even when the polymer is highly oxidized, the number of electrons removed per monomer unit is probably less than one, if we assume the level of oxidation is comparable to that observed in polythiophene derivatives.<sup>28</sup> Additionally, the alternating structure of the backbone may localize holes away from the bithiazolyl groups, lessening the effect of oxidation even further. Even though the observed effect is relatively small, it is important to note that oxidation of both ferrocene centers in  $(4\text{-ferrocenylpyridine})_2\text{Re}(\text{CO})_3\text{Cl}$  causes a shift of only 4-7  $\text{cm}^{-1}$  in the CO stretching frequencies.<sup>5</sup> This shift is probably close to what can be expected for poly-3 in which the backbone has one hole per monomer unit, even if the hole is more localized on the bithiophene unit. Small changes in electron density as a result of changes in the redox state of a pendant ligand have also been demonstrated to alter reactivity to a remarkable extent.<sup>15</sup> Shifts of only 15  $\text{cm}^{-1}$  in the carbonyl stretching frequency have been shown to result in differences of up to 200 times in the rate of nucleophilic attack at a carbonyl carbon in a Re carbonyl complex with a pendant chelating cobaltocene ligand.

This illustrates that the shifts in CO stretching frequency we observe upon oxidation of poly-3 could be significant in altering the rate of a reaction at the Re center.

## Experimental Section

**General.** All manipulations were carried out under air unless otherwise noted. Ether and THF were distilled from sodium benzophenone ketyl. Toluene was distilled from sodium. Chloroform and acetonitrile (Aldrich anhydrous) were used as received. Dichloromethane was distilled from P<sub>2</sub>O<sub>5</sub>. 2,2,4-trimethylpentane was spectrophotometric grade and was not purified. Solvents for chromatography were reagent grade and were not purified prior to use. <sup>1</sup>H NMR spectra were acquired on Varian XL-300 or Bruker AC-250 instruments. FTIR spectra were acquired on a Nicolet 60SX FTIR instrument. X-ray photoelectron spectra were obtained on a Surface Science Instruments Model SSX-100 spectrometer using monochromatic Al K $\alpha$  radiation and operating at 10<sup>-8</sup> Torr. A 1 mm spot size was used. Elemental analyses were performed by Oneida Research Services Inc.

2-Trimethylstannylthiazole<sup>35</sup> and 2,2'-bithiazole<sup>36</sup> were prepared as described in the literature.

**(2,2'-Bithiazole)Re(CO)<sub>3</sub>Cl (4).** 2,2'-Bithiazole (0.100 g, 5.94 mmol) and Re(CO)<sub>5</sub>Cl (0.215 g, 5.94 mmol) were added to 50 mL 2,2,4-trimethylpentane. The mixture was heated to reflux for 5 min. during which time the starting materials dissolved and an orange solid precipitated. This solid was collected on a frit and was washed with hot 2,2,4-trimethylpentane to remove any residual starting materials. The solid was then dissolved in CH<sub>2</sub>Cl<sub>2</sub> and reprecipitated by adding hexanes, yielding 0.236 g **4** (84%). <sup>1</sup>H NMR (acetone-d<sub>6</sub>):  $\delta$  8.35 (d, 3.4 Hz, 2H), 8.25 (d, 3.4 Hz, 2H). IR (CH<sub>2</sub>Cl<sub>2</sub>): 2028, 1926, 1902 cm<sup>-1</sup>. UV/vis: (THF) 412 (4700), 344 (16,000), 332 (19,000), 260 (11,000). MS: Anal. Calcd. for C, 22.81; H, 0.85; N, 5.91. Found: C, 22.75 ; H, 0.67 ; N, 5.88 . mp > 250 °C.

**(2,2'-Bithiazole)Re(CO)<sub>3</sub>(CH<sub>3</sub>CN)PF<sub>6</sub> (5).** A solution of (2,2'-bithiazole)Re(CO)<sub>3</sub>Cl (0.435 g, 0.918 mmol) dissolved in 50 mL acetonitrile was prepared and AgPF<sub>6</sub> (0.400 g, 1.58 mmol) was added. The mixture was refluxed in the dark for one hour and then cooled and filtered. The solvent was removed *in vacuo*, and the residual

solid dissolved in  $\text{CH}_2\text{Cl}_2$  and filtered through a Celite plug. The solvent was removed *in vacuo* and the solids dissolved in a minimal amount of  $\text{CH}_3\text{CN}$ . Ether was added to precipitate the product as a yellow solid which was collected on a frit yielding 0.184 g **5** (32%).  $^1\text{H NMR}$  (acetone- $d_6$ ):  $\delta$  8.35 (d, 3.4 Hz, 2H), 8.25 (d, 3.4 Hz, 2H). IR ( $\text{CH}_2\text{Cl}_2$ ): 2044, 1944  $\text{cm}^{-1}$ . UV/vis: (THF) 336 (18,000). Anal. Calcd. for  $\text{C}_{11}\text{H}_7\text{N}_3\text{O}_3\text{S}_2\text{PF}_6\text{Re}$ : C, 21.16; H, 1.13; N, 6.73. Found: C, 21.00; H, 1.04; N, 6.57. mp 202 °C.

**5,5'-trimethylstannyl-2,2'-bithiazole (6)**. A solution of diisopropylamine (1.3 mL, 17 mmol) in 10 mL THF was cooled to  $-78^\circ\text{C}$ . To this solution was added *n*-butyllithium (4.0 mL, 2.36-M in hexanes, 9.4 mmol) via syringe. The mixture was allowed to warm to room temperature for 5 min. and then re-cooled to  $-78^\circ\text{C}$ . 2,2'-Bithiazole (0.75 g, 4.4 mmol) in 10 mL THF was then added. A solid precipitated during the addition. The mixture was stirred at  $-78^\circ\text{C}$  for one hour and then trimethylstannylchloride (9.4 mL, 1.0 M in THF, 9.4 mmol) was added and the solution warmed to room temperature. Stirring was continued for 2 hours, after which time saturated  $\text{NaHCO}_3$  (50 mL) was added followed by addition of ether (100 mL) and subsequent extraction. The organic layer was separated and dried over anhydrous  $\text{MgSO}_4$ . The solvent was removed *in vacuo* and the resulting residue was washed with hexanes leaving a brown solid. The resulting solid was filtered yielding 1.4 g (63%) **6**.  $^1\text{H NMR}$  ( $\text{CDCl}_3$ ):  $\delta$  7.77 (s, 2 H), 0.41 (s, 18H). Anal. Calcd. for  $\text{C}_{12}\text{H}_{20}\text{N}_2\text{S}_2\text{Sn}_2$ : C, 29.19; H, 4.08; N, 5.67. Found: C, 29.00; H, 4.15; N, 5.80.

**5,5'-(2-thienyl)-2,2'-bithiazole (1)**. A solution of 2-bromothiophene (0.60 mL, 6.2 mmol), 5,5'-trimethylstannyl-2,2'-bithiazole (1.5 g, 3.0 mmol), and  $\text{PdCl}_2[\text{PPh}_3]_2$  (90 mg, 0.13 mmol) in 20 mL THF was prepared and refluxed for 12 hours. The solvent was removed *in vacuo*, and ether was added to the residual material. The resulting yellow solid was filtered off and washed well first with ether (100 mL) and then with hexanes (100 mL). The residue was then dissolved in  $\text{CH}_2\text{Cl}_2$  and filtered through a Celite pad,

followed by sublimation *in vacuo* to yield 0.14 g (14%) **1** as a bright yellow solid.  $^1\text{H}$  NMR ( $\text{CDCl}_3$ ):  $\delta$  7.89 (s, 2 H), 7.32 (d, 4.5 Hz, 2 H), 7.25 (d, 3.6 Hz, 2H), 7.06 (dd, 4.5 Hz and 3.6 Hz, 2H).  $^{13}\text{C}$  NMR ( $\text{CDCl}_3$ ):  $\delta$  159.3, 139.6, 134.7, 132.7, 128.2, 126.4, 126.3. UV/vis: (THF) 400 (35,000), 258 (29,000), mp 208 °C. HRMS:  $m/e$  331.9569 ( $\text{M}^+$  calcd. for  $\text{C}_{14}\text{H}_8\text{S}_4\text{N}_2$ : 331.95704).

**Electrochemistry.** All electrochemical measurements were conducted using a Pine RDE-4 bipotentiostat and a Kipp and Zonen XY recorder either in a nitrogen filled Vacuum Atmosphere drybox or in a sealed flask under argon. Dichloromethane was distilled from  $\text{P}_2\text{O}_5$  and stored in the drybox.  $[\textit{n}\text{-Bu}_4\text{N}]\text{PF}_6$  was recrystallized from ethanol and dried in a vacuum oven overnight. The reference electrode was either a silver wire or a saturated calomel electrode (SCE), and the counter electrode a 1  $\text{cm}^2$  piece of Pt gauze. The silver wire was referenced to the cobaltocene/cobaltocenium couple.

Anodic electropolymerizations were all conducted either on large 2 x 4 cm pieces of silicon wafers which had been coated with 1000 Å of Pt for specular reflectance spectroscopy and XPS measurements or on ITO/glass electrodes for UV/vis absorption spectroscopy. For potential dependent conductivity measurements Au microelectrode arrays were used.<sup>37,38</sup> The microelectrodes were cleaned by placing a drop of freshly prepared 3:1  $\text{H}_2\text{SO}_4$  / 30%  $\text{H}_2\text{O}_2$  on the electrode for 10 seconds, followed by characterization in 5 mM  $\text{Ru}(\text{NH}_3)_6$  aqueous solution.

The temperature dependent conductivity measurements were performed in a nitrogen atmosphere over the temperature range 25 °C to -60 °C. Polymer was deposited on a microelectrode array as above, oxidized to +1.4 V vs. Ag and the array was put in a narrow glass tube which was immersed into an isopropanol bath. The temperature of the bath was varied using a cold finger immersion cooler.

**Polymer preparation and derivatization.** 5,5'-(2-thienyl)-2,2'-bithiazole was electropolymerized anodically from 5-10 mM  $\text{CH}_2\text{Cl}_2$  solution containing 0.1 M  $[\textit{n}\text{-Bu}_4\text{N}]\text{PF}_6$ . The working electrode was held at +1.5 V vs. Ag wire for 3-4 minutes to

derivatize the surface with polymer. The resulting films were reacted with a solution of  $\text{Re}(\text{CO})_5\text{Cl}$  in  $\text{CHCl}_3$  by immersing the film in the refluxing solution for 3-4 minutes. To remove any residual  $\text{Re}(\text{CO})_5\text{Cl}$  the film was then washed by dipping several times in a refluxing  $\text{CHCl}_3$  solution. To generate the cationic Re species on the polymer, the derivatized film was refluxed in a  $\text{CH}_3\text{CN}$  solution containing  $\text{AgPF}_6$  for 1 hr. The film was then rinsed with hot  $\text{CH}_3\text{CN}$  to remove any residual  $\text{AgPF}_6$ .

**Spectroelectrochemistry.** The FTIR spectra of the neutral polymer films were acquired using a Spectra-Tech specular reflectance accessory. The IR spectra of the polymer film as a function of potential were acquired by holding the film at a given potential until the residual current is negligible, and then removing the film while still under potential control and taking the IR spectrum immediately.

**References.**

- (1) Bitterwolf, T. E. *Polyhedron* **1988**, *7*, 409.
- (2) Box, J. W.; Gray, G. M. *Inorg. Chem.* **1987**, *26*, 2774.
- (3) Tolman, C. A. *Chem. Rev.* **1977**, *77*, 313.
- (4) Tourillon, G. in "Handbook of Conducting Polymers"; T. A. Skotheim, Ed.; Marcel Dekker: New York, 1986; Vol. 1; pp 293.
- (5) Miller, T. M.; Ahmed, K.; Wrighton, M. S. *Inorg. Chem.* **1989**, *26*, 2347.
- (6) Elschenbroich, C.; Stohler, F. *Angew. Chem.; Int. Ed. Engl.* **1975**, *14*, 174.
- (7) Kotz, J. C.; Nivert, C. L. *J. Organomet. Chem.* **1973**, *52*, 387.
- (8) Kotz, J. C.; Nivert, C. L.; Lieber, J. M.; Reed, R. C. *J. Organomet. Chem.* **1975**, *91*, 87.
- (9) Rudie, A. W.; Lichtenberg, D. W.; Katcher, M. L.; Davison, A. *Inorg. Chem.* **1978**, *17*, 2859.
- (10) Colbron, S. B.; Robinson, B. H.; Simpson, J. *Organometallics* **1983**, *2*, 943.
- (11) Creager, S. E.; Murray, R. W. *Inorg. Chem.* **1987**, *26*, 2612.
- (12) Rieke, R. D.; Henry, W. P.; Arney, J. S. *Inorg. Chem.* **1987**, *26*, 420.
- (13) Kadish, K. M.; Tabard, A.; Zrineh, A.; Ferhat, M.; Guiland, R. *Inorg. Chem.* **1987**, *26*, 2459.
- (14) Shu, C. F.; Wrighton, M. S. *Inorg. Chem.* **1988**, *27*, 4326.
- (15) Lorkovic, I.; Wrighton, M. S. *submitted to J. Am. Chem. Soc.* **1993**,
- (16) Wrighton, M.; Morse, D. L. *J. Am. Chem. Soc.* **1974**, *96*, 998.
- (17) Luong, J. C.; Faltynek, R. A.; Wrighton, M. S. *J. Am. Chem. Soc.* **1980**, *102*, 7892.
- (18) Wright, M. E. *Macromolecules* **1989**, *22*, 3256.
- (19) Nishihara, H.; Funaki, H.; Shimura, T.; Aramaki, K. *Synth. Met.* **1993**, *55-57*, 942.
- (20) Munoz-Escalona, A.; Di Filippo, G. *Makromol. Chem.* **1977**, *178*, 659.

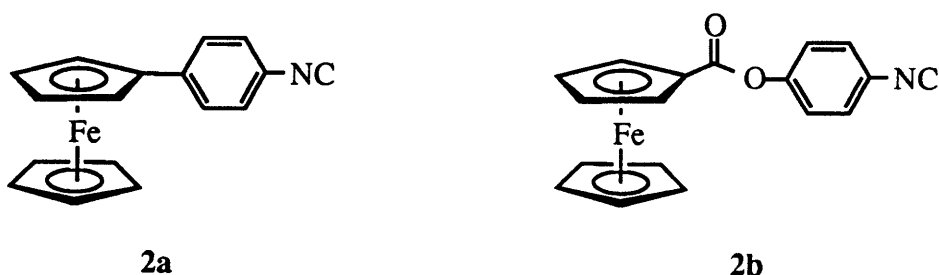


- (21) Mirrazaei, R.; Parker, D.; Munro, H. S. *Synth. Met.* **1989**, *30*, 265.
- (22) Eaves, J. G.; Munro, H. S.; Parker, D. *Inorg. Chem.* **1987**, *26*, 644.
- (23) Cosnier, S.; Deronzier, A.; Roland, J.-F. *J. Electroanal. Chem.* **1990**, *285*, 133.
- (24) Bevierre, M.-O.; Mercier, F.; Mathey, F.; Jutand, A.; Amatore, C. *New. J. Chem.* **1991**, *15*, 545.
- (25) Bolognesi, A.; Catellani, M.; Destri, S.; Porzio, W. *Synth. Met.* **1987**, *18*, 129.
- (26) Catellani, M.; Destri, S.; Porzio, W.; Themans, B.; Bredas, J. L. *Synth. Met.* **1988**, *26*, 259.
- (27) Tanaka, S.; Kaeriyama, K.; Hiraide, T. *Makromol. Chem., Rapid Commun.* **1988**, *9*, 743.
- (28) Ofer, D.; Crooks, R. M.; Wrighton, M. S. *J. Am. Chem. Soc.* **1990**, *112*, 7869.
- (29) Ofer, D.; Wrighton, M. S. *J. Am. Chem. Soc.* **1988**, *110*, 4467.
- (30) Ofer, D.; Park, L. Y.; Wrighton, M. S.; Schrock, R. R. *Chem. Mater.* **1991**, *3*, 573.
- (31) Patil, A. O.; Heeger, A. J.; Wudl, F. *Chem. Rev.* **1988**, *88*, 183.
- (32) Zingales, F.; Graziani, M.; Faraone, F.; Belluco, U. *Inorg. Chim. Acta.* **1967**, *1*, 172.
- (33) Caspar, J. V.; Meyer, T. J. *J. Phys. Chem.* **1983**, *87*, 952.
- (34) Ziessel, R.; Youinou, M.-T.; Balegroune, F.; Grandjean, D. *J. Organomet. Chem.* **1992**, *441*, 143.
- (35) Dondoni, A.; Mastellari, A. R.; Medici, A.; Negrini, E.; Pedrini, P. *Synthesis* **1986**, 757.
- (36) Dondoni, A.; Fogagnolo, M.; Medici, A.; Negrini, E. *Synthesis* **1987**, 185.
- (37) Paul, E. W.; Ricco, A. J.; Wrighton, M. S. *J. Phys. Chem.* **1985**, *89*, 1441.
- (38) Kittlesen, G. P.; White, H. S.; Wrighton, M. S. *J. Am. Chem. Soc.* **1984**, *106*, 7389.

### Chapter 3

**Synthesis and Reactivity of Novel Conducting Polymers Containing Platinum(II) in the Backbone: Polymers Derived from Oxidation of *cis*(5'-(2,5-Bithienyl))<sub>2</sub>(4-isocyanophenylferrocene)<sub>2</sub>platinum(II) and *cis*(2-Thienyl)<sub>2</sub>(4-isocyanophenylferrocene)<sub>2</sub>platinum(II)**

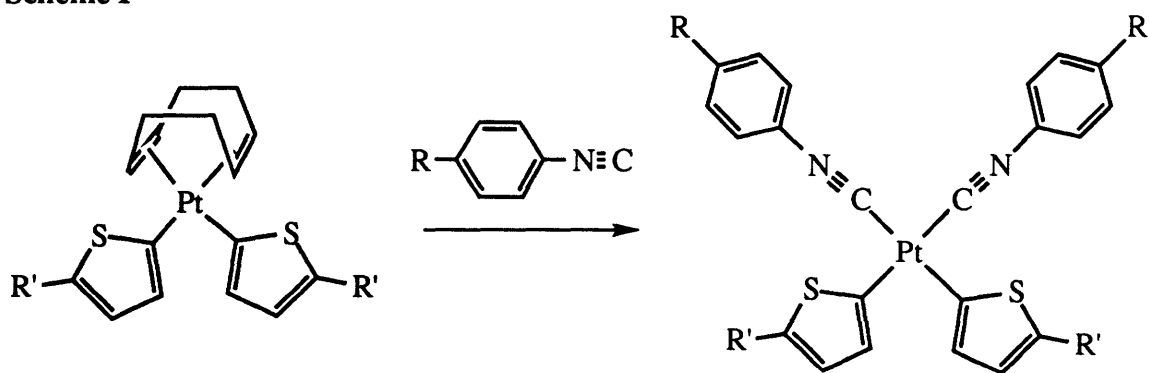
In this chapter the preparation and characterization of *cis*(5'-(2,5-bithienyl))<sub>2</sub>(4-isocyanophenylferrocene)<sub>2</sub>platinum(II) **1a**, shown in Scheme I, which undergoes oxidative polymerization to form a novel conducting polymer poly[*cis*(5'-(2,5-bithienyl))<sub>2</sub>(4-isocyanophenylferrocene)<sub>2</sub>platinum(II)], poly-**1a** is described. We have also prepared two related monomers, *cis*(5'-(2,5-bithienyl))<sub>2</sub>(4-isocyanophenylferrocenoate)<sub>2</sub>platinum(II), **1b** and *cis*(2-thienyl)<sub>2</sub>(4-isocyanophenylferrocene)<sub>2</sub>platinum(II), **1c** to study the effect of monomer structure on the polymerization. Importantly, analogs of **1a-1c** have been prepared,<sup>1,2</sup> and a critical finding is that the Pt(II) center extends the degree of  $\pi$ -delocalization<sup>2</sup> in the bithienyl and bisbithienyl species. Interestingly, the isonitrile ligands **2a** and **2b** can be reversible exchanged in the polymers derived from **1a-1c** and these processes can be studied quantitatively by electrochemical methods to detect the ferrocene centers.



We prepared the Pt(II) complexes represented by **1a-c** with the expectation that polymerization upon oxidation would occur *via* oxidative coupling in the  $\alpha$  positions of the thienyl ligands. The fact that the Pt(II) centers extends the  $\pi$ -conjugation<sup>2</sup> suggests that **1a-1c** should behave as polymerizable oligomers of thiophene. However, oxidative degradation processes at the Pt(II) may also be competitive, and Pt(IV) formation may promote reductive elimination of the thienyl ligands.

In order to circumvent problems from oxidative degradation upon polymerization, we have prepared the related oligomer, [Pt(1,5-cyclooctadiene)(2,2':5',2'':5'',2'''-tetrathiophene)]<sub>n</sub>, **3a**, by reaction of (1,5-cyclooctadiene)dichloroplatinum with

Scheme I

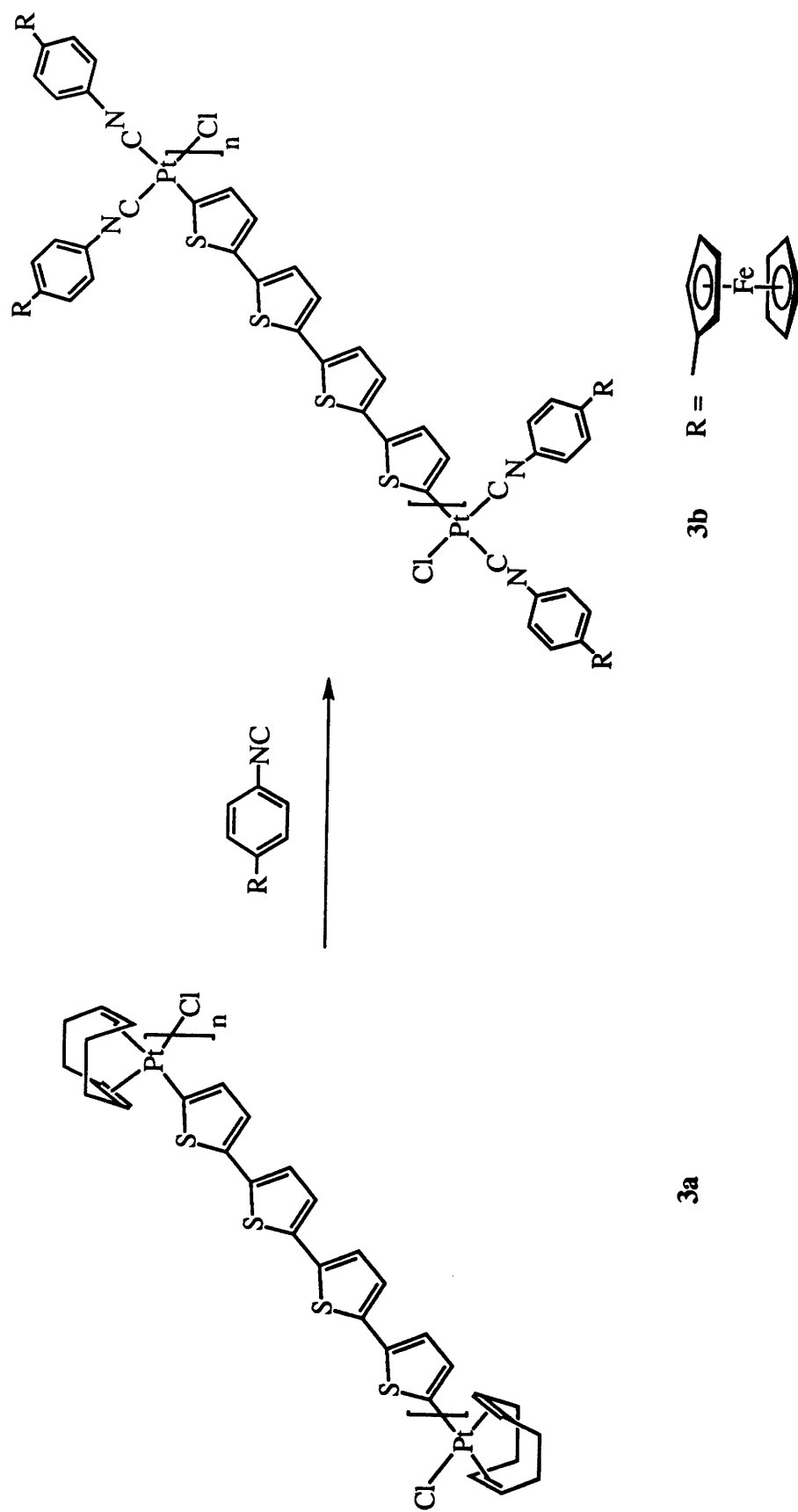


	1a	1b	1c
R			
R'			H

5,5'''-di(tributylstannyl)-2,2':5',2'':5'',2'''-tetrathiophene, **4** as shown in Scheme II. After displacement of the 1,5-cyclooctadiene with **2a** this oligomer, **3b**, has a structure analogous to that proposed for poly-**1a**. However, it is synthesized using chemical procedures which avoid the oxidative degradation accompanying polymerization of **1a-1c**.

There are numerous examples of metal-containing conducting polymers, many of them bridged macrocyclic metal complexes.<sup>3</sup> Often, these polymers are conducting by virtue of good  $\pi$ - $\pi$  overlap between adjacent macrocycles, and the metal group acts only as a structural element, rather than participating in the conductivity. Conjugated polymers<sup>4-21</sup> and oligomers<sup>22-29</sup> containing metals in the polymer backbone in which the linking group between metal centers is similar in structure to a fragment of an organic conducting polymer have also been synthesized. Although conductivity has been predicted in many of these polymers, very few examples exist where conductivity has been demonstrated.<sup>6,17</sup> In addition, although many organic conducting polymers can be conveniently prepared by electrosynthesis, none of the previously synthesized metal containing conducting polymers have been prepared by this technique. Electrochemical reduction of  $[\text{Ni}(\text{PPh}_3)_2(p\text{-C}_6\text{H}_4\text{Br})\text{Br}]$  has been shown to yield an aryl-nickel polymer, for which a polyphenylene backbone interrupted by Ni(II) was proposed. However, conductivity could not be demonstrated.<sup>30</sup> Other workers have shown that polythiophene derivatives containing methylene<sup>31</sup> or heteroatomic<sup>32</sup> bridges which interrupt the conjugation are still moderately conducting. A recent theoretical study has concluded that square planar Pt(II) groups are electronically favorable for electrical conductivity in metal oligoene polymers.<sup>33</sup> Our work described herein demonstrates an example of a conducting polymer which has been prepared from a monomer containing a metal group which interrupts the conjugation in the backbone. The reversible substitution chemistry at the Pt(II) centers of poly-**1a** and -**1c** suggests that a variety of derivatives can be easily prepared.

Scheme II



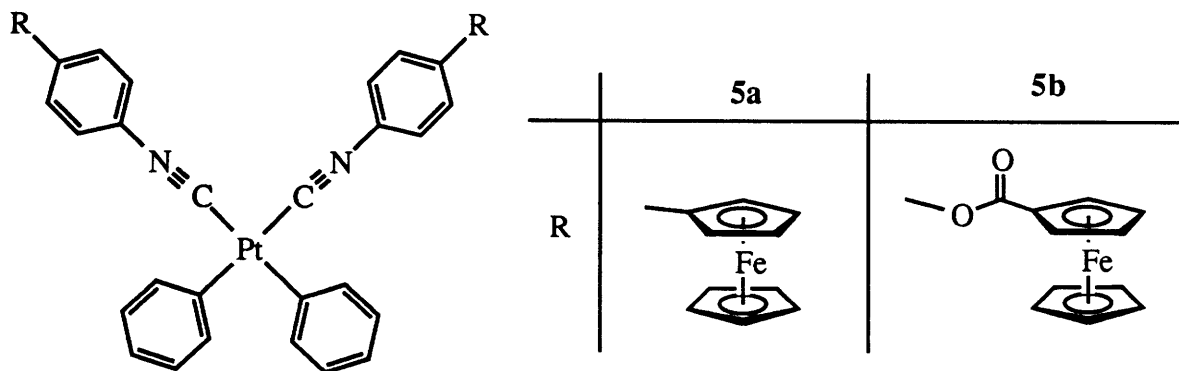
## Results and Discussion

**Preparation and Characterization of Monomers 1a-1c.** The monomers **1a-1c** were all prepared in a similar fashion by displacement of 1,5-cyclooctadiene from either *cis*(5'-(2,5-bithienyl)<sub>2</sub>(1,5-cyclooctadiene)platinum(II), **6** or *cis*(2-thienyl)<sub>2</sub>(1,5-cyclooctadiene)platinum(II) by the isonitriles **2a** and **2b** in CH<sub>2</sub>Cl<sub>2</sub> at 25 °C, Scheme I. In addition, the 1,5-cyclooctadiene in **1a-1c** may also be displaced by phosphines under the same conditions, allowing a variety of different monomers to be prepared via this route. **1a-1c** are characterized by two intense bands in the isonitrile stretching region of the infrared spectrum. The UV-vis spectral data for these complexes and the corresponding ligands **2a** and **2b** are collected in Table I. The band positions and extinction coefficients of **2a** and **2b** indicate that these compounds behave as aryl substituted ferrocenes, with several high energy  $\pi$ - $\pi^*$  bands present and a weak band at ~ 450 nm due to the d-d transition in the ferrocenyl group. The UV-vis spectra of the complexes **1a** and **1b** contain bands corresponding to those present in the ligands **2a** and **2b** overlapping with bands analogous to those observed in the spectrum of **6**. Absorption bands with maxima at 328 and 374 nm appear in the spectrum of **6**, we assign these to  $\pi$ - $\pi^*$  transitions of the bithienyl ligands, perturbed by the presence of the Pt group. Both the bands in **6** appear to lower energy of the single, intense absorption in the spectrum of 2,2'-bithiophene, providing evidence that in **6**, the Pt extends the conjugation. An analog of **1a** and **1b** which has no low energy absorptions due to the coordinated isonitrile is *cis*(5'-(2,5-bithienyl)<sub>2</sub>(*t*-butylisonitrile)<sub>2</sub>platinum(II). The spectrum of this complex contains a band with a maximum at 350 nm and a shoulder at ~ 396 nm. Thus, the isonitrile and 1,5-cyclooctadiene ligands cause only small shifts in the positions and intensities of the bands, allowing us to conclude that these bands must indeed be associated with the bithienyl ligands on the Pt.

### Preparation and Characterization of Oxidatively Formed Polymers from 1a-1c.

Films of poly-**1a** were prepared by anodic electropolymerization of **1a** and characterized

electrochemically in 0.1 M  $[(n\text{-Bu})_4\text{N}]\text{PF}_6/\text{CH}_2\text{Cl}_2$  after rinsing with  $\text{CH}_2\text{Cl}_2$  to remove residual monomer, Figure 1a. Deposition of poly-**1a** is readily observed by the naked eye as a red film. The reversible redox wave at +0.55 V vs. Ag can be assigned to the ferrocene centers and the surface coverage of ferrocenyl groups is  $\sim 2.5 \times 10^{-7}$  mol  $\text{cm}^{-2}$ . We assign the broad feature at approximately +0.95 V vs. Ag in the forward sweep of the cyclic voltammogram of poly-**1a** to polymer oxidation. For comparison, cyclic voltammetry of *cis*-(phenyl)<sub>2</sub>(4-ferrocenylphenylisonitrile)<sub>2</sub>Pt, **5a**, at a glassy carbon electrode shows a reversible wave attributed to the ferrocene centers at  $E_{1/2} = +0.59$  V, consistent with our assignments of the wave at +0.55 V in poly-**1a** as due to the ferrocene centers.



Electropolymerization of **1b** to form poly-**1b** under the same conditions as for **1a** occurs at +1.25 V vs. Ag, and similar coverages are obtained. The ferrocenyl groups in poly-**1b** show an oxidation peak at a more positive potential, +0.85 V, than in poly-**1a**, +0.55 V, consistent with the shift in ferrocenyl potential in **5b**, +0.80 V, vs. **5a**, +0.59 V.

The presence of the isocyanide units in poly-**1a** is demonstrated by specular reflectance infrared spectroscopy, Figure 2. The solution infrared spectrum of **1a** has two intense peaks due to the isocyanide group at 2198 and 2172  $\text{cm}^{-1}$ , Table I. The infrared spectrum of **2a** contains a single strong isocyanide band at 2126  $\text{cm}^{-1}$ . Specular reflectance infrared spectroscopy of poly-**1a** on a Au macroelectrode shows a broad absorption with a peak at 2195  $\text{cm}^{-1}$  and a shoulder at 2170  $\text{cm}^{-1}$ . The correspondence between the IR spectrum of poly-**1a** and **1a** in solution is good, but the broad spectral feature for the



**Table I.** IR and UV-vis spectroscopic data

Compound	IR ( $\nu_{\text{NC}}$ ) <sup>a</sup>	IR ( $\nu_{\text{CO}}$ ) <sup>a</sup>	UV-vis ( $\epsilon \times 10^{-3}$ ) <sup>b</sup>
<b>1a</b>	2198, 2172		258 (37), 302 (60), 372 (33), 446 (13)
<b>1b</b>	2199, 2173	1734	268 (32), 328 (17), 386 (13), 436 (7.3)
<b>1c</b>	2199, 2170		256 (62), 300 (79), 346 (37), 464 (5.3)
<b>2a<sup>c</sup></b>	2127		254 (17), 290 (18), 354 (2.7), 452 (0.9)
<b>2b</b>	2130	1733	240 (16), 264 (10), 316 (2.1), 350 (0.8), 450 (0.4)
<b>5a</b>	2186, 2155		262 (38), 300 (50), 370 (8.5), 458 (2.7)
<b>5b</b>	2188, 2158	1734	272 (11), 325 (4), 308 (5.2), 450 (0.3)
<b>7</b>			328 (16), 374 (15)
<b>3a</b>			432 (20) <sup>d</sup>
<b>3b</b>	2184, 2163 <sup>e</sup>		316 (48), 396 (30), 430 (36) <sup>d</sup>
<b>3c</b>	2259, 2226, 2212, 2187, 2149 <sup>e</sup>		430 (24) <sup>d</sup>
<b>4T<sup>f</sup></b>			392 (44)

<sup>a</sup> CH<sub>2</sub>Cl<sub>2</sub> solution. Band positions in cm<sup>-1</sup>. <sup>b</sup> THF solution. Band positions in nm. Extinction coefficients in M<sup>-1</sup>cm<sup>-1</sup>. <sup>c</sup> Reference 42. <sup>d</sup> Approximate values calculated assuming oligomers are n = 3. <sup>e</sup> KBr. <sup>f</sup> 2,2':5',2'':5'',2'''-Tetrathiophene. Reference 45.

**Figure 1.** (a) Cyclic voltammetry of electrodeposited film of poly-**1a** on Au microelectrodes in 0.1 M [(*n*-Bu)<sub>4</sub>N]PF<sub>6</sub>/CH<sub>2</sub>Cl<sub>2</sub>. (b) I<sub>D</sub>-V<sub>G</sub> characteristic in the same medium for the same pair of derivatized microelectrodes. (c) Cyclic voltammogram of the same film of poly-**1a** after 15 minutes immersed in **2b**/CH<sub>2</sub>Cl<sub>2</sub>. (d) I<sub>D</sub>-V<sub>G</sub> characteristic of the film shown in (c). (e) Cyclic voltammogram of the same film of poly-**1a** after 15 minutes further immersion in **2a**/CH<sub>2</sub>Cl<sub>2</sub>. (f) I<sub>D</sub>-V<sub>G</sub> characteristic of the film shown in (e).

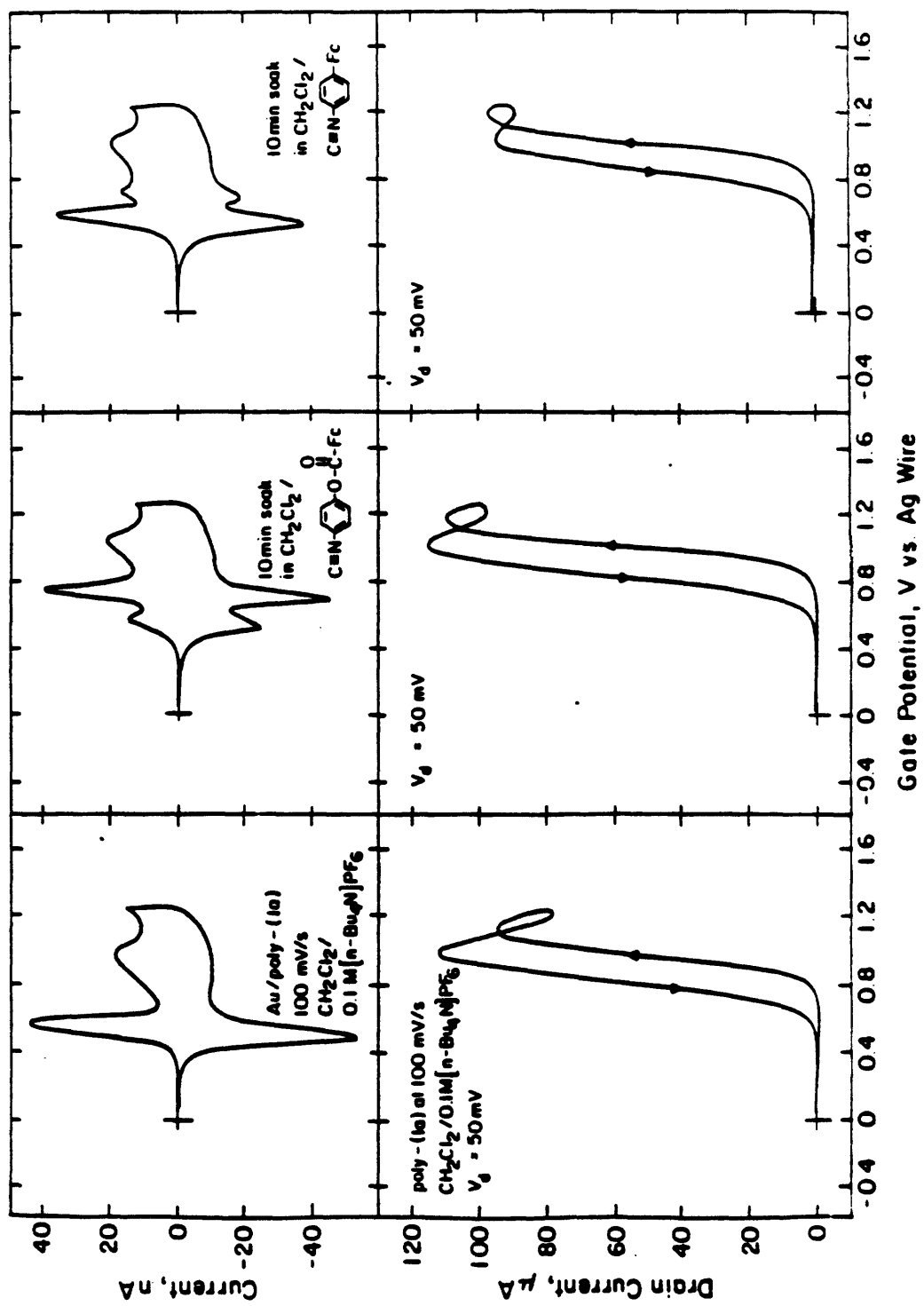
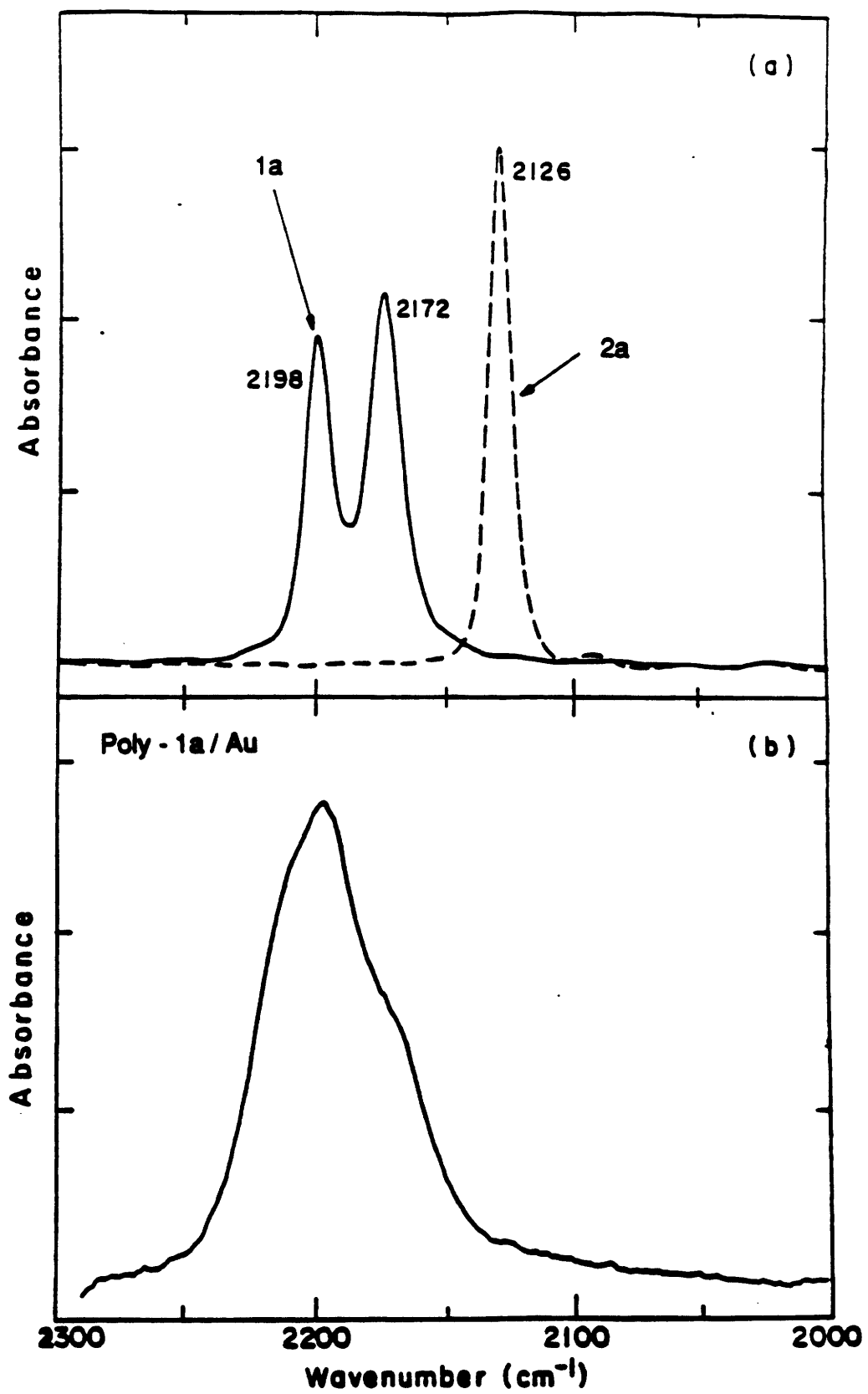


**Figure 2.** (a) Solution infrared spectra of the isonitrile stretching region of **1a** and **2a** in  $\text{CH}_2\text{Cl}_2$ . (b) Specular reflectance infrared spectrum of poly-**1a** on a Au macroelectrode in the same region.



polymer suggests that not all of the isonitrile groups are in identical environments. This may result from the ill-defined structure of the electrodeposited polymer, or from partial decomposition of the polymer during deposition (*vide infra*).

We studied the relative conductivity of poly-**1a** as a function of potential. Pairs of closely spaced ( $\sim 1 \mu\text{m}$ ) individually addressable microelectrodes ( $\sim 2 \mu\text{m} \times 100 \mu\text{m}$ ) developed in these laboratories have been useful in making *in situ* measurements of the potential dependence of conductivity of conducting polymers.<sup>34-40</sup> By applying a small fixed potential,  $V_D$ , between two adjacent polymer coated microelectrodes and at the same time varying their potential versus a reference electrode,  $V_G$ , we are able to record plots of drain current,  $I_D$ , vs. gate voltage,  $V_G$ .  $I_D$  is directly proportional to the conductivity of the polymer, hence the  $I_D$  vs.  $V_G$  plot is a plot of relative conductivity as a function of potential. The  $I_D$ - $V_G$  plot for poly-**1a** is shown in Figure 1b. The peak conductivity corresponds to the position of the anodic peak at +0.95 V vs. Ag in the cyclic voltammogram, and hysteresis in the  $I_D$ - $V_G$  plot typical of other conducting polymers is observed.<sup>37</sup> Little conductivity is observed in the potential region where the ferrocene centers are electroactive. The maximum conductivity on the positive sweep is approximately  $0.1 \Omega^{-1}\text{cm}^{-1}$ . For comparison, we find polythiophene formed by oxidative polymerization of 2,2'-bithiophene (under the same conditions of concentration, solvent, electrolyte, and potential as for **1a**) has a conductivity of  $1 \Omega^{-1}\text{cm}^{-1}$  at the potential of maximum conductivity (+1.1 V vs. Ag) on the positive sweep.

Films of poly-**1a** electropolymerized onto Au macroelectrodes were examined by XPS to establish elemental composition. These results are shown in Table II along with the results from an XPS spectrum obtained for a sample of the monomer **1a** cast from solution, for which the elemental composition is known exactly, Figure 3. The Pt to Fe ratios for monomer and polymer are similar, though not identical. In order to estimate the accuracy of determining the elemental composition of these samples quantitatively by XPS we acquired spectra at three spots on a single sample of **1a**, and the average values

along with standard deviations are shown in Table II. Since we observe significant deviation between separate analyses on a single sample, without taking into account instrumental variations and differences in surface impurities, we conclude that the element ratios are only approximate. The effect of beam damage on the samples was assessed by repeated analysis of a single sample of **1a** without moving the beam. We found that the element ratios changed as the number of scans the sample was exposed to increased, hence beam damage introduces additional uncertainty into the element ratios. Nonetheless, we have found that the Pt to S ratio is consistently lower in samples of poly-**1a** than in the monomer, **1a**. We have found that the Pt/S ratio is dependent on the exact conditions under which poly-**1a** is prepared. The cyclic voltammogram of a polymer sample on which XPS analysis was done was examined, and we found that the integrated area of the ferrocene wave in this sample was smaller in comparison to the polymer oxidation wave than the corresponding ratio for polymer deposited on microelectrodes, shown in Figure 1a. We attribute these differences to differences in current density between the electrodes, and found that even larger electrodes had even higher yet Pt/S ratios. Calculation of the Pt/S ratio for the polymer shown in Figure 1a, by comparison of the integrated areas of the ferrocene and polymer waves from samples for which the composition has been determined by XPS, reveals that the poly-**1a** on microelectrodes should have a Pt/S ratio similar to that of the monomer **1a** cast onto Au. The XPS spectra also show that the Pt 4f peaks appear at similar binding energies for both **1a** and poly-**1a** and are consistent with Pt(II).<sup>41</sup> Electrodeposition of Pt(0) into the polymer film shows new Pt 4f peaks 2 eV lower in binding energy than those in the polymer, confirming that the Pt in the polymer is indeed Pt(II).

The high S content in poly-**1a** compared to pure **1a** suggests that an undesired reaction occurs, either during polymerization or electrochemical characterization. Reductive elimination of the bithienyl ligands from oxidized **1a** would give tetrathiophene, a species that would oxidatively polymerize at the potentials where it

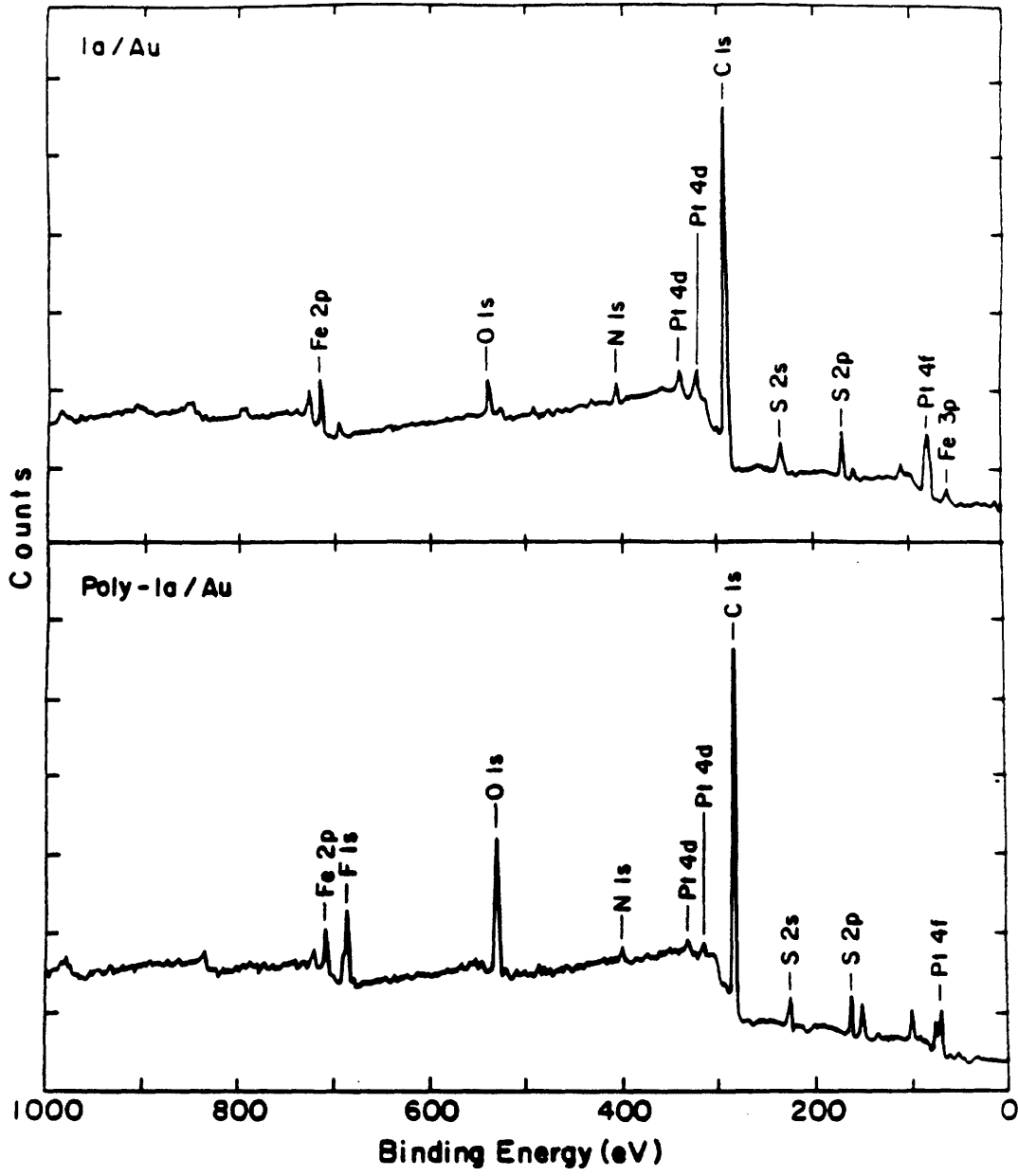
**Table II.** XPS Compositions and Element Ratios of Polymers and Monomer **1a**.

Compound	Binding Energy (Relative Amount) <sup>d,e</sup>		
	Pt(4f <sub>7/2</sub> )	Fe(2p <sub>3/2</sub> )	S(2p <sub>3/2</sub> )
<b>Poly-1a<sup>a</sup></b>	73.7 (1)	707.7 (0.48)	163.8 (6.0)
<b>1a<sup>a</sup></b>	73.2 (1)	708.1 (0.64 ± 0.05)	164.1 (3.4 ± 0.2)
<b>Poly-1c<sup>a</sup></b>	73.5 (1)	707.5 (0.75)	163.9 (3.6)
<b>1c<sup>a</sup></b>	73.6 (1)	707.9 (0.46 ± 0.02)	163.8 (2.0 ± 0.3)
<b>3a<sup>b</sup></b>	74.4 (1)	-	164.8 (3.7)
<b>3b<sup>b</sup></b>	72.9 (1)	707.1 (0.6)	163.2 (4.0)
<b>3c<sup>c</sup></b>	73.4 (1)	-	163.7 (3.3)

<sup>a</sup> Au substrate. <sup>b</sup> In substrate. <sup>c</sup> Cast from THF on Au. <sup>d</sup> Binding energies are in eV and are corrected to the C 1s peak at 284.0 eV. <sup>e</sup> Element ratios are based on Pt and are corrected using sensitivity factors.



**Figure 3.** XPS spectrum of (a) thin film of **1a** on Au and (b) poly-**1a** on Au.



might be formed. Thus, polythiophene containing no Pt may form. In addition, coupling of bithienyl or tetrathienyl units with the oxidized **1a** monomers may yield polymers which are richer in thiophene than for simple polymerization of **1a**. In order to understand whether such coupling reactions are viable in the formation of polymers from **1a** and **1b**, we attempted copolymerizations from solutions containing combinations of two polymerizable monomers: **1a** + terthiophene; **1a** + tetrathiophene; and **1b** + terthiophene. Electropolymerization from a solution containing 10 mM **1a** and 10 mM terthiophene occurs at +1.05 V vs. Ag. Cyclic voltammetry of the deposited polymer formed in this experiment shows that the ratio of the polymer oxidation peak in the cyclic voltammogram to the ferrocene oxidation peak is similar to what is obtained when pure **1a** is electropolymerized. Since terthiophene alone does not polymerize at +1.05 V vs. Ag, whereas **1a** does, we conclude that the terthiophene is not taken up into the polymer to a significant extent, and relatively little formation of polythiophene or copolymer rich in polythiophene units occurs. Electropolymerization from solutions of 10 mM **1b** and 10 mM terthiophene at +1.05 V shows similar results: very little terthiophene is incorporated into the polymer. When the potential is increased to +1.25 V in the copolymerization of **1a** and terthiophene the cyclic voltammogram of the resulting polymer shows an increase in the area of the polymer oxidation wave in comparison to the ferrocenyl wave; indicating an increase in the amount of terthiophene that is incorporated. At +1.25 V terthiophene polymerizes, so we conclude that at this potential both monomers are oxidized and are incorporated into the growing polymer. When the polymerization of **1b** and terthiophene is carried out at +1.25 V the polymer oxidation wave decreases in size in comparison to the ferrocenyl wave vs. the polymer formed from pure **1b**.

We also examined the effect of adding tetrathiophene to solutions of **1a** on the electropolymerization. Electropolymerization from solutions containing 10 mM tetrathiophene and 10 mM **1a** occurs at +1.05 V. At this potential, little change in the

cyclic voltammogram of the resulting polymer from that of pure poly-**1a** is observed. Hence, little tetrathiophene is incorporated into the polymer; consistent with the fact that tetrathiophene alone can only be polymerized at potentials above +1.05 V. At +1.25 V some tetrathiophene is incorporated as indicated by the ratio of the polymer oxidation wave to the ferrocenyl wave. These results demonstrate that intentional addition of tetrathiophene, a possible product of oxidative degradation of **1a** and **1b**, results in some incorporation of tetrathiophene into the polymer, but only at potentials where tetrathiophene alone can also be electropolymerized. We conclude that it is unlikely that incorporation of tetrathiophene (generated by degradation of **1a**) is significant when **1a** is electropolymerized alone. If this were happening we would expect to observe a greater effect upon intentional addition of tetrathiophene to the polymerization solution.

Further understanding of the factors involved in the electropolymerization of **1a** can be obtained by examining the electrochemical behavior of (2-thienyl)<sub>2</sub>(4-isocyanophenylferrocene)<sub>2</sub>platinum, **1c**. We prepared **1c** with the expectation that like other thiophene oligomers, the potential at which oxidative polymerization occurs should be dependent on the length of the oligomer. We expected **1c** to polymerize at more positive potentials than **1a** or **1b**. Indeed, this is the case and we find that electropolymerization of **1c** occurs only when the electrode is scanned to +1.75 V vs. Ag. Even, at this potential, polymer growth is slow, and thick films cannot be formed without degradation. The cyclic voltammogram of a thin film of poly-**1c**, deposited on a Pt electrode ( $\sim 2 \times 10^{-3} \text{ cm}^2$ ) is shown in Figure 4a. The reversible wave at +0.64 V vs. Ag is assigned to the ferrocenyl centers, and the broad feature at approximately +1.0 V vs. Ag to polymer oxidation. The surface coverage of ferrocenyl groups is  $\sim 4 \times 10^{-8} \text{ mol cm}^{-2}$ . The area of the ferrocenyl wave compared to the polymer wave is larger in poly-**1c** than in poly-**1a**, as expected, since the thiophene content of the monomer **1c** should be higher than that of **1a**. The product of reductive elimination from **1c** would be 2,2'-bithiophene, which can be polymerized at +1.5 V vs. Ag. If oxidized **1c** were

reductively eliminating 2,2'-bithiophene, we would expect formation of polythiophene at +1.5 vs. Ag. No polymer growth is observed at +1.5 V, implying that the rate of reductive elimination at this potential must be slow, making the effective concentration of 2,2'-bithiophene at the electrode too low to allow polymerization to occur. The XPS spectra of poly-**1c** and a thin film of **1c** on Au, Figure 5, show that poly-**1c** contains Pt, S, Fe as well as N and C, however as with poly-**1a**, the ratio of Pt to S in the sample is lower than expected in comparison to the ratio in the monomer **1c**, Table II. We conclude that reductive elimination might be occurring to some extent in the polymerization of **1c** based on the low Pt content compared to monomer. However, formation of a Pt containing polymer clearly competes with the degradation process. Deposition of poly-**1c** onto Au microelectrodes under the same conditions yields a thin red film, but we could not obtain films sufficiently thick to bridge two microelectrodes, in order to record an  $I_D$ - $V_G$  plot. Electropolymerization from solutions containing 10 mM **1c** and 10 mM terthiophene occurs at +1.5 V. Cyclic voltammetry of the resulting polymer shows the presence of ferrocenyl centers in the polymer, but the amount of **1c** incorporated into the polymer is lower than that in polymer prepared from pure **1c**, as shown by the area under the ferrocenyl redox wave, in comparison to the polymer oxidation wave. Since a copolymer forms at a potential where **1c** alone does not polymerize, we conclude that oxidized terthiophene reacts with **1c** yielding Pt containing polymer. Thus, the ratio of Pt(II) centers (from **1a**, **1b** or **1c**) to polythiophene can be varied by adjusting the potential at which the copolymerization is done, and by varying the monomers used.

**Isonitrile Exchange Reactions.** In order to further characterize the electrodeposited films of poly-**1a**, exchange experiments in which the bound isonitrile ligand is displaced by another isonitrile from solution were done. In solution, reaction of ~ 0.1 mM **1a** in  $CDCl_3$  with excess (5:1) **2b** affords no observable reaction at room temperature over several hours. However, mild heating to 40 °C for several minutes yields ligand exchange as evidenced by peaks characteristic of ligated **2b** in the  $^1H$  NMR spectrum.

**Figure 4.** (a) Cyclic voltammetry of electrodeposited film of poly-**1c** on a Pt macroelectrode in 0.1 M [(*n*-Bu)<sub>4</sub>N]PF<sub>6</sub>/CH<sub>2</sub>Cl<sub>2</sub>. (b) Cyclic voltammogram of the same film of poly-**1c** after 15 minutes immersed in **2b**/CH<sub>2</sub>Cl<sub>2</sub>. (c) Cyclic voltammogram of the same film of poly-**1c** after 15 minutes further immersion in **2a**/CH<sub>2</sub>Cl<sub>2</sub>

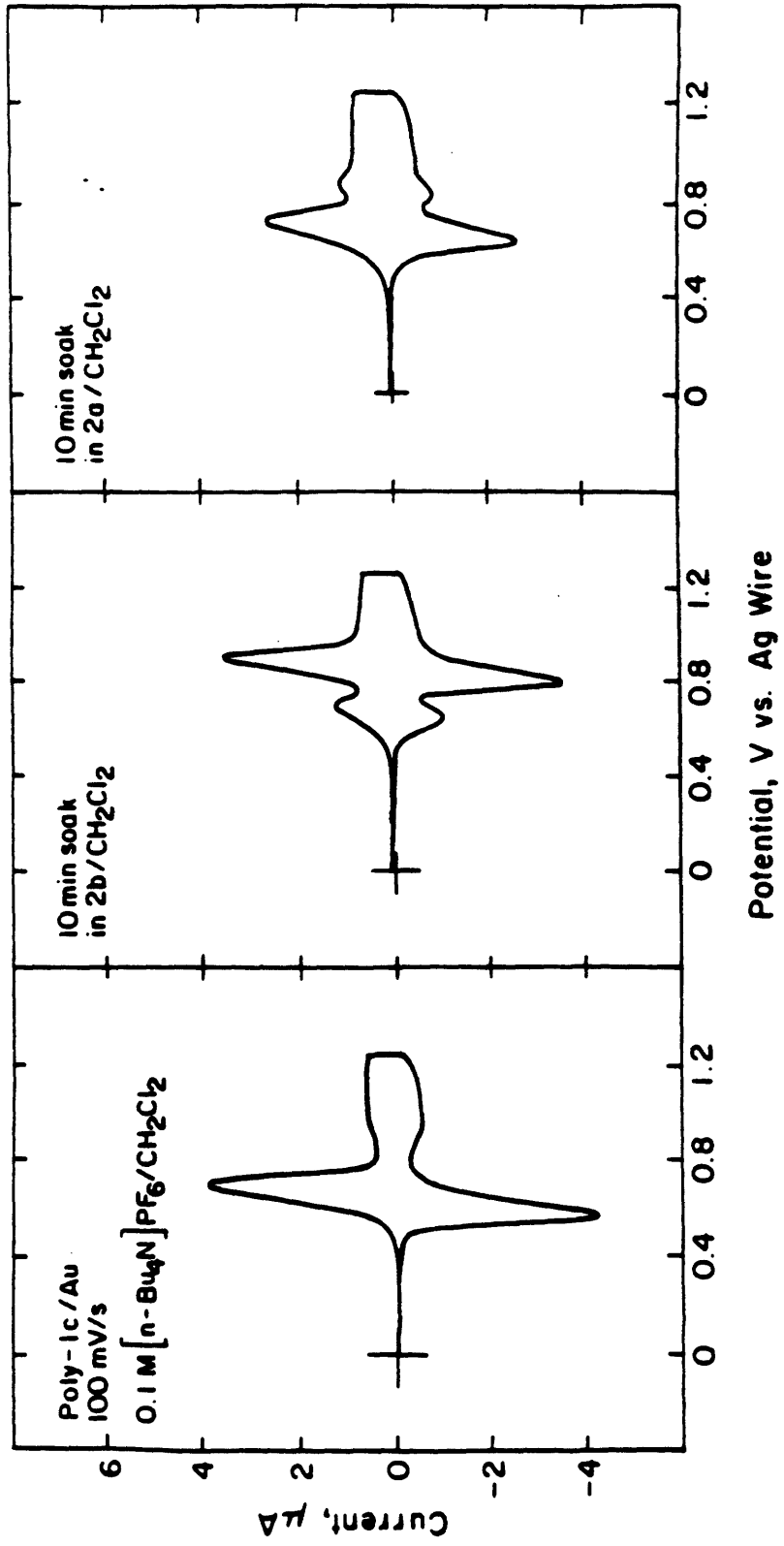
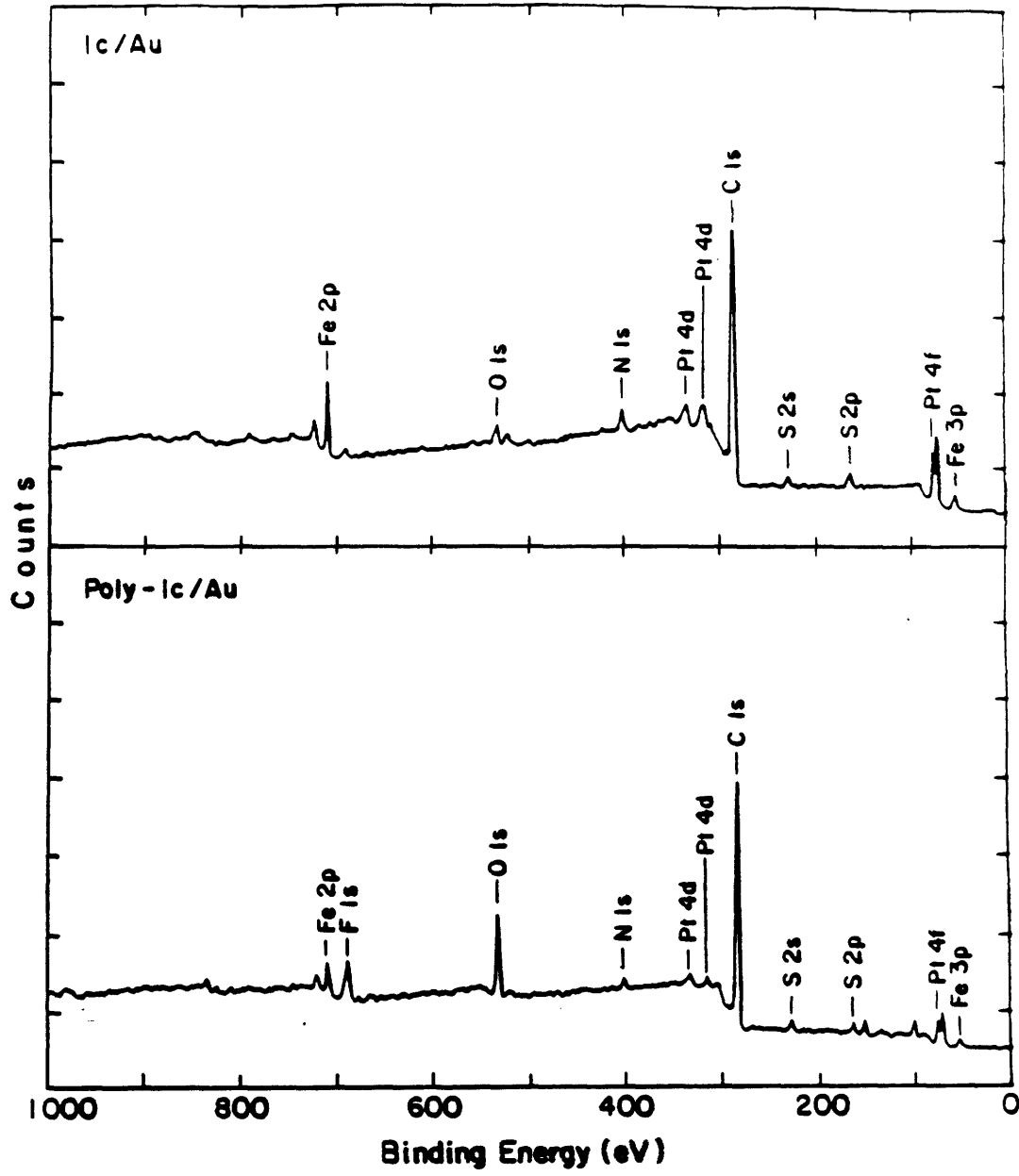


**Figure 5.** XPS spectrum of (a) thin film of **1c** on Au and (b) poly-**1c** on Au.





Samples of poly-**1a** electropolymerized onto microelectrode arrays were immersed in 10 mM solutions of **2b** in CH<sub>2</sub>Cl<sub>2</sub> for 10 min at room temperature. After rinsing with CH<sub>2</sub>Cl<sub>2</sub>, the cyclic voltammogram and I<sub>D</sub>-V<sub>G</sub> plot were obtained, Figure 1c and 1d. The cyclic voltammogram of the polymer reacted with **2b** shows a new redox wave at +0.7 V which we assign to ligated **2b** (as in poly-**2b**), while the smaller wave at +0.55 V is due to residual ligated **2a**. The reacted film, now containing **2b**, was immersed for 10 min in a 10 mM solution of **2a** in CH<sub>2</sub>Cl<sub>2</sub>, and rinsed with CH<sub>2</sub>Cl<sub>2</sub>. The cyclic voltammogram and I<sub>D</sub>-V<sub>G</sub> plot obtained thereafter are shown in Figure 1e and 1f. The area of the redox wave assigned to ligated **2a** has increased. A small amount of residual ligated **2b** remains at +0.7 V. Importantly, the sum of the integrated areas for the ferrocenyl redox waves decreases only ~ 5 % from Figure 1a to 1e, indicating that only a small amount of the coordinated isonitrile is lost during the substitution reactions. Thus, the isonitrile ligands can be efficiently exchanged in poly-**1a** by **2b** to yield poly-**2b**. This suggests that a variety of substituted derivatives of poly-**1a** are accessible via simple ligand exchange processes.

Films of poly-**1c** also react with **2b** in CH<sub>2</sub>Cl<sub>2</sub>. A cyclic voltammogram of the resulting film is shown in Figure 4b. As with poly-**1a**, the exchange is reversible, and reaction of the **2b** substituted films with **2a**, results in the reappearance of the reversible feature in the cyclic voltammogram attributed to coordinated **2a**. The integrated area under the ferrocenyl waves decreases to a greater extent than observed for the analogous substitutions in poly-**1a**, presumably because more rapid decomposition occurs in poly-**1c** vs. poly-**1a**.

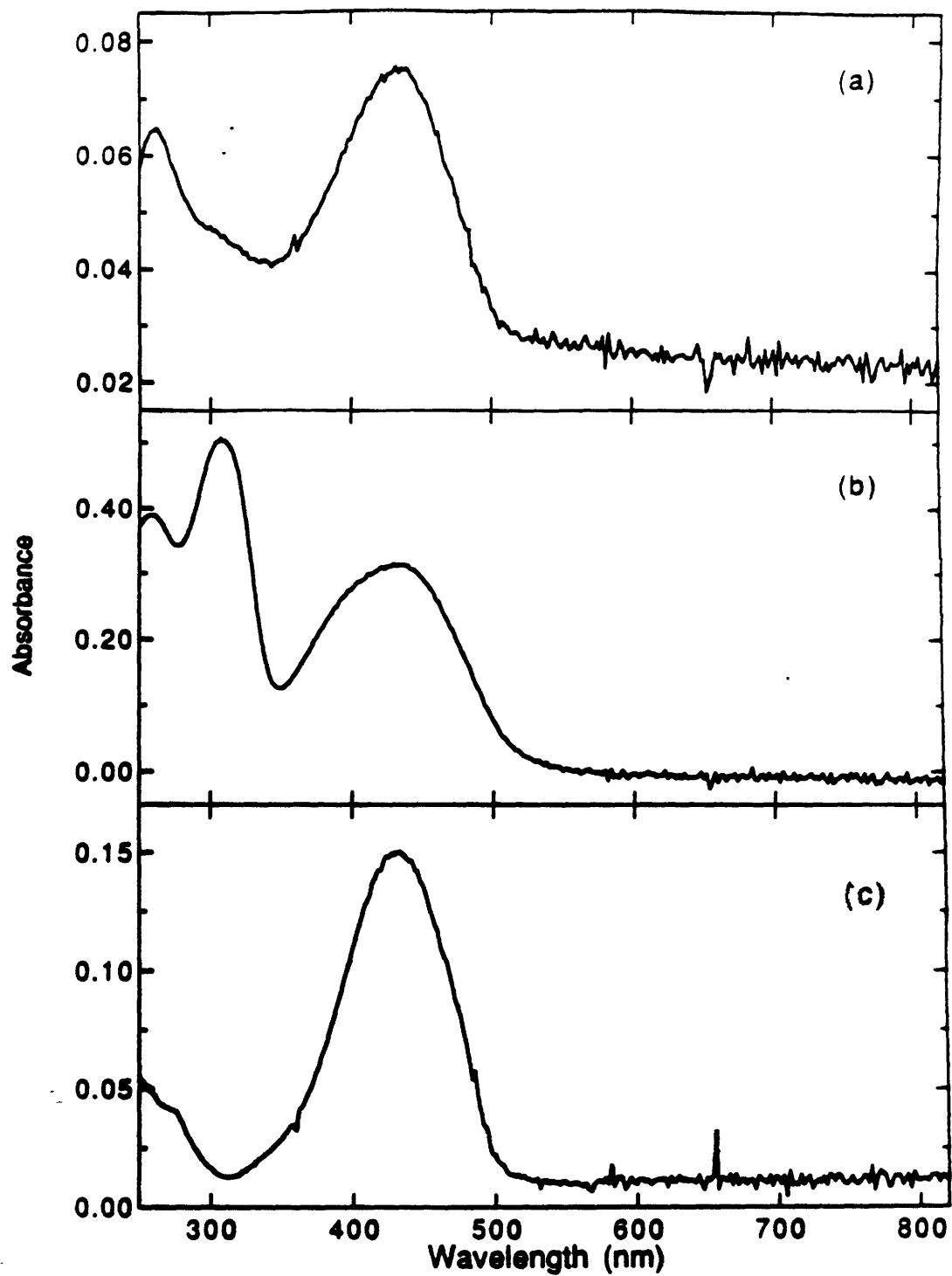
**Preparation and Characterization of 3a and 3b.** An alternative synthetic approach to the preparation of a polymer with the same structure as poly-**1a** is to chemically couple difunctionalized thiophene oligomers with metal moieties containing two reactive groups. The oligomers prepared in this manner can be characterized by standard techniques after synthesis but prior to electrochemical oxidation. Using this approach, **3a**, which we

propose to have the structure shown below, was prepared by reaction of **4** and (1,5-cyclooctadiene)dichloroplatinum. The cyclooctadiene ligands are expected to be labile in such complexes and replaceable by isonitriles such as **2a** and **2b**, since we find that **6** reacts with **2a** and **2b** to form **1a** and **1b** respectively, Scheme I.

Elemental analysis of **3a** is consistent with an oligomeric structure in which  $n = 2-3$ , and the oligomers are capped primarily with Pt-Cl moieties, since the Sn content is very low, and the Cl content is as expected for  $n = 2-3$ . The UV-vis spectrum of **3a** in tetrahydrofuran (THF) contains an absorption band at 432 nm, Figure 6a. In comparison, the spectrum of tetrathiophene has a band with  $\lambda_{\text{max}}$  at 392 nm ( $\epsilon \approx 44,000 \text{ M}^{-1}\text{cm}^{-1}$ ), Table I. The shift to lower energy in the spectrum of **3a** is consistent with a longer conjugation length than that observed tetrathiophene, analogous to the shift observed in the spectrum of **6**, compared to bithiophene (*vide supra*).

We find that the coordinated 1,5-cyclooctadiene could be displaced by suspending **3a** in solutions of isonitriles. Such chemistry yields derivatives of **3a** analogous to poly-**1a** and poly-**1b**. Suspensions of **3a** were reacted with **2a** in THF at room temperature for 12 h yielding **3b**, slightly soluble in some solvents (THF,  $\text{CHCl}_3$ ,  $\text{CH}_2\text{Cl}_2$ ). The infrared spectrum of **3b** is consistent with formation of a *cis* bisisonitrile Pt(II) species. The UV-vis spectrum has two bands, Figure 6b. The peak at 316 nm is a ligand based absorption (**1a** also has a strong band at 316 nm), while the lower energy band is due to the oligomer backbone (cf. **3a**). Reaction of suspensions of **3a** with *t*-butylisonitrile for 10 min in THF at room temperature yields **3c**; this was readily soluble in several solvents ( $\text{CHCl}_3$  and THF), therefore characterization of this oligomer by solution techniques was possible. The methyl region of the  $^1\text{H}$  NMR spectrum contains several peaks, and we attribute these to different environments for the *t*-butyl group depending on the other ligands on the Pt. There are three sets of broad peaks in the thiophene region, corresponding to the three different protons in the tetrathiophene moiety broadened due to the slightly different shifts depending on position in the oligomer. The solution IR

**Figure 6.** UV-vis spectrum of (a) **3a**, (b) **3b**, (c) **3c** in  $\text{CHCl}_3$ .



spectrum of **3c** contains bands due to the isonitrile groups, both on terminal, chloro-substituted Pt groups, and on internal Pt moieties. The UV-vis spectrum has features similar to those observed for **3a** and **3b**, Figure 6c. Since **3c** is soluble, and films can be cast from solution, we were able to examine the thin film electrochemistry of the oligomer. The cyclic voltammogram and  $I_D$ - $V_G$  plot for a thin film of **3c** are shown in Figure 7. The approximate conductivity of the polymer at +1.0 V vs. Ag wire, the positive limit of the scan, is  $0.03 \Omega^{-1}\text{cm}^{-1}$ . Electrochemical cycling (>10 scans) from 0 to +1.25 V vs. Ag in  $\text{CH}_3\text{CN}$  causes degradation of **3c**. There is a shift in the absorption maximum to lower energy by approximately 25 nm and the conductivity increases. Both of these changes are consistent with formation of polythiophene via oxidative degradation.

Powder samples of **3a** and **3b** pressed into In foil, and thin film samples of **3c** cast from THF on Au were all characterized by XPS, Table II. The Pt to S ratio for **3a-3c** is approximately 1:4. **3b** was also analyzed for Fe, and the Fe to Pt ratio is approximately 0.6 to 1; consistent with what is expected by comparison with the XPS analysis of **1a**, a complex with a similar elemental composition to that proposed for **3b**.

Immersion of a freshly prepared film of **3c** in a 10 mM solution of **2a** in  $\text{CH}_3\text{CN}$  for 15 min, followed by washing the film with  $\text{CH}_3\text{CN}$ , results in incorporation of the **2a** into the film, forming surface-confined **3b**, Figure 8, assuming all the *t*-butylisonitrile groups are exchanged by **2a**. This is evidenced by the appearance of an absorption band at 330 nm in the UV-vis spectrum in the film, as well as an additional wave in the cyclic voltammogram which we assign to the coordinated ferrocenyl center of **2a** in the oligomer. There are other changes in the cyclic voltammogram of the reacted oligomer, including a shift to a more positive potential of the oxidation feature which appears at +1.2 V in **3c**. The displacement is accompanied by a change in the  $I_D$ - $V_G$  plot. The drain current decreases by approximately 50% upon reaction with **2a**. This change is associated with the displacement reaction, however it is unclear that the change results

**Figure 7.** (a) Cyclic voltammetry of film of **3c** on Pt microelectrodes in 0.1 M [(*n*-Bu)<sub>4</sub>N]PF<sub>6</sub>/CH<sub>3</sub>CN. (b) I<sub>D</sub>-V<sub>G</sub> characteristic in the same medium for the same pair of derivatized microelectrodes.

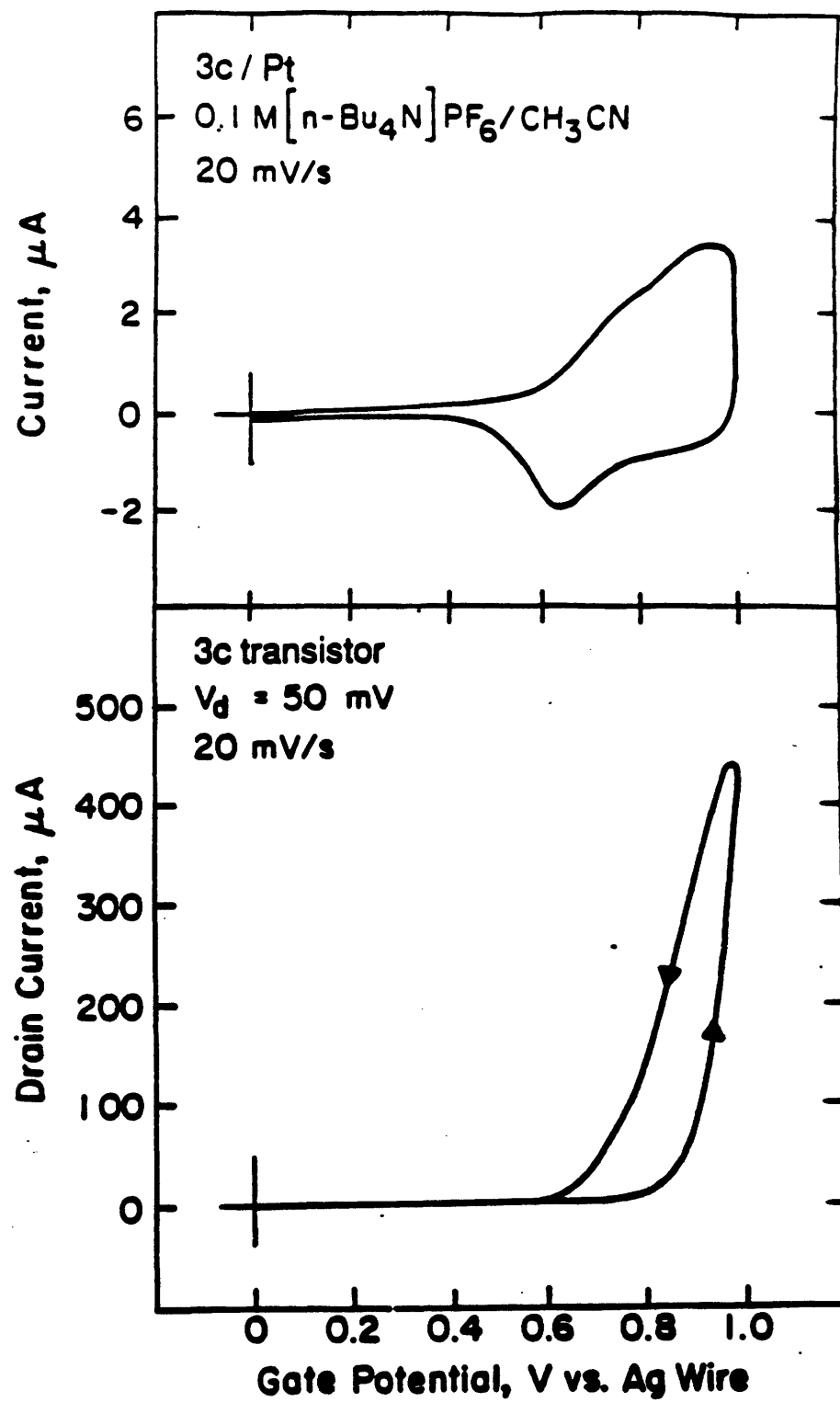
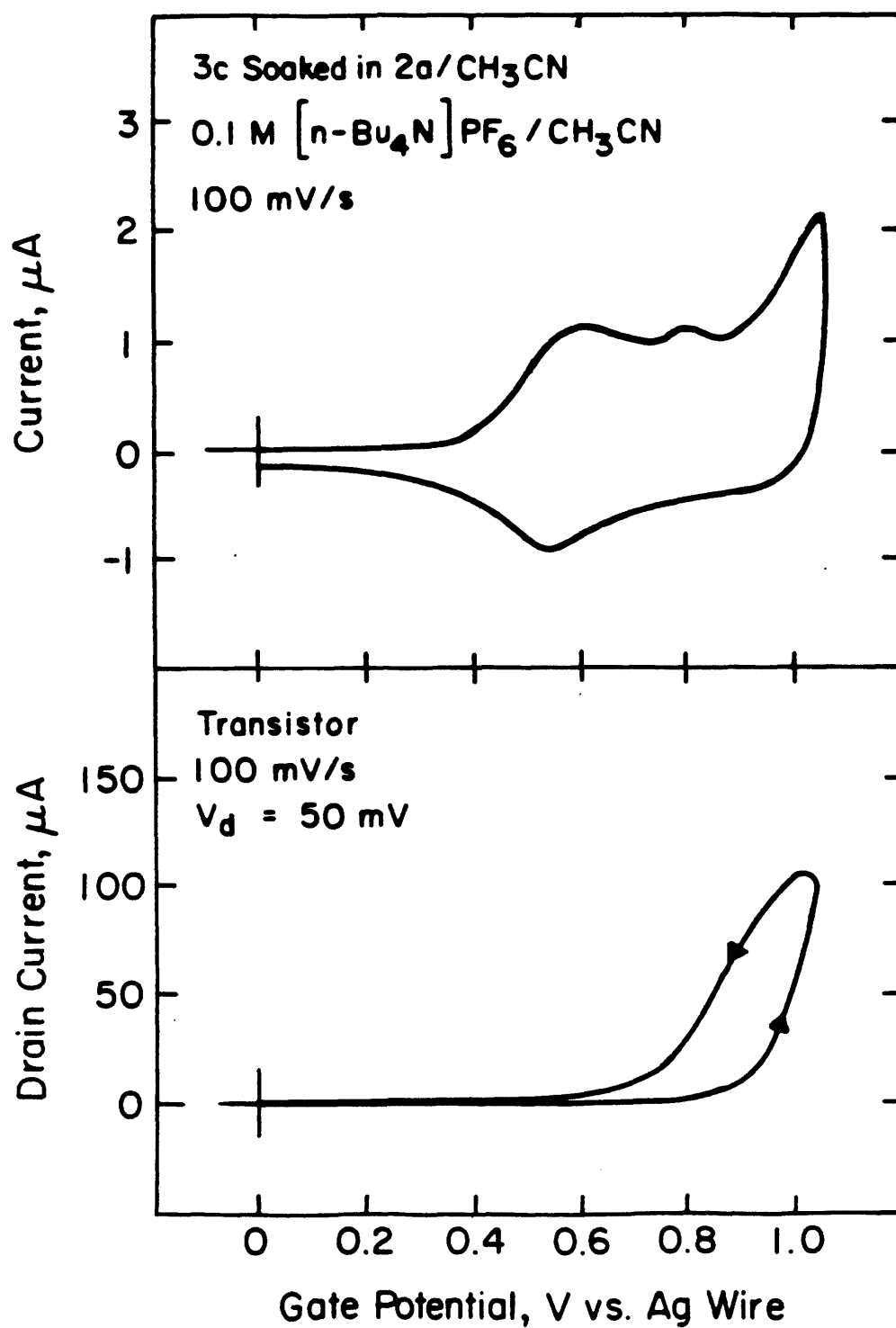




**Figure 8.** (a) Cyclic voltammetry of film of **3c** after immersion in a CH<sub>3</sub>CN solution of **2b**, on Pt microelectrodes in 0.1 M [(*n*-Bu)<sub>4</sub>N]PF<sub>6</sub>/CH<sub>3</sub>CN. (b) I<sub>D</sub>-V<sub>G</sub> characteristic in the same medium for the same pair of derivatized microelectrodes.



only from incorporation of **2a** in the polymer, since **3b** prepared by reaction of **3a** with **2b** readily dissolves in CH<sub>3</sub>CN upon oxidation of the ferrocenyl groups. Thus, the observed change in the cyclic voltammogram of **3c** after reaction with **2b** may be the result of partial dissolution of the film when the incorporated ferrocenyl centers are oxidized.

## Conclusions

The preparation of the novel conducting polymer poly-**1a**, by anodic electropolymerization has been reported. Though insoluble, characterization of this polymer using XPS, surface reflectance IR, and electrochemistry is possible. One important characteristic of poly-**1a** is the reversible substitution of the isonitrile ligands. The exchange of **2a** for **2b** in poly-**1a** causes only a small change in the  $I_D$ - $V_G$  of the polymer, but this is not unexpected since the structural differences between the two polymers is insignificant at the Pt center. Preliminary results show that larger changes in the  $I_D$ - $V_G$  by reactions of the Pt center in poly[*cis*(5'-(2,5-bithienyl))- (triphenylphosphine)<sub>2</sub>platinum(II)] a polymer with a structure analogous to poly-**1a** are possible. Future work will be focused on studies of substitution chemistry and associated changes in the  $I_D$ - $V_G$  characteristics, in order to assess the chemical sensitivity of the conductivity of the polymers.

We have found that **1a** and **1b** can be electropolymerized at a lower potential than the product of reductive elimination from **1a** or **1b**, tetrathiophene. These results indicate that should tetrathiophene be formed, it can only be incorporated into the polymer by reaction of oxidized **1a** or **1b** with neutral tetrathiophene. We do not believe this is occurring to a significant extent, since intentional addition of tetrathiophene to the electropolymerization solution does not cause significant changes in the cyclic voltammogram of the resulting polymer. Additionally, **1c** alone can not be electropolymerized at +1.5 V yet at this potential the product of reductive elimination from **1c**, bithiophene, polymerizes. We conclude that the reductive elimination from **1c** must be occurring to an insignificant extent at +1.5 V. Electropolymerization from a solution containing both terthiophene and **1c** does occur at +1.5 V, and the resulting polymer contains a significant fraction of ferrocenyl groups. Thus, oxidized terthiophene must react with neutral **1c** yielding **1c** containing polymer.

The preparation of the analogs **3a-c** by chemical methods demonstrates an alternative route to the preparation of metal-thiophene polymers which does not involve an oxidation reaction. Thin films of these polymers are shown to be moderately conducting, and isonitrile substitution reactions, analogous to those demonstrated in poly-**1a**, can be carried out. The behavior of these oligomers, in which we know the backbone contains the Pt(II) group, supports our conclusions about the structure of the electropolymerized materials.

## Experimental Section.

**General Methods.** All manipulations were carried out using standard Schlenk techniques. Dichloromethane was distilled from P<sub>2</sub>O<sub>5</sub>. Tetrahydrofuran was distilled from sodium/benzophenone ketyl. Diisopropylamine was distilled from KOH. Solvents for chromatography were reagent grade and were not purified prior to use. <sup>1</sup>H NMR spectra were acquired on Varian XL-300 or Bruker AC-250 instruments. FTIR spectra were acquired on a Nicolet 60SX FTIR instrument. UV-vis spectra were acquired on a HP 8452A diode array spectrometer. Elemental analyses were performed by Oneida Research Services Inc. 4-isocyanophenylferrocene,<sup>42</sup> ferrocenoyl chloride,<sup>43</sup> 5'-(trimethylstannyl)-2,5-bithiophene,<sup>44</sup> (phenyl)<sub>2</sub>(1,5-cyclooctadiene)Pt,<sup>1</sup> 2,2':5',2'':5'',2'''-tetrathiophene,<sup>45</sup> (1,5-cyclooctadiene)dichloroplatinum,<sup>46</sup> and (2-thienyl)<sub>2</sub>(1,5-cyclooctadiene)platinum<sup>1</sup> were prepared as described in the literature.

### ***cis*(5'-(2,5-Bithienyl)<sub>2</sub>(1,5-cyclooctadiene)platinum(II) (6).**

(1,5-cyclooctadiene)dichloroplatinum (0.500 g, 1.34 mmol) and 5'-(trimethylstannyl)-2,5-bithiophene (0.970 g, 2.95 mmol) were dissolved in CH<sub>2</sub>Cl<sub>2</sub> (20 mL) and refluxed overnight. The solvent was removed *in vacuo* and the residual solid washed with hexanes and ether yielding 0.61 g **7** (97%). <sup>1</sup>H NMR ((CD<sub>3</sub>)<sub>2</sub>SO): δ 6.49 (dd, 1 Hz and 4.9 Hz, 2H), 6.31 (d, 3.5 Hz, 2H), 6.22 (dd, 1 Hz and 3.5 Hz, 2H), 6.14 (dd, 3.5 Hz and 4.9 Hz, 2H), 5.80 (d, 3.5 Hz, 2H), 4.59 (m, 4H), 1.72 (m, 8H). MS (EI) 633 (1), 525 (2), 330(100).

### ***cis*(5'-(2,5-Bithienyl)<sub>2</sub>(4-isocyanophenylferrocene)<sub>2</sub>platinum(II) (1a).**

(5'-(2,5-bithienyl)<sub>2</sub>(1,5-cyclooctadiene)platinum(64.9 mg, 0.139 mmol) and 4-isocyanophenylferrocene (80 mg, 0.279 mmol) were dissolved in CH<sub>2</sub>Cl<sub>2</sub> (10 mL). The mixture was stirred for 45 min. The solvent was removed *in vacuo* and the residual solid washed with hexanes yielding 69 mg **1a** (53 %). <sup>1</sup>H NMR (CDCl<sub>3</sub>): δ 7.49 (d, 4H, 9 Hz), 7.39 (d, 4H, 9H), 7.20 (d, 3.7 Hz, 2H), 7.09 (d, 3.6 Hz, 2H), 7.08 (d, 5 Hz, 2H), 6.94 (dd, 5Hz, 2 H), 6.90 (d, 3.7 Hz, 2H). MS (FAB) 769 (83) (M<sup>+</sup>), 481 (100). Anal. Calcd.

for  $C_{50}H_{36}N_2S_4PtFe_2$ : C, 54.60; H, 3.30; N, 2.54. Found: C, 54.96; H, 3.66; N, 2.48. mp 220 °C (dec).

***cis*(5'-(2,5-Bithienyl)<sub>2</sub>(4-isocyanophenylferrocenoate)<sub>2</sub>platinum(II) (1b).** (5'-(2,5-Bithienyl)<sub>2</sub>(1,5-cyclooctadiene)platinum (50 mg, 0.08 mmol) and 4-isocyanophenylferrocene (58 mg, 0.18 mmol) were dissolved in  $CH_2Cl_2$  (10 mL). The mixture was stirred for 30 min. The solvent was removed *in vacuo* and the residual solid washed with hexanes yielding 71 mg **1** (75 %).  $^1H$  NMR ( $CDCl_3$ ):  $\delta$  7.54 (d, 9 Hz, 4H), 7.27 (d, 9 Hz, 4H), 7.19 (d, 4 Hz, 2H), 7.09 (d, 3.6 Hz, 2H), 7.08 (d, 5 Hz, 2H), 6.93 (dd, 5 Hz, 3.6 Hz, 2H), 6.89 (d, 3.6 Hz, 2H), 4.94 (t, 2 Hz, 4H), 4.53 (t, 2 Hz, 4 H), 4.28 (s, 10 H).

***cis*(2-Thienyl)<sub>2</sub>(4-isocyanophenylferrocene)<sub>2</sub>platinum(II) (1c).** (2-Thienyl)<sub>2</sub>(1,5-cyclooctadiene)<sub>2</sub>platinum (100 mg, 0.21 mmol) and 4-isocyanophenylferrocenoate (135 mg, 0.47 mmol) were dissolved in  $CH_2Cl_2$  (10 mL). The mixture was stirred for 60 min. The solvent was removed *in vacuo* and the residual solid washed with hexanes yielding 140 mg **2** (71%).  $^1H$  NMR ( $CDCl_3$ ):  $\delta$  7.48 (d, 8.5 Hz, 4H), 7.44 (d, 4.5 Hz, 2H), 7.37 (d, 8.5 Hz, 4H), 7.12 (dd, 3, 4.5 Hz, 2H), 6.98 (d, 3 Hz, 2H), 4.65 (t, 2 Hz, 4H), 4.39 (t, 2 Hz, 4H), 4.53 (s, 10H).

***cis*(Phenyl)<sub>2</sub>(4-isocyanophenylferrocene)<sub>2</sub>platinum(II) (5a).** (Phenyl)<sub>2</sub>(1,5-cyclooctadiene)<sub>2</sub>platinum (50 mg, 0.11 mmol) and 4-isocyanophenylferrocene (69 mg, 0.24 mmol) were dissolved in  $CH_2Cl_2$  (10 mL). The mixture was stirred for 30 min. The solvent was removed *in vacuo* and the residual solid washed with hexanes yielding 80 mg **5a** (79%).  $^1H$  NMR ( $CDCl_3$ ):  $\delta$  7.93 (m, 8H), 7.27 (d, 8 Hz, 4H), 7.05 (t, 7 Hz, 4H), 6.92 (t, 7 Hz, 2H), 4.62 (d, 1.5 Hz, 4H), 4.37 (d, 1.5 Hz, 4H), 4.00 (s, 10H).

***cis*(Phenyl)<sub>2</sub>(4-isocyanophenylferrocenoate)<sub>2</sub>platinum(II) (5b).** (Phenyl)<sub>2</sub>(1,5-cyclooctadiene)<sub>2</sub>platinum (45 mg, 0.10 mmol) and 4-isocyanophenylferrocenoate (72 mg, 0.22 mmol) were dissolved in  $CH_2Cl_2$  (10 mL). The mixture was stirred for 60 min. The solvent was removed *in vacuo* and the residual solid washed with hexanes yielding 70 mg

**5b** (70%).  $^1\text{H NMR}$  ( $\text{CDCl}_3$ ):  $\delta$  7.44 (d, 8 Hz, 4H), 7.42 (d, 7 Hz, 4H), 7.22 (d, 8 Hz, 4H), 7.05 (t, 7 Hz, 4H), 6.95 (t, 7 Hz, 2H), 4.94 (t, 1.8 Hz, 4H), 4.53 (t, 1.8 Hz, 4H), 4.28 (s, 10H).

**4-Nitrophenylferrocenoate (8)**. A solution of ferrocenoyl chloride (4.90 g, 18.2 mmol), 4-nitrophenol (2.74 g, 19.7 mmol) and pyridine (1 mL) in THF (100 mL) was prepared. The solution was allowed to reflux overnight. More pyridine (2 mL) was added and the reaction was refluxed another hour. The reaction was cooled and water (100 mL) and ether (100 mL) were added. Separation of the organic phase, followed by drying over anhydrous  $\text{MgSO}_4$  and evaporation of the solvent yielded the crude product. Final purification was by chromatography (silica,  $\text{Et}_2\text{O}$ ) yielding 4.44 g (66%) **8**.  $^1\text{H NMR}$  ( $\text{CDCl}_3$ ):  $\delta$  8.30 (d, 9Hz, 2H), 7.36 (d, 9Hz, 2H), 4.96 (t, 2Hz, 2H), 4.55 (t, 2Hz, 2H), 4.30 (s, 5H). IR ( $\text{CH}_2\text{Cl}_2$ ):  $1733\text{ cm}^{-1}$ . Anal. Calcd. for  $\text{C}_{17}\text{H}_{13}\text{NO}_4\text{Fe}$ : C, 58.15; H, 3.73; N, 3.99. Found: C, 58.20; H, 4.30; N, 3.80. mp  $115\text{ }^\circ\text{C}$ .

**4-Aminophenylferrocenoate (9)**. 4-Nitrophenylferrocenoate (2.30 g, 6.20 mmol) was dissolved in ethanol (100 mL) and platinum oxide (0.04 g, 0.18 mmol) was added. Hydrogen was bubbled through the suspension for several minutes and then the flask was pressurized with hydrogen (18 lbs) and stirred for 2 hours. During this time the mixture became yellow. The solvent was removed *in vacuo* and the residual solid purified by chromatography (silica,  $\text{Et}_2\text{O}$ ) to yield 1.73 g (82%) of **9**.  $^1\text{H NMR}$  ( $\text{CDCl}_3$ ):  $\delta$  6.92 (d, 9 Hz, 2H), 6.67 (d, 9 Hz, 2H), 4.90 (t, 1.8 Hz, 2H), 4.44 (t, 1.8 Hz, 2H), 4.25 (s, 5H), 3.60 (s, 2H). IR ( $\text{CH}_2\text{Cl}_2$ ):  $1721\text{ cm}^{-1}$ . Anal. Calcd. for  $\text{C}_{17}\text{H}_{15}\text{NO}_2\text{Fe}$ : C, 63.58; H, 4.71; N, 4.36. Found: C, 63.44; H, 5.02; N, 4.47. mp  $123\text{ }^\circ\text{C}$ .

**4-Formamidophenylferrocenoate (10)**. 4-Aminophenylferrocenoate (1.50 g, 4.40 mmol) was dissolved in ethyl formate (50 mL) and refluxed overnight. Water (100 mL) and methylene chloride (100 mL) were added and the product was extracted. The organic layer was washed once with water (100 mL), dried over anhydrous  $\text{MgSO}_4$ , and the solvent removed *in vacuo*. The crude product was purified by chromatography (silica,



Et<sub>2</sub>O) yielding 0.96 g (59%) **10**. <sup>1</sup>H NMR (CDCl<sub>3</sub>): δ 8.63 (d, 11 Hz, 1H), 8.34 (d, 1.8 Hz, 1H), 7.81 (d, 12 Hz, 2H, broad), 7.56 (d, 9 Hz, 2H), 7.41 (s, 1H), 7.2-7.1 (m, 4H), 4.94 (m, 2H), 4.50 (m, 2H), 4.29 (s, 5H). <sup>13</sup>C NMR (CDCl<sub>3</sub>): δ 170.5, 162.2, 158.7, 147.3, 134.9, 132.2, 123.0, 122.2, 120.9, 120.2, 72.1, 72.0, 70.7, 70.0. IR (CH<sub>2</sub>Cl<sub>2</sub>): 1725, 1702 cm<sup>-1</sup>. Anal. Calcd. for C<sub>18</sub>H<sub>15</sub>NO<sub>3</sub>Fe: C, 61.92; H, 4.33; N, 4.01. Found: C, 61.60; H, 4.22; N, 4.25. mp 128 °C.

**4-Isocyanophenylferrocenoate (2b)**. 4-Formamidophenylferrocenoate (0.80 g, 2.1 mmol) and diisopropylamine (1.40 mL, 10.0 mmol) were dissolved in CH<sub>2</sub>Cl<sub>2</sub> (7 mL) and cooled to 0 °C under Ar. POCl<sub>3</sub> (0.50 mL, 5.4 mmol) was added dropwise, and the solution stirred 1 h at 0 °C. After warming to room temperature a solution of Na<sub>2</sub>CO<sub>3</sub> (1.0 g) in water (10 mL) was added and the solution stirred 1 h at room temperature. CH<sub>2</sub>Cl<sub>2</sub> was added (50 mL) and the product extracted. The organic layer was washed once with water (100 mL), dried over anhydrous MgSO<sub>4</sub>, and the solvent removed *in vacuo*. The product was purified by chromatography (alumina, Et<sub>2</sub>O) yielding 0.29 g (39%) **3**. <sup>1</sup>H NMR (CDCl<sub>3</sub>): δ 7.43 (d, 9 Hz, 2H), 7.21 (d, 9 Hz, 2H), 4.93 (d, 1.9 Hz, 2H), 4.52 (d, 1.9 Hz, 2H), 4.28 (s, 5H). <sup>13</sup>C NMR (CDCl<sub>3</sub>): δ 169.7, 164.3, 151.0, 127.5, 122.8, 72.3, 70.7, 70.0, 69.2. IR (CH<sub>2</sub>Cl<sub>2</sub>): 2130, 1733 cm<sup>-1</sup>. Anal. Calcd. for C<sub>17</sub>H<sub>13</sub>NFe: C, 65.29; H, 4.26; N, 4.23. Found: C, 65.09; H, 4.14; N, 4.19. mp 114 °C.

**5,5'''Di(tributylstannyl)-2,2':5',2'':5'',2'''-tetrathiophene (4)**. 2,2':5',2'':5'',2'''-Tetrathiophene (1.00 g, 3.03 mmol) was dissolved in THF (150 mL) and cooled in an ice bath. *n*-BuLi (2.7 mL, 2.37 M in hexanes, 6.40 mmol) was added via syringe, and the mixture was allowed to warm to room temperature and left stirring overnight. Tributylstannylchloride (1.73 mL, 6.40 mmol) was added and the solution left stirring for a further 24 hours. The solvent was removed *in vacuo* and ether (100 mL) added. The ether layer was washed with water (2 x 100 mL), dried over MgSO<sub>4</sub> and the ether removed yielding 2.30 g (96%) of a dark brown oil, which was used without further

purification.  $^1\text{H}$  NMR ( $\text{C}_6\text{D}_6$ ):  $\delta$  7.30 (d, 3.4 Hz, 2H), 7.08 (d, 3.4 Hz, 2H), 6.92 (d, 3.8 Hz, 2H), 6.82 (d, 3.8 Hz, 2H).  $^{13}\text{C}$  NMR ( $\text{CDCl}_3$ ):  $\delta$  142.3, 136.9, 136.3, 136.0, 135.5, 124.8, 124.0, 29.0, 27.3, 13.8, 11.0.

**Preparation of Polymers.** Poly-**1a** was prepared by cycling an electrode between 0 and +1.25 V vs. Ag wire in a 5-10 mM solution of **1a** in 0.1 M [*n*-Bu] $_4$ N]PF $_6$ /CH $_2$ Cl $_2$ . Electropolymerization was on two Au microelectrodes (100  $\mu\text{m}$  x 2  $\mu\text{m}$ )<sup>39,47</sup> or Au macroelectrodes (~ 2 cm x 2 cm, and separated from each other by ~ 2  $\mu\text{m}$ ) and yielded red films of poly-**1a**. Prior to use the microelectrodes were cleaned by placing a drop of freshly prepared 3:1 H $_2$ SO $_4$ /30% H $_2$ O $_2$  on the electrode for 10 s, followed by characterization in 5 mM Ru(NH $_3$ ) $_6$  aqueous solution by scanning from 0 to -0.5 V vs. SCE and recording the diffusion limited wave for the Ru reduction.

Oligomer **3a** was prepared by reaction of **4** (0.500 g, 0.55 mmol) and (1,5-cyclooctadiene)dichloroplatinum (0.241 g, 0.644 mmol) dissolved in 50 mL THF and refluxed under Ar for 15 hours. During the reaction a solid precipitated and was collected by filtration. The solid was washed with hexanes yielding 0.26 g of poly-**2** as a dark yellow solid. Anal.: C, 42.26; H, 3.40; N, 0.08; S, 16.81; Cl, 3.13; Sn, 0.63. **3b** was prepared by stirring a suspension of **3a** (50 mg) and **2a** (46 mg, 0.16 mmol) in THF for 12 hours. The THF was removed *in vacuo* and the product washed with hexanes. **3c** was prepared by stirring a suspension of **3a** (50 mg) and *t*-butylisonitrile (3 drops) in THF (5 mL) for 1 hr. The suspension dissolved almost immediately. The THF was removed *in vacuo* and the product washed with hexanes.  $^1\text{H}$  NMR ( $\text{CDCl}_3$ ):  $\delta$  7.15-7.07 (m, 2H), 7.02-6.85 (m, 4H), 6.78-6.72 (m, 2H), 1.67, 1.62, 1.57, 1.54 (broad singlets, total integration 20 H).

**Electrochemistry.** Cyclic voltammetry was conducted using a Pine RDE-4 bipotentiostat and a Kipp and Zonen XY recorder either in a nitrogen filled Vacuum Atmosphere drybox or in a sealed flask under argon. Dichloromethane was distilled from P $_2$ O $_5$  and stored in the drybox. [*n*-Bu $_4$ N]PF $_6$  was recrystallized from ethanol and dried in

a vacuum oven overnight. The reference electrode was a silver wire and the counter electrode a 1 cm<sup>2</sup> piece of Pt gauze. The silver wire was referenced to the cobaltocene/cobaltocenium couple. Constant potential coulometry was done using a PAR 173 potentiostat and a PAR 179 coulometer. Cyclic voltammetry and I<sub>D</sub>-V<sub>G</sub> measurements of cast films was done on highly interdigitated Pt microelectrode arrays which have been previously described.<sup>38</sup>

**XPS and Surface Reflectance IR.** XPS spectra were obtained on a Surface Science Instruments Model SSX-100 spectrometer using monochromatic Al K $\alpha$  radiation and operating at 10<sup>-8</sup> Torr. A 1 mm spot size was used. Surface reflectance IR spectra were acquired using a Spectra-Tech reflectance accessory. Electropolymerized samples were prepared on pieces of silicon wafers (1-8 cm<sup>2</sup>) which had been coated with 1000 Å of Au. Thin films of **1a** and **2a** were cast from CH<sub>2</sub>Cl<sub>2</sub> onto the same substrates. **3a-c** were pressed as solids into In foil for XPS and were cast from THF solution for surface reflectance IR.

**References.**

- (1) Eaborn, C.; Odell, K. J.; Pidcock, A. *J. Chem. Soc., Dalton* **1978**, 357.
- (2) Kotani, S.; Shiina, K.; Sonogashira, K. *J. Organomet. Chem.* **1992**, 492, 403.
- (3) Hanack, M.; Datz, A.; Fay, R.; Fischer, K.; Keppeler, U.; Koch, J.; Metz, J.; Mezger, M.; Schneider, O.; Schulze, H.-J. in "Handbook of Conducting Polymers"; T. A. Skotheim, Ed.; Marcel Dekker: New York, 1986.
- (4) Marder, T. B.; Lesley, G.; Yuan, Z.; Fyfe, H. B.; Chow, P.; Stringer, G.; Jobe, I. R.; Taylor, N. J.; Williams, I. D.; Kurtz, S. K. *ACS Symp. Ser.* **1991**, 455, 606.
- (5) Khan, M. S.; Davies, S. J.; Kakkar, A. K.; Schwartz, D.; Lin, B.; Johnson, B. F. G.; Lewis, J. *J. Organomet. Chem.* **1992**, 424, 87.
- (6) Dray, A. E.; Wittmann, F.; Friend, R. H.; Donald, A. M.; Khan, M. S.; Lewis, J.; Johnson, B. F. G. *Synth. Met.* **1991**, 41-43, 871.
- (7) Kotani, S.; Shiina, K.; Sonogashira, K. *Appl. Organomet. Chem.* **1991**, 5, 417.
- (8) Johnson, B. F. G.; Kakkar, A. K.; Khan, M. S.; Lewis, J. *J. Organomet. Chem.* **1991**, 409, C12.
- (9) Fujikura, Y.; Sonogashira, K.; Hagihara, N. *Chem. Lett.* **1975**, 1067.
- (10) Sonogashira, K.; Takahashi, S.; Hagihara, N. *Macromolecules* **1977**, 10, 879.
- (11) Sonogashira, K.; Kataoka, S.; Takahashi, S.; Hagihara, N. *J. Organomet. Chem.* **1978**, 160, 319.
- (12) Sonogashira, K.; Ohga, K.; Takahashi, S.; Hagihara, N. *J. Organomet. Chem.* **1980**, 188, 237.
- (13) Takahashi, S.; Kariya, M.; Yatake, T.; Sonogashira, K.; Hagihara, N. *Macromolecules* **1978**, 11, 1063.
- (14) Takahashi, S.; Murata, E.; Sonogashira, K.; Hagihara, N. *J. Polym. Sci. Chem. Ed.* **1980**, 18, 661.
- (15) Takahashi, S.; Ohyama, Y.; Murata, E.; Sonogashira, K.; Hagihara, N. *J. Polym. Sci. Polym. Chem. Educ.* **1980**, 18, 349.

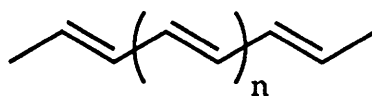
- (16) Takahashi, S.; Morimoto, H.; Murata, E.; Kataoka, S.; Sonogashira, K.; Hagihara, N. *J. Polym. Sci. Polym. Chem. Educ.* **1982**, *20*, 565.
- (17) Nalwa, H. S. *Appl. Organomet. Chem.* **1990**, *4*, 91.
- (18) Hagihara, N. J.; Sonogashira, K.; Takahashi, S. *Adv. Poly. Sci.* **1981**, *41*, 149.
- (19) Chisholm, M. H. *Angew. Chem.* **1991**, *103*, 690.
- (20) Nishihara, H.; Shimura, T.; Ohkubo, A.; Matsuda, N.; Aramaki, K. *Adv. Mater.* **1993**, *5*, 752.
- (21) Ochmanska, J.; Pickup, P. G. *Can. J. Chem.* **1991**, *69*, 653.
- (22) Davies, S. J.; Johnson, B. F. G.; Khan, M. S.; Lewis, J. *J. Chem. Soc., Chem. Commun.* **1991**, 187.
- (23) Davies, S. J.; Johnson, B. F. G.; Lewis, J.; Khan, M. S. *J. Organomet. Chem.* **1991**, *401*, C43.
- (24) Fyfe, H. B.; Mlekuz, M.; Zargarian, D.; Taylor, N. J.; Marder, T. B. *J. Chem. Soc., Chem. Commun.* **1991**, 188.
- (25) McDonald, R.; Sturge, K. C.; Hunter, A. D.; Shilliday, L. *Organometallics* **1992**, *11*, 898.
- (26) Nast, R.; Grouhi, H. *J. Organomet. Chem.* **1979**, *182*, 197.
- (27) Onitsuka, K.; Ogawa, H.; Joh, T.; Takahashi, S.; Yamamoto, Y.; Yamazaki, H. *J. Chem. Soc. Dalton Trans.* **1991**, 1531.
- (28) Wong, A.; Kang, P. C. W.; Tagge, C. D.; Leon, D. R. *Organometallics* **1990**, *9*, 1992.
- (29) Wright, M. E. *Macromolecules* **1989**, *22*, 3256.
- (30) Schiavon, G.; Zotti, G.; Bontempelli, G. *J. Electroanal. Chem.* **1984**, *161*, 323.
- (31) Kossmehl, G. *Makromol. Chem., Macromol. Symp.* **1986**, *4*, 45.
- (32) Kossmehl, G. A. in "Handbook of Conducting Polymers"; T. A. Skotheim, Ed.; Marcel Dekker: New York, 1986; pp 351.
- (33) Frapper, G.; Kertesz, M. *Inorg. Chem.* **1993**, *32*, 732.

- (34) Thackerey, J. W.; White, H. S.; Wrighton, M. S. *J. Phys. Chem.* **1985**, *89*, 5133.
- (35) Park, L. Y.; Ofer, D.; Gardner, T. J.; Schrock, R. R.; Wrighton, M. S. *Chem. Mater.* **1992**, *4*, 1388.
- (36) Ofer, D.; Wrighton, M. S. *J. Am. Chem. Soc.* **1988**, *110*, 4467.
- (37) Ofer, D.; Crooks, R. M.; Wrighton, M. S. *J. Am. Chem. Soc.* **1990**, *112*, 7869.
- (38) Ofer, D.; Park, L. Y.; Wrighton, M. S.; Schrock, R. R. *Chem. Mater.* **1991**, *3*, 573.
- (39) Kittlesen, G. P.; White, H. S.; Wrighton, M. S. *J. Am. Chem. Soc.* **1984**, *106*, 7389.
- (40) Natan, M. J.; Wrighton, M. S. in "Progress in Inorganic Chemistry"; S. J. Lippard, Ed.; John Wiley and Sons: New York, 1989; Vol. 37.
- (41) Kim, K. S.; Winograd, N.; Davis, R. E. *J. Am. Chem. Soc.* **1971**, *93*, 6296.
- (42) Hickman, J. J.; Zou, C.; Ofer, D.; Harvey, P. D.; Wrighton, M. S.; Laibinis, P. E.; Bain, C. E.; Whitesides, G. M. *J. Am. Chem. Soc.* **1989**, *111*, 7271.
- (43) Pauson, P. C.; Watts, W. E. *J. Chem. Soc.* **1963**, 2990.
- (44) Rossi, R.; Carpita, A.; Ciafalo, M.; Houben, J. L. *Gazz. Chim. Ital.* **1990**, *120*, 793.
- (45) Shabana, R.; Galal, A.; Mark, H. B. J.; Zimmer, H.; Gronowitz, S.; Hornfeldt, A. *Phosphorus, Sulfur and Silicon* **1990**, *48*, 239.
- (46) McDermott, J. X.; White, J. F.; Whitesides, G. M. *J. Am. Chem. Soc.* **1976**, *98*, 6521.
- (47) Paul, E. W.; Ricco, A. J.; Wrighton, M. S. *J. Phys. Chem.* **1985**, *89*, 1441.

## **Chapter 4**

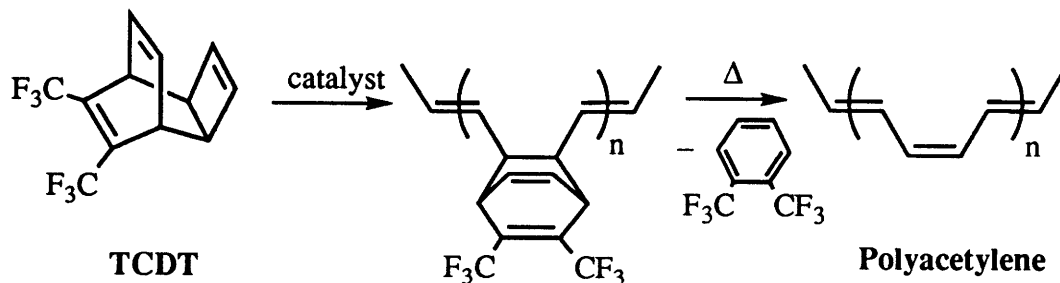
### **Electrochemical Properties of Cyclopolymers of 1,6-Heptadiyne Derivatives Prepared Using Well-Defined Alkylidene Complexes**

Polyacetylene,  $(\text{CH})_n$ , the conjugated polymer with the simplest structure, has been extensively studied, both theoretically and experimentally.<sup>1,2</sup> Polyacetylene is highly conductive when doped,<sup>3</sup> particularly when oriented,<sup>4</sup> and its simple structure has stimulated theoretical interest in the basis of conductivity in conjugated materials.



polyacetylene

Polyacetylene was first prepared from acetylene gas using Ziegler type catalysts.<sup>5,6</sup> Unfortunately, the polyacetylene prepared directly by these and other routes is insoluble. Several routes to polyacetylene that involve soluble precursor polymers have been developed. Grubbs and coworkers prepared polybenzvalene, an unstable precursor polymer which is converted to polyacetylene thermally.<sup>7,8</sup> A similar approach was developed by Feast using 7,8-bistrifluoromethyl-tricyclo[4.2.2.0<sup>2,5</sup>]deca-3,7,9-triene (TCDT) as the monomer (see below).<sup>9-12</sup> After polymerization, the polymer can be heated to cause elimination of 1,2-(trifluoromethyl)benzene in a retro-Diels-Alder type reaction yielding polyacetylene. This preparation is often called the Durham route, after the researchers who discovered the technique at the University of Durham. All of these methods for the preparation of polyacetylene still lead to intractable material.





One approach to making polyacetylene which is tractable has been to put substituents on the backbone. The polymers formed in this way are soluble, and therefore can be cast into films; however, the polymers usually have a dramatically lower average conjugation length, and in some cases aggregate.<sup>13-19</sup> The conductivity of the substituted materials has in general been much lower than the parent, unsubstituted polyacetylene, a fact which has been attributed to the low conjugation lengths.

A potentially interesting class of polyenes are those prepared by cyclopolymerization of 1,6-heptadiyne derivatives. These polymers have been prepared using several classical methods, including Ziegler-Natta catalysts,<sup>20,21</sup> Pd(II) catalysts<sup>22-25</sup> and olefin-metathesis catalysts.<sup>26-43</sup> The polymers are often insoluble, and no control of chain length has been reported. Using well-defined alkylidene complexes as catalysts a variety of polymers have been prepared by ring-opening metathesis polymerization of norbornenes and norbornadienes<sup>44</sup> Fox and Schrock reported that such a catalyst,  $\text{Mo}(\text{CHCMe}_2\text{Ph})(\text{NAr})(\text{OR}_{\text{F6}})_2$ ,  $\text{Ar} = 2,6\text{-}i\text{-Pr}_2\text{-C}_6\text{H}_3$ ,  $\text{OR}_{\text{F6}} = \text{OCMe}(\text{CF}_3)_2$  (**1**), could be used to effect living cyclopolymerization of a 1,6-heptadiyne, diethyldipropargylmalonate.<sup>45</sup> The polymers were highly soluble and highly conjugated, properties which made the polymers potential candidates for soluble, conducting derivatives of polyacetylene.

Previously, our group has studied the electrochemistry of Durham polyacetylene, prepared using the Schrock catalyst, **1**.<sup>46</sup> The precursor route permitted casting of thin films of the precursor film followed by heating to effect the retro-Diels-Alder directly on the microelectrodes. These experiments, done in liquid  $\text{SO}_2$  as the electrochemical solvent, demonstrated that polyacetylene had a finite window of conductivity as a function of electrochemical potential. Because the method used to prepare the polymers was a living polymerization, samples of different chain lengths could be readily prepared. The conductivity as a function of chain length of the polymer, as well as the conductivity of shorter polyenes was studied.

In this chapter the electrochemical characterization polymers prepared by cyclopolymerization of dipropargyl malonate esters using a well-defined alkylidene complex as the catalyst is described. The preparation, characterization and study of some of the other properties of these polymers are described elsewhere.<sup>47,48</sup> The solution and thin-film cyclic voltammetry of a series of polymers, in which both the nature of the ester group and the chain-length are varied, is reported. The potential dependence of the conductivity of thin-films of the homopolymers is studied. Cyclic voltammetry and conductivity measurements were also done on thin-films of copolymers, prepared from monomer solutions containing both a 1,6-heptadiyne and TCDT.

## Results and Discussion

Homopolymers of diethyl dipropargylmalonate, **2** and di-(1R,2S,5R)-(-)-menthyl dipropargylmalonate, **3** were prepared using **1** as a catalyst in DME (Scheme I). The polymerization reaction was terminated, usually after approximately 60 minutes, in a Wittig-like reaction by adding benzaldehyde. Random copolymers of TCD and **3** each containing a total of 50 equivalents of the two monomers were also prepared. Random copolymers containing **2** and TCDT (poly[(TCDT)<sub>x</sub>(**2**)<sub>y</sub>]) were synthesized in high yield and had low polydispersities (Table I).

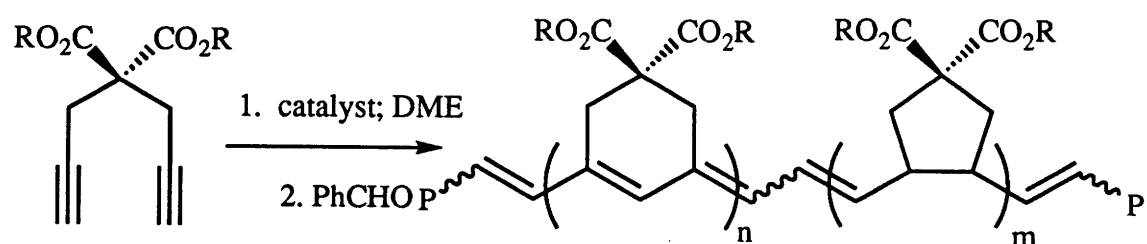
### Solution Electrochemistry of Poly(**2**) and Poly(**3**(-)).

Solutions of the poly(**2**)<sub>n</sub> prepared using **1** in DME were characterized by cyclic voltammetry in 0.1 M [Et<sub>4</sub>N]AsF<sub>6</sub> / CH<sub>3</sub>CN. The cyclic voltammogram of the poly(**2**)<sub>20</sub> at 100 mV/s exhibited a poorly-defined anodic peak at 0.75 V in the potential range 0 to 1.2 V, and a corresponding small return wave at 0.65 V (Figure 1). Voltammograms of solutions of the poly(**2**)<sub>5</sub> and poly(**2**)<sub>10</sub> contained the same anodic features as poly(**2**)<sub>20</sub>, the only differences being slight shifts in peak positions. The voltammogram of a solution of poly(**2**)<sub>80</sub> under the same conditions was broad and featureless. Some anodic deposition of polymer onto the electrode was observed with cycling from 0 to 1.25 V. The voltammogram of the poly(**3**(-))<sub>20</sub> in 0.1 M [*n*-Bu<sub>4</sub>N]PF<sub>6</sub> / CH<sub>2</sub>Cl<sub>2</sub> showed only a very broad anodic feature with no discernible peaks.

### Thin Film Electrochemistry of Poly(**3**(-)).

We were unable to study the thin-film electrochemistry of poly(**2**) due to its solubility in most solvents that are suitable for electrochemistry. Poly(**3**(-)), on the other hand, was insoluble in acetonitrile and therefore we were able to characterize solution-cast thin films of these polymers by cyclic voltammetry in 0.1 M [*n*-Bu<sub>4</sub>N]PF<sub>6</sub> / CH<sub>3</sub>CN. Films of poly(**3**(-)) of various lengths exhibited a well-defined, sharp wave at 0.8 V. The cyclic voltammogram of a thin film of the poly(**3**(-))<sub>40</sub> is shown in Figure 2a. The

## Scheme I



catalyst = Mo(NAr)(CHCMe<sub>2</sub>Ph)(OR<sub>F6</sub>)<sub>2</sub>  
 (1; Ar = 2,6-*i*-Pr<sub>2</sub>-C<sub>6</sub>H<sub>3</sub>,  
 OR<sub>F6</sub> = OCMe(CF<sub>3</sub>)<sub>2</sub>)

R = Et (2), 1R,2S,5R-(-)-menthyl (3(-)),  
 1S,2R,5S-(+)-menthyl (3(+))

**Table I.** Data for Homopolymers, Random and Block Copolymers.

polymer		$M_n^a$	$M_w/M_n^a$	$\sigma$ ( $\Omega^{-1}\text{cm}^{-1}$ ) <sup>b</sup>
poly(2) <sub>5</sub>		3640	1.21	-
poly(2) <sub>10</sub>		6110	1.24	-
poly(2) <sub>20</sub>		8790	1.25	-
poly(2) <sub>80</sub>		23200	1.23	-
poly(3(-))		12300	1.19	-
poly(3(-))		25000	1.17	-
poly[(TCDT) <sub>25</sub> (3(+)) <sub>25</sub> ]	<b>4a</b>	31500	1.15	$4 \times 10^{-2}$
poly[(TCDT) <sub>30</sub> (3(+)) <sub>20</sub> ]	<b>4b</b>	29100	1.12	$6 \times 10^{-2}$
poly[(TCDT) <sub>35</sub> (3(+)) <sub>15</sub> ]	<b>4c</b>	22600	1.17	$7 \times 10^{-2}$
poly[(TCDT) <sub>50</sub> (2) <sub>50</sub> ]	<b>4d</b>	35400	1.11	$2 \times 10^{-2}$
poly[(TCDT) <sub>30</sub> (2) <sub>70</sub> ]	<b>4e</b>	31600	1.12	$3 \times 10^{-4}$
[poly(TCDT) <sub>10</sub> ] <sub>2</sub> poly(3(+)) <sub>20</sub>	<b>4f</b>	29600	1.17	$3 \times 10^{-4}$

<sup>a</sup> Determined by GPC on-line viscometry versus a polystyrene universal calibration curve (Viscotek). <sup>b</sup> Average conductivity at potential of maximum conductivity.

**Figure 1.** Cyclic voltammogram of a thin film of poly (**2**)<sub>20</sub> at a Pt electrode in 0.1 M [*n*-Et<sub>4</sub>N]AsF<sub>6</sub> / CH<sub>3</sub>CN at 100 mV/s.

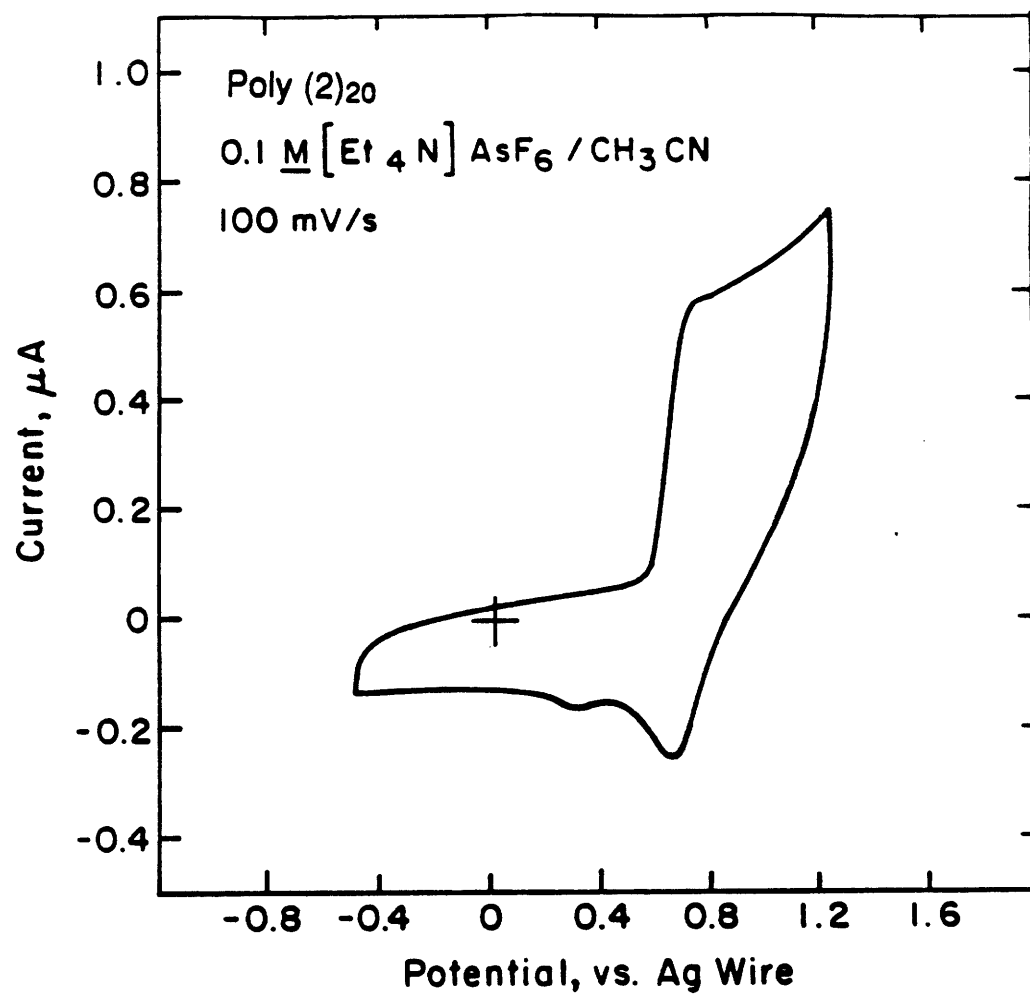
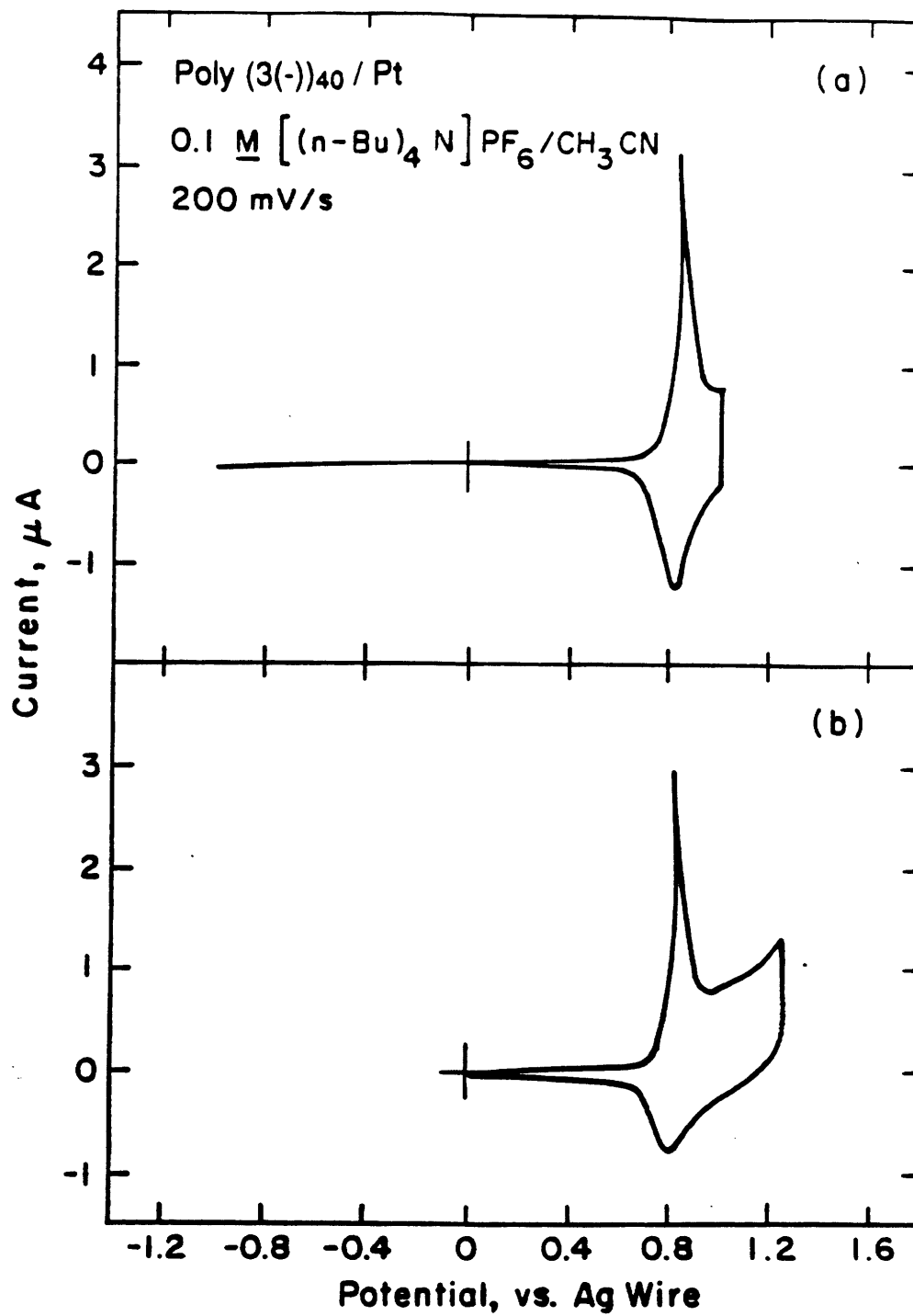


**Figure 2.** (a) Cyclic voltammogram of a thin film of poly (**3(-)**)<sub>40</sub> on a Pt electrode in 0.1 M [*n*-Bu<sub>4</sub>N]PF<sub>6</sub> / CH<sub>3</sub>CN from -1.0 V to 1.0 V vs. Ag; (b) Cyclic voltammogram of poly (**3(-)**)<sub>40</sub> from 0 V to 1.25 V.





oxidation peak at 0.85 V and the corresponding reduction peak at 0.8 V are sharp. In addition, the anodic peak current varies linearly with scan rate, as expected for a surface confined electroactive species.<sup>49</sup> Scanning to 1.2 V results in a broad oxidation of the polymer and a loss of intensity on the return wave (Figure 2b). The voltammogram of the poly(3(-))<sub>20</sub> contains a similar sharp oxidation at 0.9 V and a corresponding reduction peak at 0.85 V. Scanning to 1.5 V causes the reduction peak to almost completely disappear. Several cycles to 1.5 V caused the film to become red and eventually turn colorless, suggesting decomposition or dissolution of the polymer under these conditions.

UV/vis spectroelectrochemistry of thin films of poly(3(-))<sub>20</sub> on indium-tin oxide/glass electrodes demonstrated that the peak at 534 nm which is present for the neutral polymer film disappears upon electrochemical oxidation to 1.0 V vs. Ag in 0.1 M [*n*-Bu<sub>4</sub>N]PF<sub>6</sub>/CH<sub>3</sub>CN (Figure 3) and at the same time a new absorption appears in the near-IR region. This potential is 100 mV more positive than the oxidation peak in the cyclic voltammogram of this polymer. When the polymer sample is returned to its neutral state (0 V vs. Ag), the 534 nm band reappears though the intensity is reduced. The observed changes in spectral properties are consistent with the absorption changes observed upon oxidative doping of polyacetylene<sup>50</sup> and of substituted polyacetylenes.<sup>51</sup>

Microelectrode devices developed in these laboratories may be used for *in situ* potential dependent measurement of the conductivity of solution cast polymer films. The method has been described previously for the measurement of the conductivities of polyacetylene films.<sup>46</sup> Using this technique we measured the drain current ( $I_D$ ) as a function of gate potential ( $V_D$ ) for thin films of poly(3(-))<sub>20</sub>. The drain current flows between the "source" and "drain" microelectrodes when the sample is conducting due to the small applied drain voltage ( $V_D$ ). Surprisingly, we found that the drain current was negligible over the potential range 0 to 1.2 V, implying that the conductivity of poly(3(-))<sub>20</sub> over this potential region is very low ( $\sigma < 10^{-6} \Omega^{-1}\text{cm}^{-1}$ ). This result is quite different from the conductivity of the analogous unsubstituted poly(TCDT)<sub>20</sub> ( $\sigma = 3 \times$

$10^{-1} \Omega^{-1}\text{cm}^{-1}$ ).<sup>46</sup> The conductivities of other substituted polyacetylenes has been studied, and it has been observed that substituted polyacetylenes containing predominantly cis double bonds results in conductivities 2-3 orders of magnitude lower than the comparable trans materials.<sup>1,52</sup> It is possible that the extremely low conductivity observed in poly(**3(-)**)<sub>20</sub> is related to the presence of cis double bonds in the backbone. <sup>13</sup>C NMR analysis of poly(**3(+)**)<sub>40</sub> the ratio of five- to six-membered rings is approximately 1:1.<sup>48</sup> The five-membered rings enforce a cis conformation at the double bond which is in the ring, thus polymers containing a significant amount of five-membered rings must contain cis double bonds.

### Thin Film Electrochemistry of Copolymers

The copolymers prepared from **3(+)** and TCDT (**4a** - **4c**; Table I) were characterized by cyclic voltammetry on solution-cast thin films on Pt electrodes. Acetonitrile was used for the electrochemistry, since the films were insoluble in acetonitrile. The voltammograms of films of **4c** (70% TCDT) and **4a** (50% TCDT) which had been heated to 125 °C for 10 min are shown in Figures 4 and 5a, respectively. The anodic and cathodic features at 0.7 V for **4a** are broader than those observed for poly(**2c(-)**)<sub>20</sub>, but the separation between the anodic and cathodic peaks is still very small. As the content of TCDT is increased to 70% (**4c**), a shoulder appears at 0.9 V in the anodic scan and at 0.55 V on the return cycle (Figure 4). These shoulders are evident in voltammogram of **4b** (60% TCDT). UV/vis results suggest that the "random" copolymers of TCDT and **3(+)** actually contain largely uninterrupted sequences of poly(**3(+)**), i.e., they are virtually block copolymers.<sup>48</sup> This can be ascribed to the relatively slow polymerization of **3(+)**, presumably for steric reasons. These results suggest that long segments of unsubstituted polyacetylene may be electrochemically independent of the cyclopolymer segments and that these shoulders in the cyclic voltammogram are due to the polyacetylene fragments. (The cyclic voltammogram of

**Figure 3.** (a) UV/vis spectrum of a thin film of poly (3(-))<sub>20</sub> on an indium-tin oxide electrode held at 0 V vs. Ag in 0.1 M [*n*-Bu<sub>4</sub>N]PF<sub>6</sub> / CH<sub>3</sub>CN; (b) Same film held at 1.0 V; (c) Same film held at 0 V again.

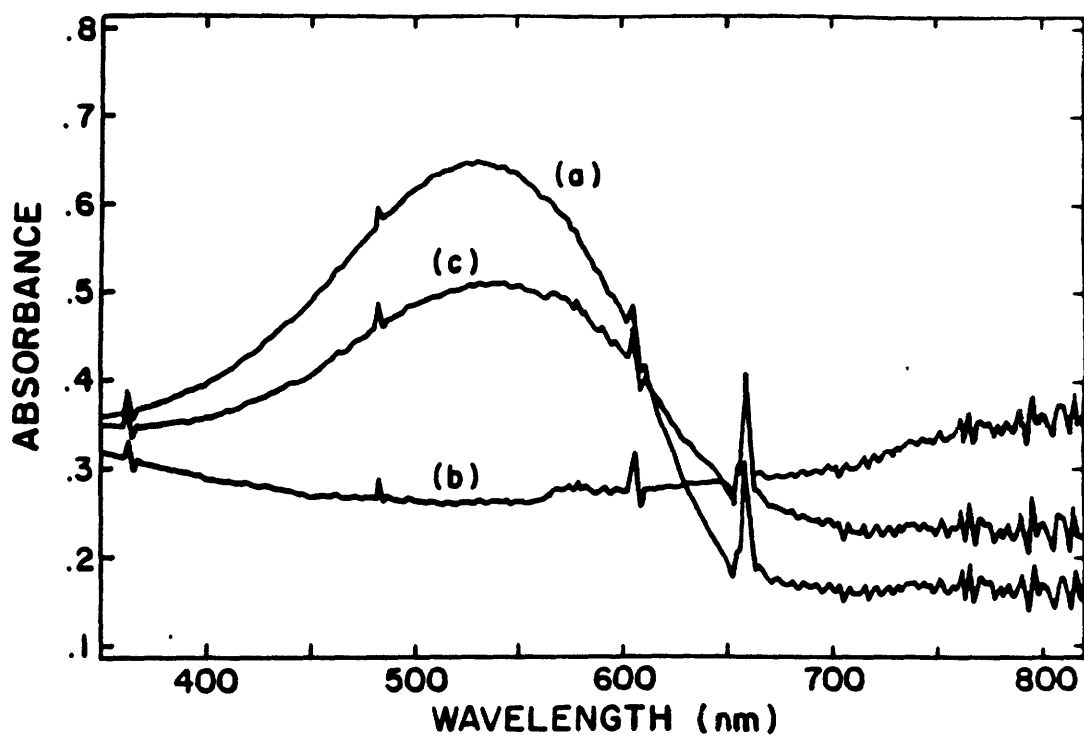
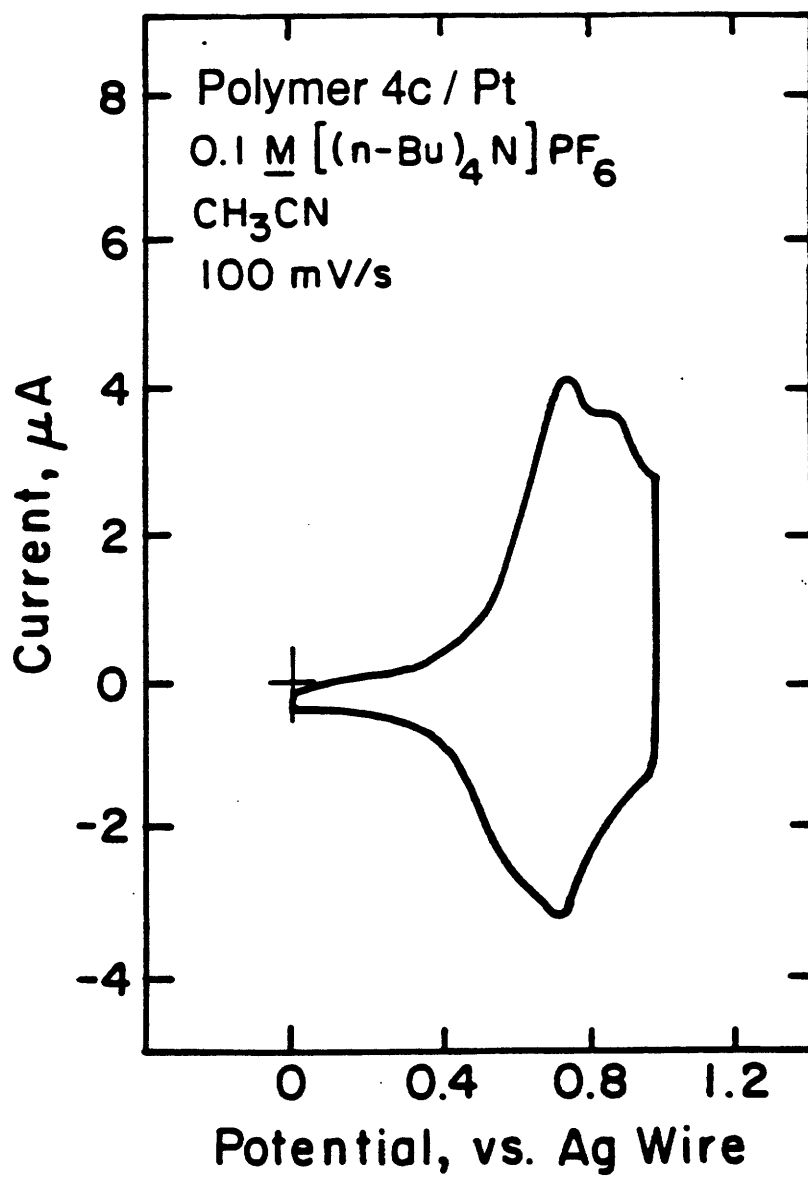


**Figure 4.** Cyclic voltammogram of a thin film of polymer **4c** on a Pt electrode in 0.1 M  $[n\text{-Bu}_4\text{N}]\text{PF}_6 / \text{CH}_3\text{CN}$ .



poly(TCDT)<sub>20</sub> under identical conditions contains an anodic peak at 0.9 V and a corresponding reduction at 0.7 V with a shoulder at 0.55 V.) Random copolymers containing TCDT and **2a** also could be characterized in this manner; the cyclic voltammogram of polymer **4d** (50% TCDT; Table I) is shown in Figure 5b. It is evident that the wave for **4d** is slightly broader than the wave for poly(**3(-)**)<sub>20</sub>.

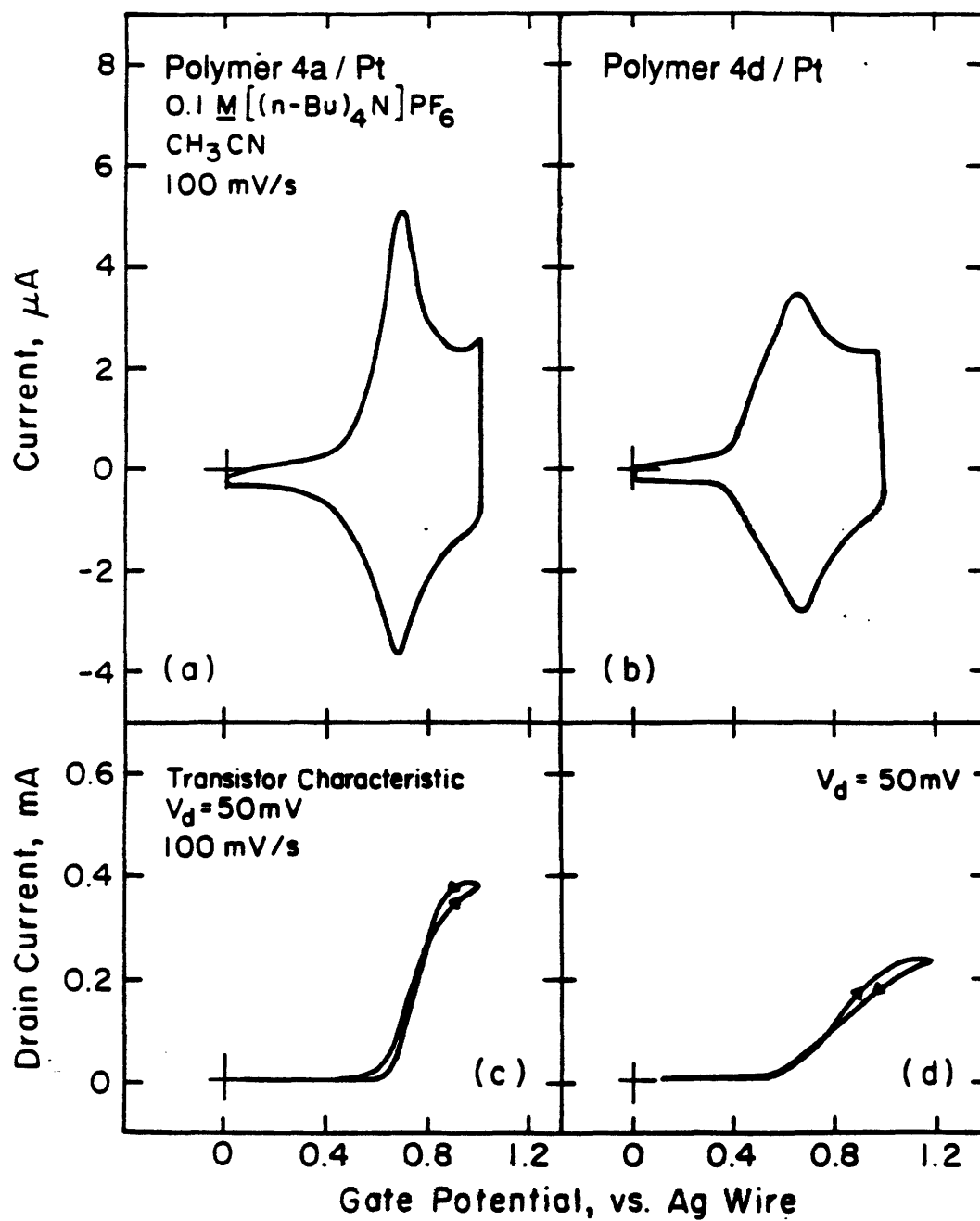
The potential dependent conductivities of copolymers **4e**, **4d**, **4a**, **4b**, **4c**, and **4f** were determined by recording the  $I_D$ - $V_G$  plots<sup>46</sup> for thin films of these polymers. These are shown in Figure 5(c) for **4a** and in Figure 5(d) for **4d**. For each of the copolymers studied by electrochemistry, we were able to calculate the average conductivity at the potential where the  $I_D$ - $V_G$  plot reaches a maximum; these data are included in Table XI. Several conclusions can be drawn from these data. First, the copolymers **4c**, **4a** and **4b** have conductivities in the  $10^{-2} \Omega^{-1}\text{cm}^{-1}$  range, a value that could be expected for unsubstituted polyacetylene samples where the average chain length is 20-30 double bonds in length.<sup>46</sup> Assuming the cyclopolymer segments contribute little to the overall conductivity since their homopolymers (consider poly(**3(-)**)<sub>20</sub>) are poorly conducting, it seems likely that in **4a-4c** the polyacetylene block is roughly 25 double bonds in length, consistent with the blocky structure of these polymers. The average conductivity of the triblock copolymer **4f** was  $3 \times 10^{-4} \Omega^{-1}\text{cm}^{-1}$ , a value that is slightly less than expected for 20 double bonds.<sup>46</sup> If the cyclopolymer block was contributing to the bulk conductivity, the measured conductivity would be greater than the observed value. For the copolymers **4d** and **4e**, in which the structure is more random, the conductivities are proportional to the TCDT content, consistent with short conducting unsubstituted polyene fragments interrupted by cyclopolymer fragments.

Conductivities of doped 1,6-heptadiyne derivatives prepared with classical catalysts have been found to be low relative to the conductivity of doped polyacetylene. Our findings confirm that the conductivity of 1,6-heptadiyne cyclopolymer is inherently



much lower than that of unsubstituted polyenes. That result should not be totally unexpected since ideally for high conductivity a highly delocalized form of the polymer, preferably trans/transoid in the case of an unsubstituted polyene, should be energetically accessible with minimal distortion of the polymer backbone. The presence of five- and six-membered rings containing bulky substituents enforces a conformation of the polymer backbone that has significant degree of conjugation, but at the same time the rings probably severely limit accessibility of highly delocalized, extended excited states.

**Figure 5.** Cyclic voltammograms of copolymer films on Pt electrodes in 0.1 M [*n*-Bu<sub>4</sub>N]PF<sub>6</sub> / CH<sub>3</sub>CN: (a) polymer **4a**; (b) polymer **4d**. I<sub>D</sub>-V<sub>G</sub> characteristics for copolymer films on interdigitated Pt electrode arrays in 0.1 M [*n*-Bu<sub>4</sub>N]PF<sub>6</sub> / CH<sub>3</sub>CN: (c) polymer **4a**; (d) polymer **4d**.



## Experimental Section

Preparation of the polymers is described elsewhere.<sup>47,48</sup> Acetonitrile for electrochemistry was Aldrich anhydrous grade; it was filtered through a plug of activated alumina before use.  $[n\text{-Bu}_4\text{N}]\text{PF}_6$  (Aldrich) was recrystallized from ethanol.  $[\text{Et}_4\text{N}]\text{AsF}_6$  was prepared from  $[\text{Et}_4\text{N}]\text{Br}$  and  $\text{LiAsF}_6$  and was recrystallized from acetone/ethanol. Both electrolytes were dried in a vacuum oven overnight before use.

**Electrochemistry.** Solution cyclic voltammetry was carried out using a Pt dot working electrode, a Pt mesh counter electrode and an oxidized silver wire as the quasi-reference electrode. The Pt dot was cleaned by cycling in 0.5 M  $\text{H}_2\text{SO}_4$  between 1.2 and -0.25 V vs. SCE as described previously.<sup>53</sup> Platinum microelectrode arrays for conductivity measurements and cyclic voltammetry of solution cast thin films were fabricated and mounted as described previously.<sup>54,55</sup> Arrays were cleaned by etching for 10 seconds with a freshly prepared 3:1 concentrated  $\text{H}_2\text{SO}_4$  : 30%  $\text{H}_2\text{O}_2$  solution, followed by cycling in 0.5 M  $\text{H}_2\text{SO}_4$  as described above.

Thin films of the polymers were cast from THF solutions directly onto the microfabricated array using a 0.5  $\mu\text{L}$  micropipette. Conductivity measurements were carried out as described previously.<sup>46</sup> In all the experiments, electrodes 1 and 4 were designated "source" and 5 and 8 designated "drain".

The UV/vis spectroelectrochemistry was carried out using in a air tight cell using a large Pt mesh counter electrode, oxidized silver wire quasi-reference and a transparent indium doped tin oxide (Delta Technologies) working electrode.

## References

- (1) Gibson, H. W. in "Handbook of Conducting Polymers"; T. J. Skotheim, Ed.; Marcel Dekker: New York, 1986; Vol. 1.
- (2) *Conjugated Polymers*; Brédas, J. L.; Silbey, R., Ed.; Kluwer: Boston, 1991.
- (3) Shirikawa, H.; Louis, E. J.; MacDiarmid, A. G.; Chiang, C. K.; Heeger, A. J. *J. Chem. Soc. Chem. Commun.* **1977**, 578.
- (4) Naarmann, H. *Synth. Met.* **1987**, *17*, 223.
- (5) Ito, T.; Shirakawa, H.; Ikeda, S. *J. Polym. Sci., Polym. Chem. Ed.* **1974**, *12*, 11.
- (6) Shirakawa, H.; Ikeda, S. *Polym. J.* **1971**, *2*, 231.
- (7) Swager, T. M.; Dougherty, D. A.; Grubbs, R. H. *J. Am. Chem. Soc.* **1988**, *110*, 2973.
- (8) Swager, T. M.; Grubbs, R. H. *J. Am. Chem. Soc.* **1989**, *111*, 4413.
- (9) Bott, D. C.; Brown, C. S.; Edwards, J. H.; Feast, W. J.; Parker, D.; Winter, J. N. *Mol. Cryst. Liq. Cryst.* **1985**, *117*, 9.
- (10) Edwards, J. H.; Feast, W. J. *Polymer* **1980**, *21*, 595.
- (11) Edwards, J. H.; Feast, W. J.; Bott, D. C. *Polymer* **1984**, *25*, 395.
- (12) Feast, W. J.; Winter, J. N. *J. Chem. Soc., Chem. Commun.* **1985**, 202.
- (13) Masuda, T.; Higashimura, T. *Adv. Polym. Sci.* **1986**, *81*, 122.
- (14) Sailor, M. J.; J., G. E.; Gorman, C. B.; Kumar, A.; Grubbs, R. H.; Lewis, N. S. *Science* **1990**, *249*, 1146.
- (15) Moore, J. S.; Gorman, C. B.; Grubbs, R. H. *J. Am. Chem. Soc.* **1991**, *113*, 1704.
- (16) Gorman, C. B.; Ginsburg, E. J.; Grubbs, R. H. *J. Am. Chem. Soc.* **1993**, *115*, 1397.
- (17) Ginsburg, E. J.; Gorman, C. B.; Marder, S. R.; Grubbs, R. H. *J. Am. Chem. Soc.* **1989**, *111*, 7621.
- (18) Klavetter, F. L.; Grubbs, R. H. *J. Am. Chem. Soc.* **1989**, *110*, 7807.
- (19) Masuda, T.; Yoshimura, T.; Higashimura, T. *Macromolecules* **1989**, *22*, 3804.
- (20) Stille, J. K.; Frey, D. A. *J. Am. Chem. Soc.* **1961**, *83*, 1697.

- (21) Gibson, H. W.; Bailey, F. C.; Epstein, A. J.; Rommelmann, H.; Kaplan, S.; Harbour, J.; Yang, X. Q.; Tanner, D. B.; Pochan, J. M. *J. Am. Chem. Soc.* **1983**, *105*, 4417.
- (22) Akopyan, L. A.; Ambartsumyan, G. V.; Matsoyan, M. S.; Ovakimyan, E. V.; Matsoyan, S. G. *Arm. Khim. Zh.* **1977**, *30*, 771.
- (23) Akopyan, L. A.; Ambartsumyan, G. V.; Grigoryan, S. G.; Matsoyan, S. G. *Vysokomol. Soedin., Ser. A* **1977**, *19*, 1068.
- (24) Akyopan, L. A.; Ambartsumyan, G. V.; Ovakimyan, E. V.; Matsoyan, S. G. *Vysokomol. Soedin., Ser. A* **1977**, *19*, 271.
- (25) Ambartsumyan, G. V.; Gevorkyan, S. B.; Kharatyan, V. G.; Gavalyan, V. B.; Saakyan, A. A.; Grigoryan, S. G.; Akopyan, L. A. *Arm. Khim. Zh.* **1984**, *37*, 188.
- (26) Ahn, H. K.; Kim, Y. H.; Jin, S. H.; Choi, S. K. *Polym. Bull.* **1992**, *29*, 625.
- (27) Cho, O. K.; Kim, Y. H.; Choi, K. Y.; Choi, S. K. *Macromolecules* **1990**, *23*, 12.
- (28) Choi, S. K. *Makromol. Chem., Macromol. Symp.* **1990**, *33*, 145.
- (29) Gal, Y. S.; Choi, S. K. *Pollimo* **1987**, *11*, 563.
- (30) Gal, Y. S.; Choi, S. K. *J. Polym. Sci., Part C* **1988**, *26*, 115.
- (31) Gal, Y. S.; Jung, B.; Cho, H. N.; Lee, W. C.; Choi, S. K. *J. Polym. Sci., Part C* **1990**, *28*, 259.
- (32) Gal, Y. S.; Choi, S. K. *J. Polym. Sci., Part A* **1993**, *31*, 345.
- (33) Han, S. H.; Kim, U. Y.; Kang, Y. S.; Choi, S. K. *Macromolecules* **1991**, *24*, 973.
- (34) Jin, S. H.; Kim, S. H.; Cho, H. N.; Choi, S. K. *Macromolecules* **1991**, *24*, 6050.
- (35) Jin, S. H.; Cho, H. N.; Choi, S. K. *J Polym Sci A-Polym Chem* **1993**, *31*, 69.
- (36) Kim, Y. H.; Gal, Y. S.; Kim, U. Y.; Choi, S. K. *Macromolecules* **1988**, *21*, 1991.
- (37) Kim, Y. H.; Choi, K. Y.; Choi, S. K. *J. Polym. Sci., Part C* **1989**, *27*, 443.
- (38) Kim, Y. H.; Kwon, S. K.; Gal, Y. S.; Choi, S. K. *J. Macromol. Sci., Pure Appl. Chem.* **1992**, *29*, 589.
- (39) Kim, Y. H.; Kwon, S. K.; Choi, S. K. *Bull. Kor. Chem. Soc.* **1992**, *13*, 459.

- (40) Koo, K. M.; Han, S. H.; Kang, Y. S.; Kim, U. Y.; Choi, S. K. *Macromolecules* **1993**, *26*, 2485.
- (41) Park, J. W.; Lee, J. H.; Cho, H. N.; Choi, S. K. *Macromolecules* **1993**, *26*, 1191.
- (42) Ryoo, M. S.; Lee, W. C.; Choi, S. K. *Macromolecules* **1990**, *23*, 3029.
- (43) Jang, M. S.; Kwon, S. K.; Choi, S. K. *Macromolecules* **1990**, *23*, 4135.
- (44) Schrock, R. R. *Acc. Chem. Res.* **1990**, *23*, 158.
- (45) Fox, H. H.; Schrock, R. R. *Organometallics* **1992**, *11*, 2763.
- (46) Park, L. Y.; Ofer, D.; Gardner, T. J.; Schrock, R. R.; Wrighton, M. S. *Chem. Mater.* **1992**, *4*, 1388.
- (47) Fox, H. H. Ph.D. Thesis, Massachusetts Institute of Technology, September, 1993.
- (48) Fox, H. H.; Wolf, M. O.; O'Dell, R.; Lin, B. L.; Schrock, R. R.; Wrighton, M. S. *J. Am. Chem. Soc.* **in press**,
- (49) Bard, A. J.; Faulkner, L. R. "Electrochemical Methods"; ; Wiley: New York, 1980.
- (50) Patil, A. O.; Heeger, A. J.; Wudl, F. *Chem. Rev.* **1988**, *88*, 183.
- (51) Jozefiak, T. H.; Ginsburg, E. J.; Gorman, C. B.; Grubbs, R. H.; Lewis, N. S. *J. Am. Chem. Soc.* **1993**, *115*, 4705.
- (52) Gorman, C. B.; Ginsburg, E. J.; Sailor, M. J.; Moore, J. S.; Jozefiak, T. H.; Lewis, N. S.; Grubbs, R. H.; Marder, S. R.; Perry, J. W. *Synth. Met.* **1991**, *41*, 1033.
- (53) Breiter, M.; Böld, W. *Electrochim. Acta* **1961**, *5*, 141.
- (54) Paul, E.; Ricco, A. J.; Wrighton, M. S. *J. Phys. Chem.* **1985**, *89*, 1441.
- (55) Kittlesen, G. P.; White, H. S.; Wrighton, M. S. *J. Am. Chem. Soc.* **1984**, *106*, 7389.

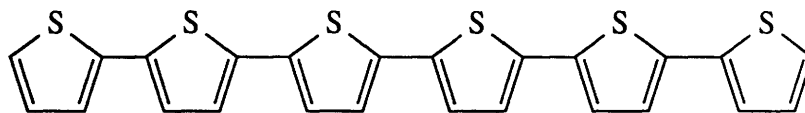
## **Chapter 5**

**Preparation and Characterization of Photovoltaic and Photoelectrochemical Devices**

**Based on  $\alpha$ -Sexithiophene**



In this chapter the preparation and characterization of photovoltaic and photoelectrochemical energy conversion devices fabricated using  $\alpha$ -sexithiophene as the active component are discussed.



$\alpha$ -Sexithiophene

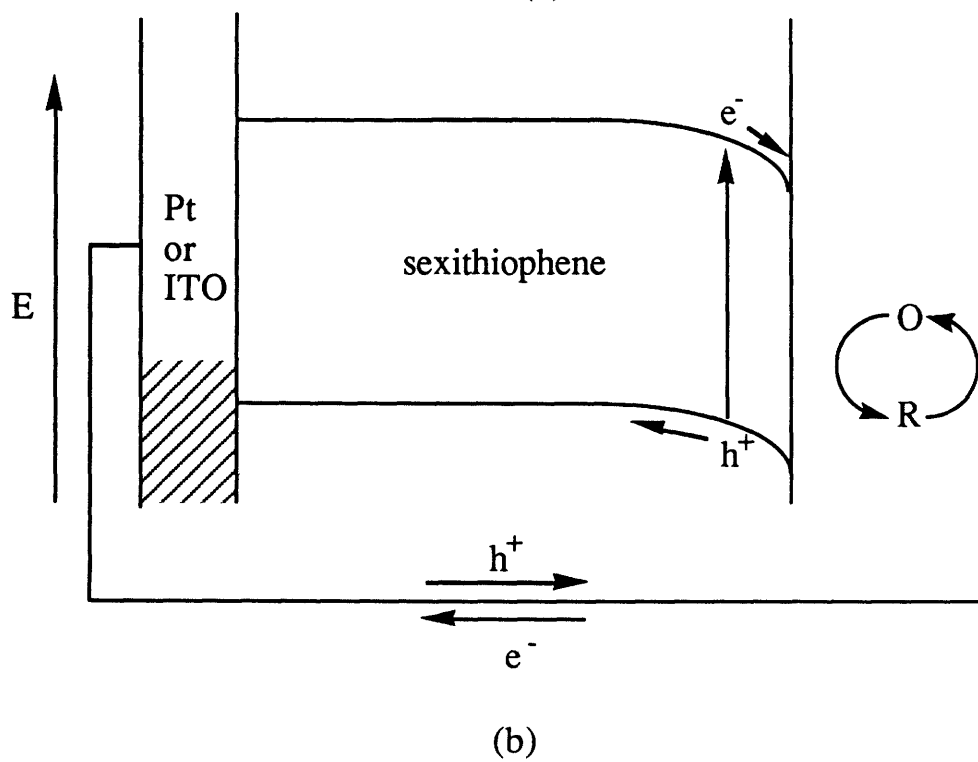
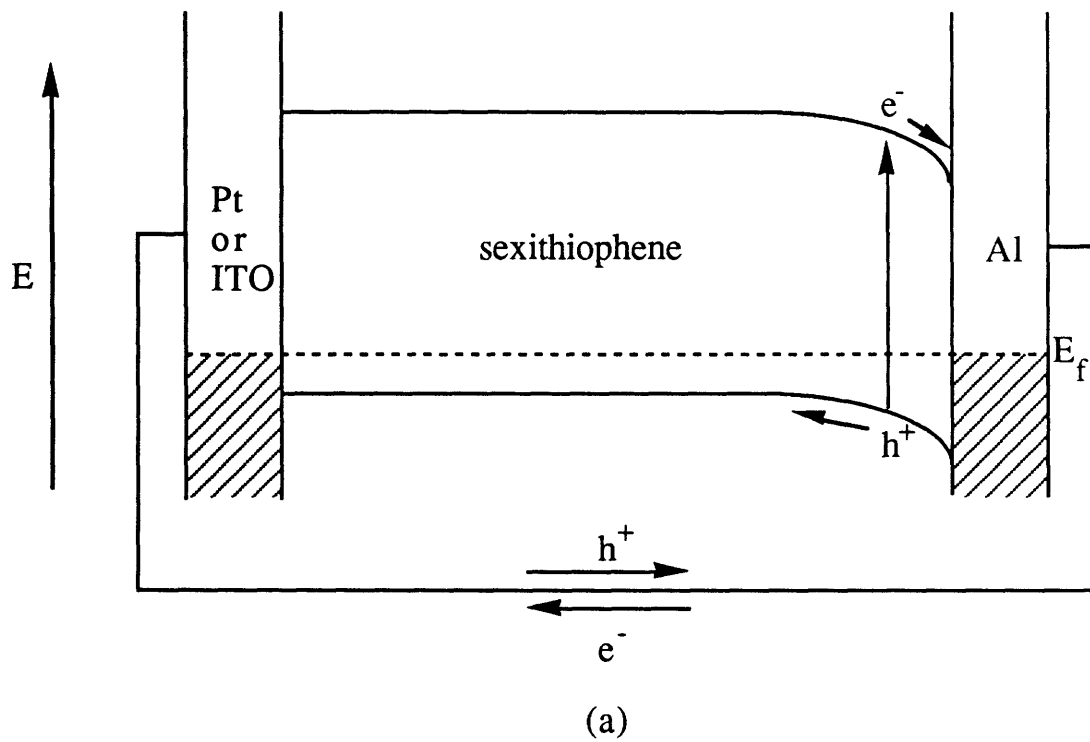
Molecular semiconductors have been well studied as materials for the preparation of solid state photovoltaic devices<sup>1-5</sup> as well as photoelectrochemical devices.<sup>6-8</sup> Such materials offer the prospect of control over device properties through structural modification of the semiconductor. The viability of using molecular semiconductors in practical devices has been limited by their poor properties, particularly their low carrier mobilities.<sup>9</sup>  $\alpha$ -Sexithiophene has been shown to have an extraordinarily high space charge carrier mobility ( $0.46 \text{ cm}^2/\text{Vs}$ ) for an organic material.<sup>10-14</sup> In comparison amorphous hydrogenated silicon has a carrier mobility of  $1 \text{ cm}^2/\text{Vs}$ .<sup>15-17</sup>  $\alpha$ -Sexithiophene is easily synthesized via several routes from readily available starting materials,<sup>18-23</sup> and large area devices may be prepared in thin film form by vacuum deposition.<sup>11,13,14</sup>  $\alpha$ -Sexithiophene has several advantages over organic conducting polymers which have also been investigated as photovoltaic<sup>5,24</sup> and photoelectrochemical<sup>25,26</sup> energy conversion materials. Since  $\alpha$ -sexithiophene is a pure material properties associated with conventional conducting polymers such as defects and traps are minimized. These properties of conducting polymers likely limit their charge carrier mobility.

Photocurrent in photovoltaic devices results from the separation of charge carriers generated by photoexcitation, Scheme Ia. Efficient separation of the charge carriers depends on the electric field generated by the metal contacts sandwiching the

active component, as well as the mobility of the charge carriers. High charge carrier mobility results in a greater probability that the carrier reaches the contact before it recombines. It is this feature of  $\alpha$ -sexithiophene that we expected to improve the efficiency of photovoltaic devices in which it is employed as the light absorber.

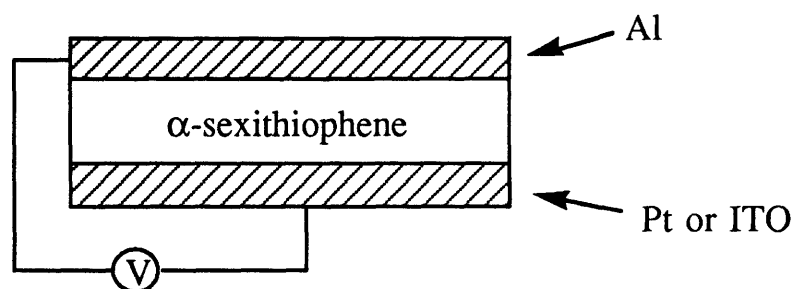
Photoelectrochemical devices function on the same principle of charge separation, however a solution redox couple is employed in place of one of the metal contacts, Scheme Ib. Since the potential of the redox couple can be varied at will, the potential of the solution can be fixed at any potential accessible with a redox couple.

**Scheme I.** Schematic of  $\alpha$ -sexithiophene photovoltaic and photoelectrochemical devices.



## Results and Discussion.

**Preparation and Characterization of Photovoltaic Devices.** We prepared photovoltaic devices by evaporation of pure  $\alpha$ -sexithiophene onto substrates (indium doped tin oxide (ITO) or Pt).



The devices were coated with thermally evaporated Al and the Al contacted with a copper clip. The thickness of the metal contacts was chosen to allow maximum transmission of incident light without causing excessive series resistance. The device characteristics were measured immediately after fabrication in order to minimize oxidation effects. The device characteristics were measured by controlling the potential across the device while measuring the current response. The effect of variation in the intensity of incident light was also measured in this way.

The current density-voltage curves of a Pt/ $\alpha$ -sexithiophene/Al and ITO/ $\alpha$ -sexithiophene/Al device at different incident monochromatic (488 nm) light intensities are shown in Figures 1 and 2 respectively. The fill factor (ratio of the maximum output power to the product of  $V_{oc}$  and  $I_{sc}$ ), quantum efficiency for electron flow ( $\Phi$ )<sup>27</sup> and overall power conversion efficiency ( $\eta$ )<sup>28</sup> have been calculated and these

**Figure 1.** Photocurrent density as a function of potential for irradiation of an Pt/ $\alpha$ -sexithiophene/Al device for different incident light intensities. Illumination is through the Al side of the device with 488 nm laser light, and intensities are corrected for the aluminum absorption.

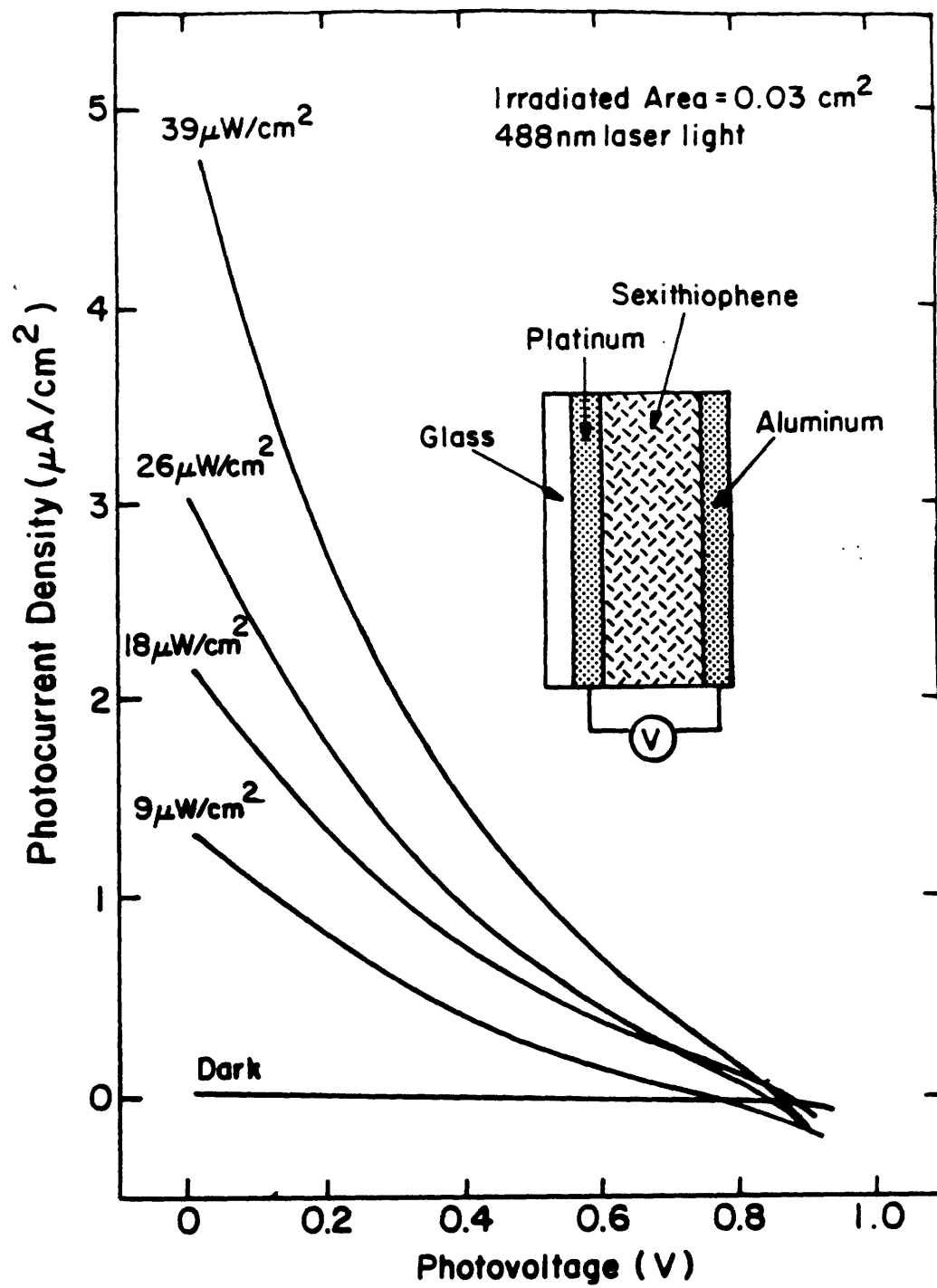
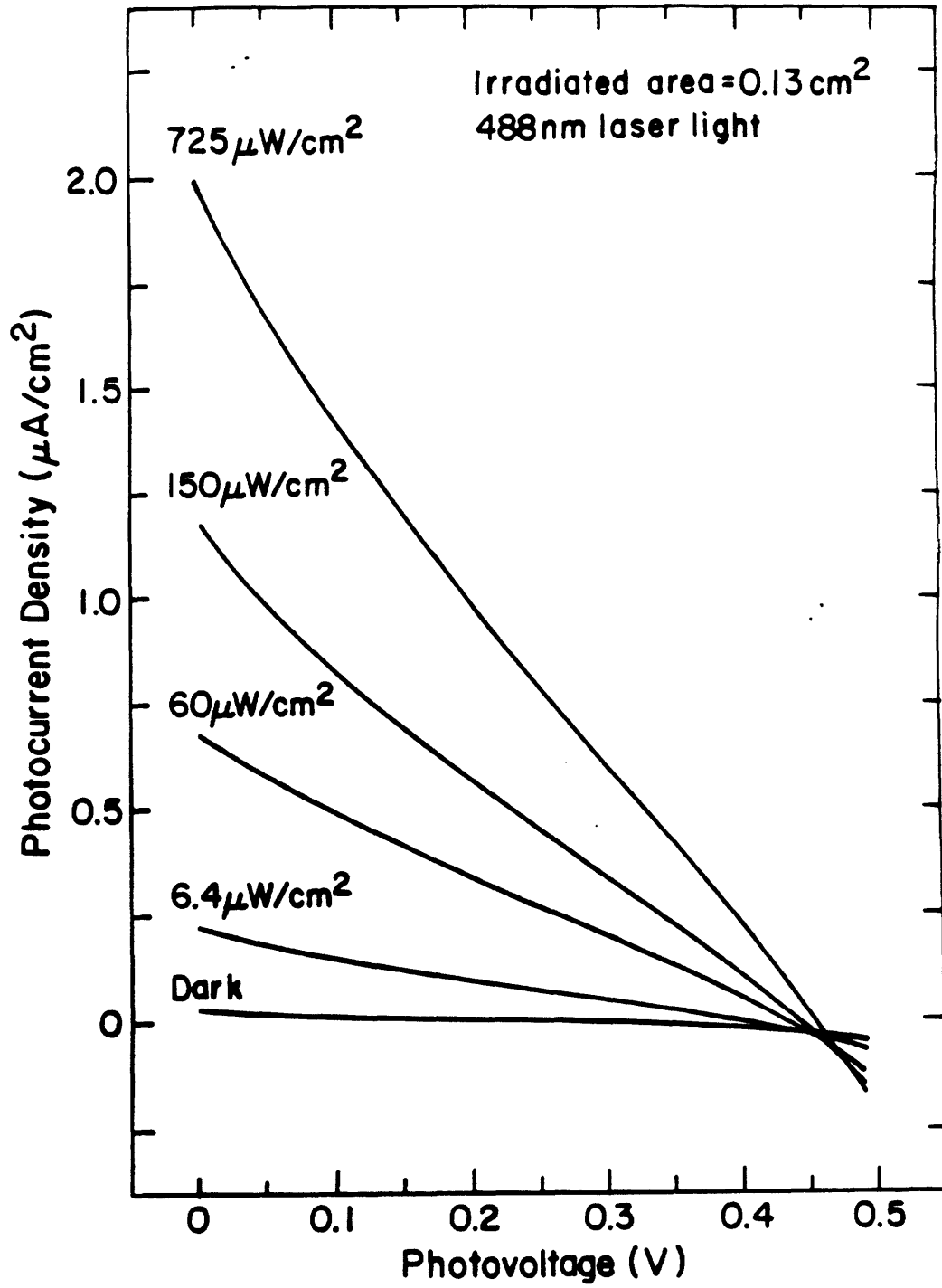


**Figure 2.** Photocurrent density as a function of potential for irradiation of an ITO/ $\alpha$ -sexithiophene/Al device for different incident light intensities. Illumination is through the Al side of the device with 488 nm laser light, and intensities are corrected for the aluminum absorption.





are shown in Table I. In the device shown in Scheme Ia electrons flow from the Al to the Pt or ITO contacts upon irradiation, consistent with the work function difference in work functions of the metals.<sup>29</sup>

The dependence of  $V_{oc}$  and  $I_{sc}$  on the incident light intensity,  $I_{inc}$ , for the ITO/ $\alpha$ -sexithiophene/Al device is shown in Figure 3. The  $V_{oc}$  reaches a maximum ( $\sim 0.4$  V) as the light intensity is increased, and this maximum is achieved at very modest light intensities. Although values as high as 1.2 V have been reported for  $V_{oc}$ ,<sup>30,31</sup> most organic photovoltaics have  $V_{oc}$  between 0.3 - 0.8 V.<sup>1-5</sup> A plot of  $\log I_{sc}$  vs.  $\log I_{inc}$ , Figure 3b, is linear with a slope of 0.5 over the whole range of light intensities studied. This behavior has been observed previously for photovoltaic devices in which a bimolecular electron-hole deactivation pathway is active, and a low thermal carrier concentration exists.<sup>28</sup> As a result, the quantum yield and power efficiency at 488 nm for the device both decrease with increasing light intensity. In many organic photovoltaic devices the electric field is not uniform across the entire thickness of the device; the space charge region does not extend from one contact to the other. Since the quantum yield for photocurrent is field dependent, light intensity changes would be expected to affect the observed quantum yield.

The photoaction spectrum of the ITO/ $\alpha$ -sexithiophene/Al device is shown in Figure 4b for irradiation through the ITO side of the device. The spectrum was normalized for the number of photons incident at each wavelength. The absorbance spectrum, Figure 4a, matches the features observed in the photoaction spectrum. When irradiation is from the ITO side only a small photocurrent is measured, Figure 4c. This behavior is consistent with the presence of a barrier at the Al-sexithiophene interface, as shown in Scheme Ia.<sup>1</sup> We believe that the carriers generated in the space charge region contribute most to the observed photocurrent. Many of the carriers in the bulk of the semiconductor decay before they diffuse into the high electric field region.

**Table I.** Performance Characteristics of Photovoltaic and Photoelectrochemical Cells Based on  $\alpha$ -Sexithiophene.

Cell	$I_{\text{inc}}$ ( $\mu\text{W}/\text{cm}^2$ )	$I_{\text{sc}}$ ( $\mu\text{A}/\text{cm}^2$ )	$V_{\text{oc}}$ (V)	FF <sup>b</sup>	$\Phi$ (%) <sup>c</sup>	$\eta$ (%) <sup>d</sup>
A <sup>a</sup>	725	2.0	0.46	0.22	0.7	0.03
A	22	0.41	0.43	0.21	4.8	0.17
A	0.22	0.032	0.22	0.22	36	0.69
B	39	4.8	0.83	0.15	0.31	1.5
C	25	2.8	0.99	0.11	-	1.2
D	34	5.3	1.4	0.42	-	0.01

<sup>a</sup> A: ITO/ $\alpha$ -sexithiophene/Al device, 488 nm light, irradiated through Al side. B: Pt/ $\alpha$ -sexithiophene/Al device, 488 nm light, irradiated through Al side. C: Pt/ $\alpha$ -sexithiophene/Al device, polychromatic light, irradiated through Al side. D: Pt/ $\alpha$ -sexithiophene device contacted with 5 mM [Cp<sub>2</sub>Co][PF<sub>6</sub>] in 0.1 M [*n*-Bu<sub>4</sub>N][PF<sub>6</sub>]. <sup>b</sup> FF =  $P_{\text{max}} / V_{\text{oc}} I_{\text{sc}}$ . <sup>c</sup> Quantum yield:  $\Phi$  (%) =  $124000 I_{\text{sc}} / \lambda I_{\text{inc}}$  ( $I_{\text{inc}}$  is incident power). <sup>d</sup> Overall power efficiency:  $\eta$  (%) =  $100 I_{\text{sc}} V_{\text{oc}} \text{FF} / I_{\text{inc}}$

**Figure 3.** (a)  $V_{oc}$  vs.  $I_{inc}$  and (b)  $I_{sc}$  vs.  $I_{inc}$  for an ITO/ $\alpha$ -sexithiophene/Al device .

Illumination is through the Al side of the device with 488 nm laser light, and intensities are corrected for Al absorption. Inset:  $\log I_{sc}$  vs.  $\log I_{inc}$ .

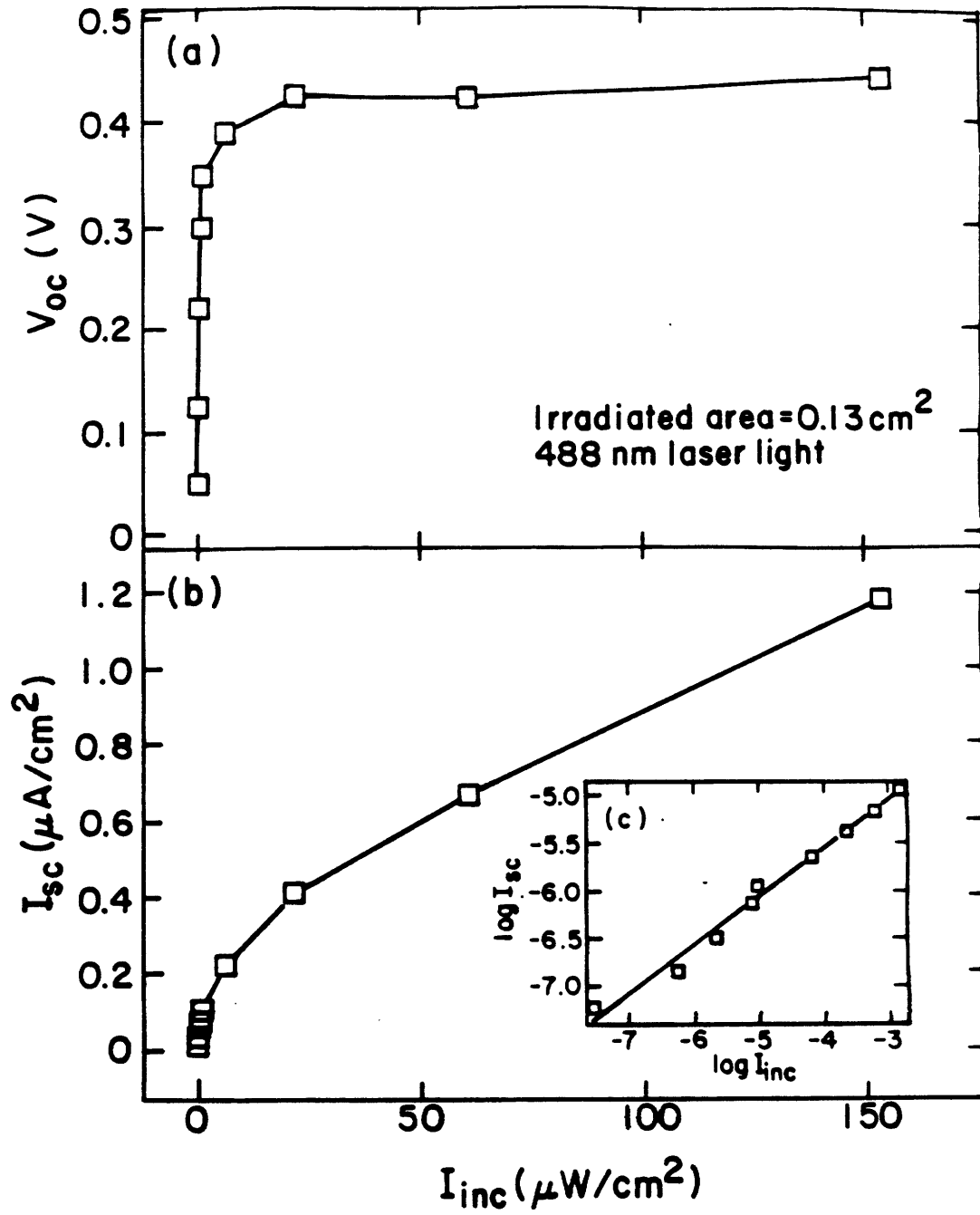
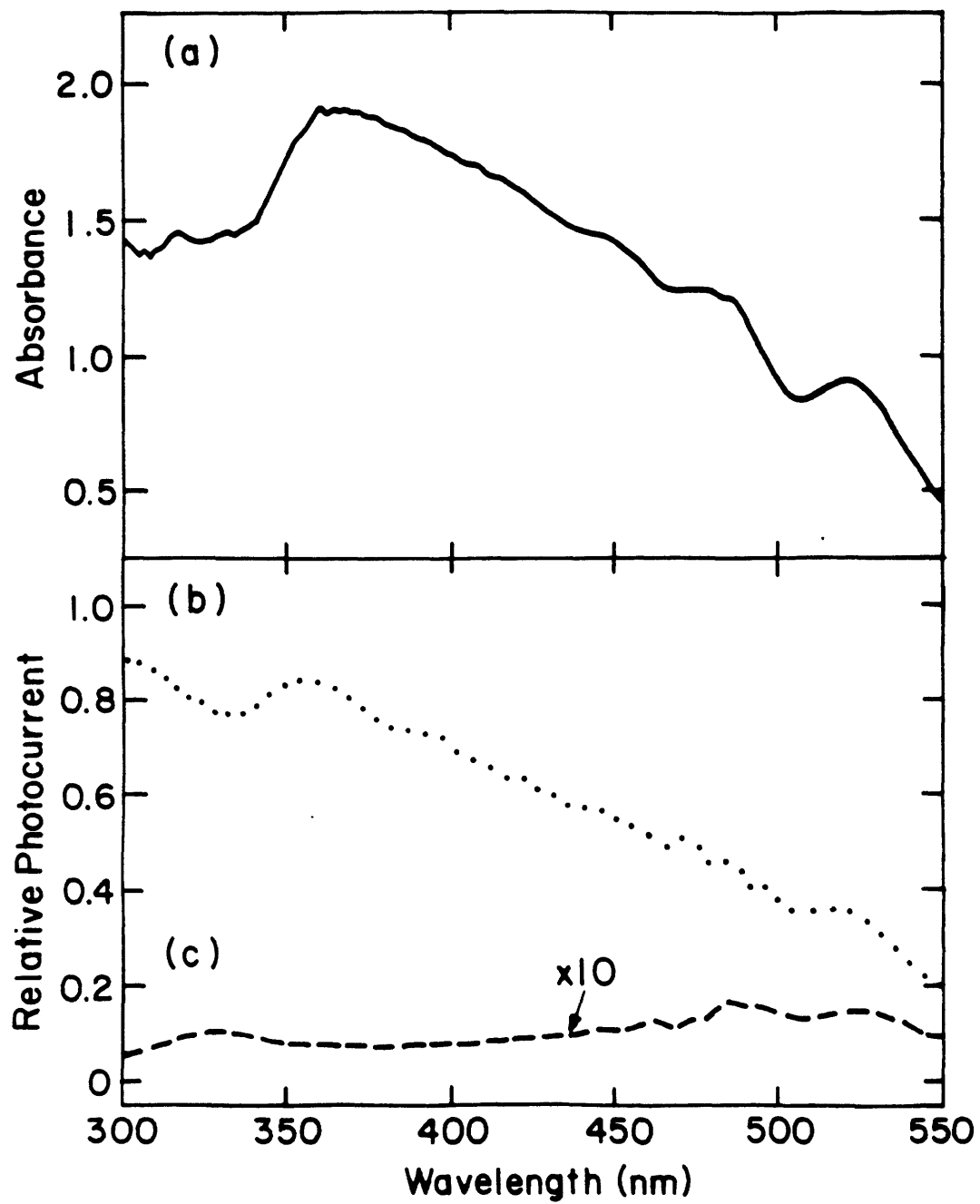


**Figure 4.** (a) Absorbance spectrum of the  $\alpha$ -sexithiophene film on ITO/glass. (b) photoaction spectra for irradiation through aluminum side and (c) ITO side. Photocurrents are corrected for Al and ITO/glass absorption and lamp intensity variations.



The dependence of  $V_{oc}$  and  $I_{sc}$  on the incident light intensity,  $I_{inc}$ , for the Pt/ $\alpha$ -sexithiophene/Al device is shown in Figure 5. In this device, at the light intensities studied,  $I_{sc}$  increases in an approximately linear fashion with increasing light intensity, in contrast to the ITO device. We attribute this difference to the presence of a stronger field across the device, yielding more efficient charge separation. Notably, the maximum  $V_{oc}$  for the Pt/ $\alpha$ -sexithiophene/Al device, Figure 5b, is approximately 0.83 V. The difference in the  $V_{oc}$  observed for the two devices may be accounted for by the difference in work functions between ITO and Pt. The work function of ITO is approximately 4.7 eV<sup>32</sup>, whereas that of Pt is 5.65 eV.<sup>29</sup> The photoaction spectrum of the Pt/ $\alpha$ -sexithiophene/Al device is shown in Figure 6a for irradiation through the Pt side of the device. The spectrum was normalized for the number of photons incident at each wavelength. The absorbance spectrum, Figure 6b, matches the features observed in the photoaction spectrum.

The fill factors for the devices are low, but they are comparable to those observed for most other organic photovoltaic devices.<sup>1-5</sup> As with other organic photovoltaic devices the sexithiophene based device has a non-uniform electric field across the thickness of the photovoltaic material and the space charge region likely does not extend from one contact to the other. In the bulk, the rate of recombination is higher leading to greater overall device resistance,<sup>1-5</sup> and low fill factors. Despite the low fill factors, the overall efficiencies ( $\eta$ ) are approximately 1% for both polychromatic and 488 nm light for the Pt/ $\alpha$ -sexithiophene/Al device, Table I. Other workers have obtained similar efficiencies at comparable light intensities with phthalocyanines,<sup>27,33,34</sup> and perylenetetracarboxylic acid derivatives layered with copper phthalocyanine.<sup>35</sup> Similar efficiencies have also been obtained at higher light intensities with merocyanines.<sup>30,31</sup>

**Photoelectrochemical Devices.** We also examined the behavior  $\alpha$ -sexithiophene films which were deposited onto Pt electrodes in photoelectrochemical cells using several

**Figure 5.** (a)  $I_{sc}$  vs.  $I_{inc}$  and (b)  $V_{oc}$  vs.  $I_{inc}$  for a Pt/-sexithiophene/Al device.

Illumination is through the Al side of the device with 488 nm laser light, and intensities are corrected for Al absorption.



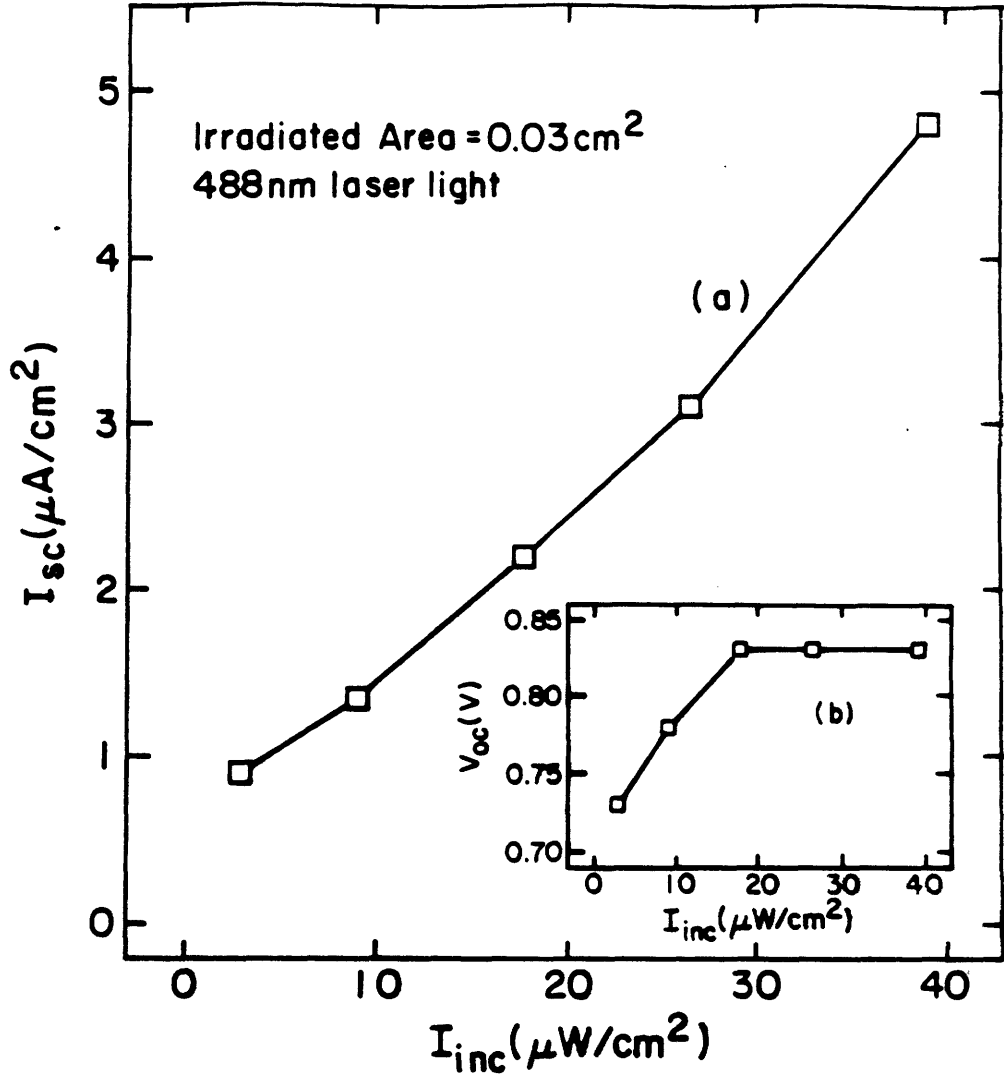
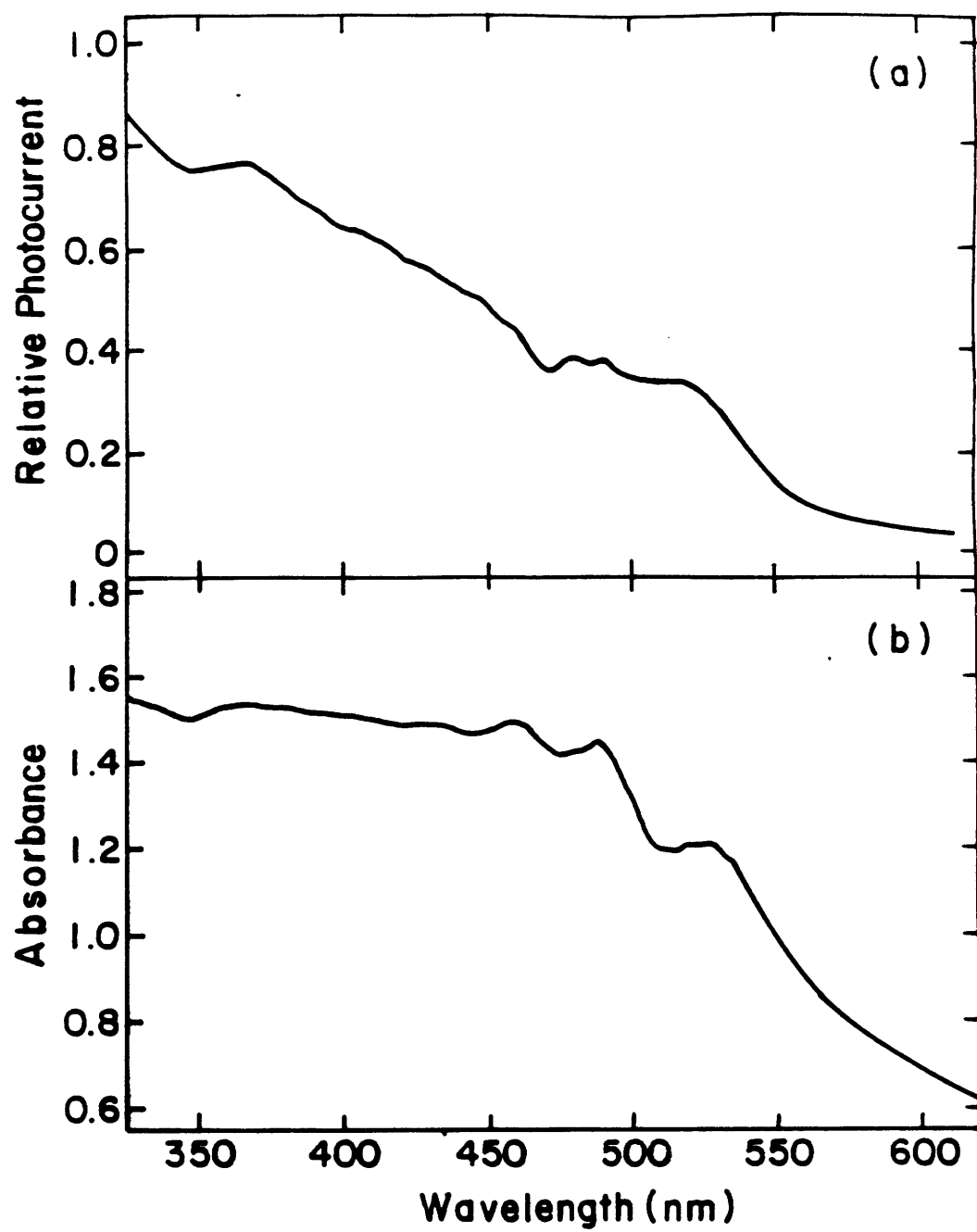


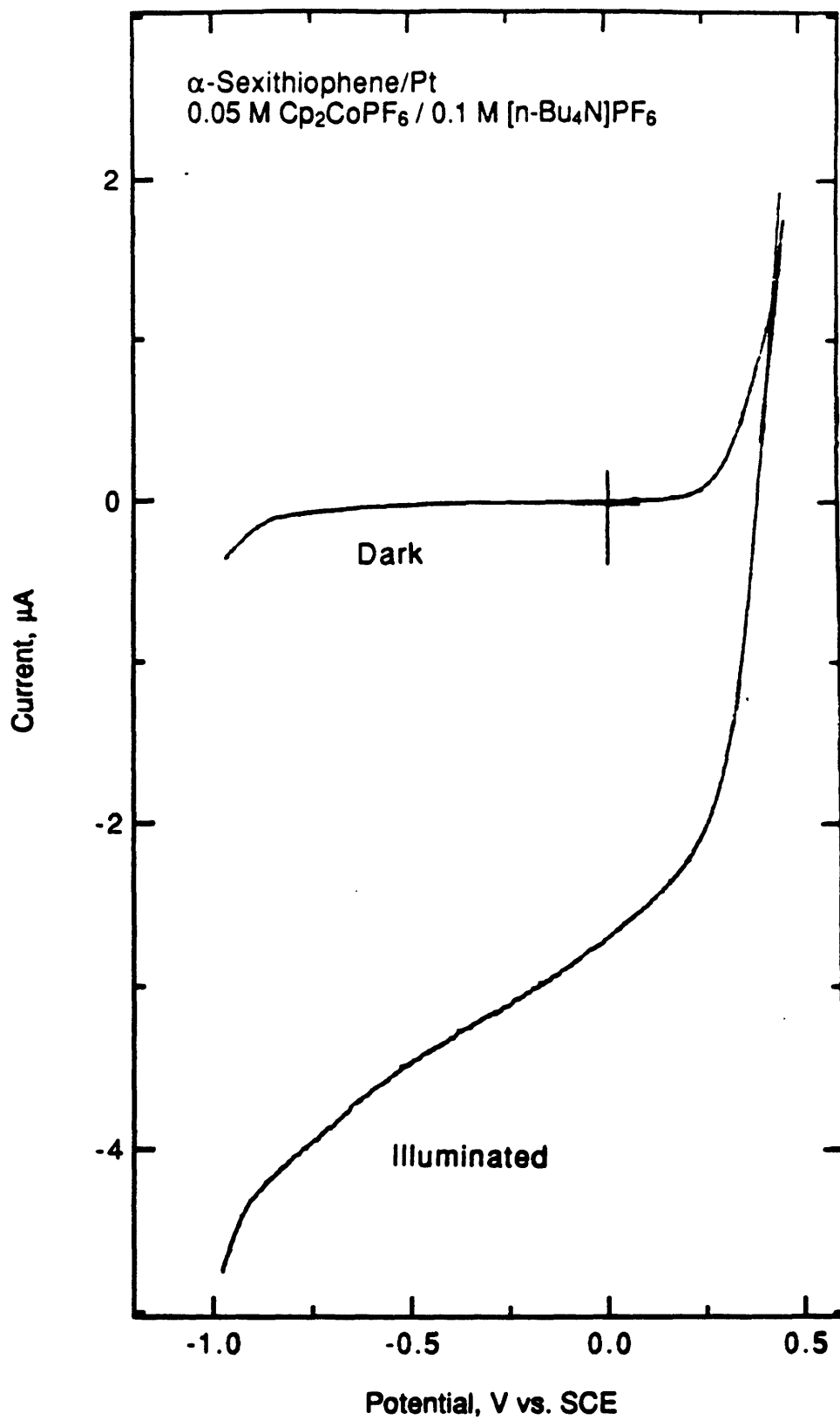
**Figure 6.** (a) Photoaction spectra for irradiation through aluminum side of a Pt/-sexithiophene/Al device and (b) absorbance spectrum of the  $\alpha$ -sexithiophene film on ITO/glass. Photocurrents are corrected for Al absorption and lamp intensity variations.



redox species in acetonitrile to contact the film. Since the  $\alpha$ -sexithiophene films behaved as p-type semiconductors in the photovoltaic cells, we chose solution species with negative reduction potentials in order to achieve large photovoltages. The photocurrent vs. potential plot for a  $\alpha$ -sexithiophene film ( $\sim 1\mu\text{m}$ ) immersed in a 5 mM  $[\text{Cp}_2\text{Co}][\text{PF}_6]$  solution containing 0.1 M  $[\text{n-Bu}_4\text{N}]\text{PF}_6$  as supporting electrolyte is shown in Figure 7. Illumination was with polychromatic light ( $50\text{ mW/cm}^2$ ). In the dark, cathodic current begins to flow at  $-0.9\text{ V}$  vs. SCE. Presumably, this dark current is due to reduction of  $[\text{Cp}_2\text{Co}]^+$  at Pt which is exposed through the pinholes in the film.

We examined the dependence of the photocurrent,  $I_{\text{ph}}$ , on light intensity. For these experiments the potential of  $\alpha$ -sexithiophene electrode was held constant at  $-0.6\text{ V}$  vs. SCE and the electrode illuminated with polychromatic light. A plot of  $\log I_{\text{ph}}$  vs.  $\log I_{\text{inc}}$  is linear. The slope of this plot is the exponent  $\gamma$  in the equation  $I_{\text{ph}} \propto I_{\text{inc}}^\gamma$ , we calculate  $\gamma$  to be 0.92 here. This value is related to the extent of recombination during transport of the electron-hole pair to the electrodes.<sup>4</sup> Thus, the rate of electron-hole recombination in these films is only weakly dependent on the incident light intensity. These preliminary results show that photoelectrochemical cells using thin films of  $\alpha$ -sexithiophene as a photocathode have low overall efficiencies but large fill factors. In these experiments it is only possible to estimate the photovoltage, since the solution potential is pinned.

**Figure 7.** Photocurrent density as a function of potential vs. SCE for irradiation of a sexithiophene/Pt device in 0.05 M  $\text{Cp}_2\text{CoPF}_6$  / 0.1 M  $[\text{n-Bu}_4]\text{NPF}_6$



**Experimental Section.**

**Synthesis.** Sexithiophene was prepared by the oxidative coupling of 2,2':5',2''-terthiophene using a variation of the literature method.<sup>23,36</sup> 2,2':5',2''-terthiophene (5.00 g) and anhydrous FeCl<sub>3</sub> (3.28 g) were stirred overnight in dry benzene. The solid which precipitates was washed with acetone and further purified via overnight Soxhlet extraction of the starting material into acetone leaving sexithiophene as a red powder. The compound was then doubly sublimed (10<sup>-5</sup> torr) yielding a bright red-orange powder. Low resolution EI mass spectrum contains molecular ion peak at m/e = 494 (100). Anal. Calcd. for C<sub>24</sub>H<sub>14</sub>S<sub>6</sub>: C, 58.30; H, 2.85. Found: C, 58.24 ; H, 3.00.

**Preparation of Devices.** Films were deposited by vacuum evaporation (10<sup>-5</sup> torr) onto Pt substrates prepared by electron beam evaporation of 100 Å Cr followed by 1000 Å Pt onto Si wafers. Prior to depositing the sexithiophene film the Pt surface was cleaned by rinsing with EtOH and H<sub>2</sub>O followed by etching in a H<sub>2</sub> and Ar plasma. Film thicknesses were determined using a Dektak profilometer. For the photovoltaic devices the Al top contacts were deposited by thermal evaporation (10<sup>-6</sup> torr) to complete the devices.

**Device Characterization.** For the monochromatic study an Ar laser (488 nm) was used as a light source, and irradiation was carried out through the Al side of the device.

Monochromatic light intensities were measured using a Tektronix J16 radiometer calibrated at 488 nm by actinometry, and were corrected for the absorbance of the Al layer. The experiments using polychromatic light used a 500 W tungsten lamp filtered through a 5 cm H<sub>2</sub>O filter. Light intensities were varied using Oriel neutral density filters. Polychromatic light intensities were measured using a Solarex reference cell. An X-Y recorder was used to record the steady-state voltage-current characteristics of the devices, and these data were recorded at 5 mV/s. In the photoelectrochemical experiments [Cp<sub>2</sub>Co][PF<sub>6</sub>] (Aldrich or Strem) in CH<sub>3</sub>CN containing 0.1 M [n-

$\text{Bu}_4\text{NPF}_6$  as supporting electrolyte were used. All the photoelectrochemical experiments were conducted under an argon atmosphere.



**References.**

- (1) Nevin, W. A.; Chamberlain, G. A. *J. Chem. Soc., Faraday Trans. 2* **1989**, *85*, 1729.
- (2) Dodelet, J.-P.; Pommier, H.-P.; Ringuet, M. J. *J. Appl. Phys.* **1982**, *53*, 4270.
- (3) Skotheim, T.; Yang, J.-M.; Otvos, J.; Klein, M. P. *J. Chem. Phys.* **1982**, *77*, 6144.
- (4) Segui, J.; Hotchandani, S.; Baddou, D.; LeBlanc, R. M. *J. Phys. Chem.* **1991**, *95*, 8807.
- (5) Glenis, S.; Horowitz, G.; Tourillon, G.; Garnier, F. *Thin Solid Films* **1984**, *111*, 93.
- (6) Crouch, A. M.; Ordonez, I.; Langford, C. H.; Lawrence, M. F. *J. Phys. Chem.* **1988**, *92*, 6058.
- (7) Ingnas, O.; Lundstrom, I. *J. Appl. Phys.* **1983**, *54*, 4185.
- (8) Tamizhmani, G.; Dodelet, J. P.; Cote, R.; Gravel, D. *Chem. Mater.* **1991**, *3*, 1046.
- (9) Simon, J.; Andre, J.-J. "Molecular Semiconductors"; ; Springer Verlag: Berlin, 1985.
- (10) Fichou, D.; Horowitz, G.; Nishikitani, Y.; Garnier, F. *Chemtronics* **1988**, *3*, 176.
- (11) Fichou, D.; Horowitz, G.; Nishikitani, Y.; Roncali, J.; Garnier, F. *Synth. Met.* **1989**, *28*, C729.
- (12) Garnier, F.; Horowitz, G.; Fichou, D. *Synth. Met.* **1989**, *28*, C705.
- (13) Horowitz, G.; Fichou, D.; Garnier, F. *Solid State Commun.* **1989**, *70*, 385.
- (14) Horowitz, G.; Fichou, D.; Peng, X.; Xu, Z.; Garnier, F. *Solid State Commun.* **1989**, *72*, 381.
- (15) Garnier, F.; Horowitz, G.; Peng, X.; Fichou, D. *Adv. Mater.* **1990**, *2*, 592.
- (16) Anderson, J. C. *Thin Solid Films* **1976**, *38*, 151.
- (17) Sze, S. M. "Physics of Semiconductor Devices"; ; Wiley: New York, 1969.
- (18) Kagan, J.; Arora, S. K. *Tetrahedron Lett.* **1983**, *24*, 4043.
- (19) Kagan, J.; Arora, S. K. *Heterocycles* **1983**, *20*, 1937.
- (20) Kagan, J.; Arora, S. K. *J. Org. Chem.* **1983**, *48*, 4317.

- (21) Nakayama, J.; Konishi, T.; Murabayashi, S.; Hoshino, M. *Heterocycles* **1987**, *26*, 1793.
- (22) Taliani, C.; Zamboni, R.; Ruani, G.; Rossini, S.; Lazzaroni, R. *J. Mol. Elec.* **1990**, *6*, 225.
- (23) Fichou, D.; Horowitz, G.; Garnier, G. *French Patent 89-07610* **1989**,
- (24) Vannikov, A. V.; Zhuravleva, T. S. *J. Mol. Electron.* **1989**, *5*, 63.
- (25) Garnier, F.; Horowitz, G.; Roncali, J.; Lemaire, M. *Ber. Bunsenges. Phys. Chem.* **1988**, *92*, 1261.
- (26) Yaohua, D.; Shaolin, M. *Electrochim. Acta* **1991**, *36*, 2015.
- (27) Loutfy, R. O.; Sharp, J. H. *J. Chem. Phys.* **1979**, *71*, 1211.
- (28) Meier, H. "Organic Semiconductors"; ; Verlag Chemie: Berlin, 1974.
- (29) "CRC Handbook of Chemistry and Physics"; ; 1983.
- (30) Morel, D. L.; Ghosh, A. K.; Feng, T.; Stogryn, E. L.; Purwin, P. E.; Fishman, C. *Appl. Phys. Lett.* **1978**, *32*, 495.
- (31) Ghosh, A. K.; Feng, T. *J. Appl. Phys.* **1978**, *49*, 5982.
- (32) Balasubramanian, N.; Subrahmanyam, A. *J. Electrochem. Soc.* **1991**, *138*, 322.
- (33) Fan, F.-R.; Faulkner, L. R. *J. Chem. Phys.* **1978**, *69*, 3341.
- (34) Loutfy, R. O.; Sharp, J. H.; Hsiao, C. K.; Ho, R. *J. Appl. Phys.* **1981**, *52*, 5218.
- (35) Tang, C. W. *Appl. Phys. Lett.* **1986**, *48*, 183.
- (36) Tamao, K.; Kodama, S.; Nakajima, I.; Kumada, M.; Minato, A.; Suzuki, K. *Tetrahedron* **1982**, *38*, 3347.